



Efficient operation of a packed bed thermal energy storage for waste heat recovery in the iron and steel industry

by Paul Schwarzmayr

A dissertation for the degree of
Doctor technicae

In the
Doctoral programme in Engineering Sciences – Mechanical Engineering

At the
Faculty of Mechanical and Industrial Engineering, TU Wien

Under the supervision of
Prof. Dr. René Hofmann, TU Wien

and
Dr. Felix Birkelbach, TU Wien

Reviewed by
Prof. Dr. Luisa F. Cabeza, Universitat de Lleida

and
Prof. Dr. André Thess, German Aerospace Center (DLR)

Author

Paul Schwarzmayr
Matr. Nr.: 01527078
paul.schwarzmayr@gmail.com
 0000-0003-4735-3447

Supervisor

Prof. Dr. René Hofmann
TU Wien
Institute of Energy Systems and
Thermodynamics
Getreidemarkt 9/E302
1060 Vienna

Co-supervisor

Dr. Felix Birkelbach
TU Wien
Institute of Energy Systems and
Thermodynamics
Getreidemarkt 9/E302
1060 Vienna

Reviewers

Prof. Dr. Luisa F. Cabeza
Universitat de Lleida
GREiA Research Group
Carrer de Pere de Cabrera
25001 Lleida

Prof. Dr. André Thess
German Aerospace Center (DLR)
Institute of Engineering Thermodynamics
Pfaffenwaldring 38-40
70569 Stuttgart

This work has been supported by the Austrian Research Promotion Agency (FFG) as part of the project *5DIndustrialTwin* (FFG project number 881140). I confirm that this dissertation needs the confirmation of the examination committee before going to press.

Affidavit

I declare in lieu of oath that I wrote this dissertation and carried out the associated research myself, using only the literature cited in this volume. If text passages from sources are used literally, they are marked as such. I confirm that this work is original and has not been submitted for examination elsewhere, nor is it currently under consideration for a dissertation elsewhere. I acknowledge that the submitted work will be checked using appropriate and state-of-the-art means (plagiarism detection software). On the one hand, this ensures that the high-quality standards of the rules of good scientific practice ("Code of Conduct") applicable at TU Wien are adhered to in the preparation of the submitted work. On the other hand, a comparison with other student theses avoids violations of my personal copyright.

Vienna, May 2024

Paul Schwarzmayr

Acknowledgments

Although the purpose of this dissertation is to prove my ability to conduct independent scientific research, the process that led to this final piece of writing involved many important people to whom I am very grateful.

Firstly, I would like to express my gratitude to my doctoral advisors, René Hofmann, Heimo Walter, and Felix Birkelbach, whose support during the past few years has been extraordinary. Thank you, René, for giving me the opportunity to work in your research group and for the effort you are putting into supporting my academic career. I really appreciate the numerous discussions and lessons we had during the last three years. Thank you, Heimo, for the many years of support, which started when I was an undergraduate student and continued throughout my graduate and doctoral studies. I always enjoy discussions with you, whether they are about technical topics or holiday plans. Felix, I think the luckiest decision I made during my PhD was on my first day at work when I chose my workplace right next to yours. Most of all, I enjoyed the countless discussions on the small table between our desks where we brainstormed about our research. Without the incredible amount of time and effort you put into guiding me through my doctoral studies, the scientific quality of my dissertation would be far from where it is right now.

Moreover, I would like to thank all of my amazing colleagues who have accompanied me during the last three years. Be it our peer meetings or small talks during coffee breaks, lunch, or after work. All these moments made my pre-doc years a time I will look back on with pleasure. Special thanks to Lukas, who contributed large parts to the research project I was working on and supported me by reviewing this dissertation. At this point, I would also like to take the opportunity to thank all my colleagues at the science center who helped me construct the test rigs I used for my research.

Finally, and probably most importantly, I am thankful to my family and my girlfriend, Stefanie. Thank you for encouraging and supporting me in all my decisions and always being enthusiastic about my research.

Abstract

The waste heat potential in the industry sector is enormous, and its exploitation can translate into significant emission savings. Packed bed thermal energy storage systems can improve the waste heat utilization rate in the iron and steel industry by decoupling the availability of excess heat and the demand for process heat. Besides the intermittent availability of waste heat, the composition of industrial exhaust gases (gas-powder two-phase flow) is one of the major challenges in this field of application. This dissertation aims to study the thermal efficiency and long-term operation of a packed bed thermal energy storage operated with high-temperature gas-powder two-phase flow. Experimental investigations considering the powder hold-up and pressure drop, as well as the thermal efficiency for these challenging operating conditions, are analyzed and discussed. During long-term partial cycle experiments, the maximum energy (90 %) and exergy (86 %) efficiencies are reached when the storage is charged from the top and discharged from the bottom. However, the results also indicate that powder particles accumulate inside the storage, and charging the storage from the bottom and discharging it from the top facilitates the removal of powder hold-up. Due to an accelerated thermocline degradation in this configuration, the partial cycle energy and exergy efficiencies are slightly lower but still greater than 85 % and 80 % respectively. This signifies the potential of packed bed thermal energy storage systems to store high-temperature heat from gas-powder two-phase flow, even if operating strategies that decrease thermal efficiency are applied.

Kurzfassung

Das Abwärmepotenzial in der Industrie ist enorm und dessen Nutzung kann zu erheblichen Emissionseinsparungen führen. Festbettwärmespeicher können durch Entkopplung der Abwärmeverfügbarkeit und des Prozesswärmebedarfs die Abwärmennutzung in der Eisen- und Stahlindustrie deutlich verbessern. Die hohe Staubbeladung von industriellem Abgas stellt jedoch eine große Herausforderungen dar. Diese Arbeit hat zum Ziel, den Wirkungsgrad und Dauerbetrieb eines Festbettwärmespeichers, der mit staubbeladenem Abgas betrieben wird, zu untersuchen. Dazu wurden Experimente zur Akkumulation von Staubpartikeln und zur Evaluierung des thermischen Wirkungsgrades durchgeführt und analysiert. Die höchsten Wirkungsgrade von 90 % (Energie) und 86 % (Exergie) werden erreicht, wenn der Speicher von oben beladen wird. Die Ergebnisse zeigen jedoch auch, dass sich Staub im Speicher absetzen kann und es für die Abreinigung dieses Staubes erforderlich ist, den Speicher von unten zu beladen. Aufgrund einer beschleunigten Degradation der Thermokline in dieser Konfiguration sind die Wirkungsgrade zwar etwas niedriger, aber immer noch höher als 85 % (Energie) bzw. 80 % (Exergie). Diese Ergebnisse verdeutlichen das Potenzial von Festbettwärmespeichern für den Betrieb mit staubbeladenem Abgas, auch wenn Betriebsstrategien erforderlich sind, die den thermischen Wirkungsgrad des Speichers negativ beeinflussen.

Contents

Research summary	1
1 Introduction	1
2 Context	4
2.1 Industrial waste heat recovery	4
2.2 Thermal energy storage	5
2.3 Packed bed thermal energy storage	8
2.4 Gas-powder two-phase flow in packed beds	12
3 Motivation	14
3.1 Research objective	17
4 Research approach	18
5 Conclusion and outlook	24
References	27
Publications	35
Publication 1	36
<i>Standby efficiency and thermocline degradation of a packed bed thermal energy storage: An experimental study</i>	
Publication 2	45
<i>Packed bed thermal energy storage for waste heat recovery in the iron and steel industry: A cold model study on powder hold-up and pressure drop</i>	
Publication 3	54
<i>Exergy efficiency and thermocline degradation of a packed bed thermal energy storage in partial cycle operation: An experimental study</i>	
Contributions to international conferences	66
Co-author publications	68

List of Figures

1	Process flow diagram of a conventional waste heat recovery system in the iron and steel industry.	4
2	Schematic setup of a vertical flow PBTES with illustrations of the direct-contact heat transfer during charging and discharging and the physical effects that cause thermocline degradation. Adapted from Esence et al. (2017).	8
3	Process flow diagram of the proposed waste heat recovery system with PBTES integration. Adapted from Kasper et al. (2024).	15
4	Optimization results of the unit commitment model for (a) the planned energy system without PBTES integration and (b) the proposed PBTES-enhanced energy system.	16
5	Process flow and instrumentation diagrams of the (a) small-scale cold model test rig and the (b) medium-scale high-temperature test rig. Adapted from Schwarzmayer et al. (2023a, 2024b).	19
6	Experimental results from Publication 2: (a) Pressure drop and void fraction; (b) Powder hold-up in the top layer; (c) Powder hold-up in the remaining layers. Adapted from Schwarzmayer et al. (2024b).	20
7	Results from Publication 1 and 3: Impact of the HTF flow direction on the efficiency of a PBTES in (a) standby and (b) partial cycle operation. Adapted from Schwarzmayer et al. (2023a, 2024a).	22

List of Tables

1	Test rig geometries, sensor equipment, and material properties of the cold model and high-temperature experimental setup. Adapted from Schwarzmayer et al. (2023a, 2024b).	18
---	--	----

Nomenclature

Acronyms

CSP	Concentrated solar power
EU	European Union
FWD	Forward
HTF	Heat transfer fluid
IEA	International Energy Agency
IPCC	Intergovernmental Panel on Climate Change
IRENA	International Renewable Energy Agency
PBTES	Packed bed thermal energy storage
PCM	Phase change material
REV	Reverse
SOC	State of charge
TES	Thermal energy storage

Roman Symbols

$\delta B_{\text{htf},k}$	Exergy transferred from/to HTF in J
$\delta B_{\text{sat},k}$	Saturation exergy losses in J
c	Specific heat capacity in $\text{J kg}^{-1} \text{K}^{-1}$
\mathcal{C}	Set of sample indices for charging
E	Energy in J
$\Delta h_{\text{s}/1}$	Latent heat of fusion in J kg^{-1}

ΔH_{R}	Reaction enthalpy in J kg^{-1}
m	Mass in kg
Δp_{i-j}	Pressure drop in kPa m^{-1}
$\delta Q_{\text{htf},k}$	Heat transferred from/to HTF in J
$\delta Q_{\text{sat},k}$	Saturation heat losses in J
\mathcal{R}	Set of sample indices for recovery/discharging
T	Temperature in K
T°	Reaction temperature in K
T_{init}	Initial temperature in K
T_{final}	Final temperature in K
T^*	Melting/solidification temperature in K
w_1	Mass fraction of liquid PCM phase in kg kg^{-1}
$W_{\text{p},k}$	Pumping work in J

Greek Symbols

η_{B}	Exergy efficiency
η_{E}	Energy efficiency
ξ_{p}	Extent of reaction in kg kg^{-1}

Subscripts

i, j	Indices of pressure measuring points
k	Index for sample number

Research summary

The present work provides a synopsis of the research articles constituting its scientific contribution as a dissertation. A concise research summary is provided in this introductory chapter to link the contents of the publications included in this dissertation.

Starting with an overview of current climate change and global warming events, the potential of waste heat recovery in the energy-intensive industry for reducing greenhouse gas emissions is outlined in Section 1. Fundamental information about state-of-the-art heat recovery systems and thermal energy storage systems – particularly packed bed thermal energy storage systems – is provided in Section 2. Section 3 delineates the motivation for the research conducted during this dissertation. After proposing packed bed thermal energy storage systems for waste heat recovery in the iron and steel industry, the research objective of this dissertation is outlined. In Section 4, the research approach to evaluate the efficiency of a packed bed thermal energy storage for using industrial waste heat is presented. This section also acts as a summary that associates the contents of each publication with the overall context of this dissertation. The first chapter is completed in Section 5 with a recapitulation of the main results of this dissertation as well as an outlook that emphasizes the importance of further research and developments concerning this topic.

The second chapter provides a collection of all the publications of this dissertation, including journal articles and contributions to scientific conferences. For core journal publications and additional conference papers, the full-length articles are reprinted along with a summary highlighting their scientific contribution to the entire work.

1 Introduction

Humanity is facing a time in which the number of temperature records broken is record-breaking (First Dog on the Moon 2023). According to the Copernicus Climate Change Service, part of the European Commission's flagship Earth observation program, July 2023 was by far the hottest month on record globally (C3S 2023). As of the 2nd of July 2023, the hottest day was recorded in August 2016 with a global average surface temperature of 16.8 °C. By the end of July 2023 (29 days later), this record was broken 29 times (new record: 17.08 °C). The consequences that arise from nearly 1.5 °C of global warming (with respect to pre-industrial levels) make their presence felt in the increased frequency and intensity of extreme weather events (IPCC 2018). In their sixth assessment report, where they assessed observed changes in weather extremes and their correlation with human-induced climate change, the Intergovernmental Panel on Climate Change (IPCC) found that climate change has already increased the magnitude and frequency of

RESEARCH SUMMARY

extreme hot events and decreased the magnitude and frequency of extreme cold events (IPCC 2021a). With global climate moving further away from its previous states, future weather events like temperature extremes, heavy precipitation, floods, droughts, extreme storms, and wildfires will be unprecedented in magnitude, frequency, location, and/or timing (IPCC 2021a). To prevent these predictions from eventuating, the driving force behind human-induced climate change – the accumulation of greenhouse gases in the earth’s atmosphere – must be stopped.

Greenhouse gases are naturally occurring gases (including carbon dioxide, water vapor, and methane) that are part of the Earth’s atmosphere and can absorb and release energy in the form of long-wave radiation (infrared light). As solar radiation is dominated by short-wave radiation (mostly visible light), it is transmitted by the atmosphere, absorbed by the earth’s surface, and radiated back in the form of long-wave radiation. Without an atmosphere that is opaque to long-wave radiation, the surface temperature on earth would be about -18°C (NASA 2023c). Providentially, the earth’s atmosphere used to contain the right amount of greenhouse gases to absorb enough energy to increase the surface temperature to congenial 15°C on average (NASA 2023c). In the past few decades, however, human activities have interfered with this fragile balance at a terrific pace. While the atmosphere’s CO_2 concentration never exceeded 300 ppm for millennia, human-caused greenhouse gas emissions during the late 20th century raised CO_2 levels beyond 400 ppm for the first time in recorded history (NASA 2023a). Multiple studies of renowned institutions (IPCC 2021b; NASA 2023b) state that the influence of human activities on the concentration of greenhouse gases in the earth’s atmosphere, and hence on global warming, is unequivocal.

Besides deforestation and farming, burning fossil fuels for energy provision is by far the greatest cause of human-induced greenhouse gas emissions (European Commission 2023). Global energy-related CO_2 emissions reached a new maximum of 36.9 Gt in 2022 (IEA 2023a). When allocating emissions from electricity generation to the major end-use sectors, 42 % (15.5 Gt) of the global energy-related CO_2 emissions are caused by the industry sector. These total emissions consist of direct emissions (25 %) from industrial processes and indirect emissions (17 %) due to electricity consumption (IEA 2023b). Direct emissions in the industry sector are mostly caused by industrial processes that generate CO_2 as a by-product (reduction of iron ore, calcination of limestone, ...) and by burning fossil fuels to generate high-temperature heat.

According to the IPCC’s special report on global warming of 1.5°C (IPCC 2018), energy efficiency is one of the key ways to reduce global greenhouse gas emissions. The International Energy Agency’s (IEA) former executive director Maria van der Hoeven even stated that energy efficiency is the world’s first fuel in clean energy transition (IEA 2013). Investing in energy efficiency has multiple benefits for various stakeholders (IEA 2019). Since energy efficiency reduces the total energy demand, it also reduces the reliance on imports of fossil fuels. Thereby, energy efficiency contributes to both long- and short-term energy security. Energy efficiency improvements can also positively impact energy affordability if implemented on a large enough scale across several markets. Additionally, energy efficiency provides various environmental benefits by reducing the

RESEARCH SUMMARY

overall energy demand. The most popular of these benefits is the reduction of greenhouse gas emissions as a contribution to climate change mitigation. Without the improvements in energy efficiency in the past two decades, today's energy-related CO₂ emissions would be 12 % higher (IEA 2019). For more details on the versatile benefits of energy efficiency, the author refers to a report of the IEA (2019). Although energy efficiency plays a crucial role in the decarbonization of all major greenhouse gas emitting sectors, including industry, transportation, buildings, and power generation, the present dissertation focuses on the implementation of energy efficiency in the iron and steel industry, for it is the sector with the highest potential for emission savings.

Since iron- and steel-making processes often involve chemical reactions and require high-temperature heat, this industry sector is probably the most challenging to decarbonize. According to the IEA's pathway to net-zero emissions in 2050, the iron and steel industry will be one of the last sectors to still use significant amounts of fossil fuels (IEA 2022). Therefore, improving energy efficiency is particularly important to get the iron and steel industry on track to accomplish global net-zero emissions by 2050. In industrial processes, energy efficiency aims to minimize the amount of energy needed to produce a certain amount of goods. Considering that more than one-quarter of the industry sector's final energy consumption in the European Union (EU) is discharged as hot exhaust gases (i.e., waste heat) (Bianchi et al. 2019), the potential for energy and emission savings is enormous. Although estimated values for the available waste heat potential reported in the literature (Bianchi et al. 2019; Forman et al. 2016; Panayiotou et al. 2017; Papapetrou et al. 2018) vary widely, the conclusion is always the same: The waste heat potential across all sectors is tremendous and, if utilized, it can significantly contribute to the reduction of primary energy consumption and greenhouse gas emissions. Concerning the industry sector, the reasons for this massive amount of untapped waste heat potential are, among others, the fluctuating availability of excess heat and the challenging operating conditions. These challenges can be met by utilizing a robust type of thermal energy storage to increase the flexibility and resilience of industrial waste heat recovery systems. Therefore, the present dissertation investigates the potential, suitability, and performance of a packed bed thermal energy storage to increase the utilization rate of waste heat recovery systems in the iron and steel industry.

2 Context

The major barriers to utilizing the enormous waste heat potential in the iron and steel industry are of economic and technological nature. Besides the challenging operating conditions that push conventional waste heat recovery systems to their limits, the main issue of industrial waste heat recovery is the temporal mismatch between excess heat availability and process heat demand. Packed bed thermal energy storage (PBTES) systems, a sensible type of thermal energy storage (TES), are resistant to aggressive industrial exhaust gases and capable of storing high-temperature heat with comprehensive efficiencies. Therefore, they can provide enough flexibility to increase the waste heat utilization rate in the iron and steel industry in an economically efficient way.

2.1 Industrial waste heat recovery

Two types of waste heat sources must be differentiated when considering waste heat recovery in the industry sector. The first and easy-to-handle type of waste heat sources are continuous processes, where the heat of hot exhaust streams can be reused directly to preheat cold input streams. The second type of waste heat sources, discontinuous (batch) processes, is much more challenging. The fluctuating availability of waste heat from discontinuous processes results in a temporal mismatch between excess heat availability and process heat demand, which increases the complexity of waste heat recovery. To that end, TES systems can make a valuable contribution by decoupling the waste heat source from the process heat conversion system. In conventional waste heat recovery systems (Sprecher et al. 2019), hot exhaust gas is used to produce super-heated steam via radiation heat exchangers, which is then stored in a steam storage system. Therefore, the waste heat recovery system consists of an exhaust gas system and a high/medium pressure steam system (Keplinger et al. 2018). As depicted in the process flow diagram of a conventional waste heat recovery system in Figure 1, several factors limit the waste heat utilization rate to less than 45 % (Ja'fari et al. 2023) of the theoretically available waste heat. Since industrial exhaust gases are usually contaminated with high amounts of dust/powder,

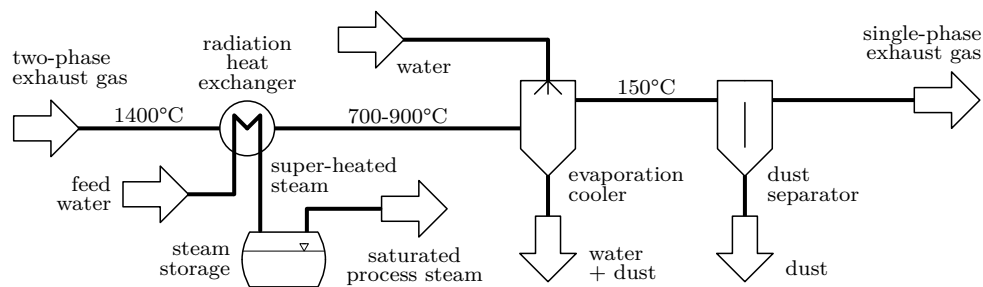


Figure 1: *Process flow diagram of a conventional waste heat recovery system in the iron and steel industry.*

the only type of heat exchangers that are reasonably applicable in this case are radiation heat exchangers. However, due to the physical nature of radiative heat transfer, only heat at temperatures above 700 °C to 900 °C can be recovered in this configuration. The remaining heat is dissipated into the environment by injecting water into the hot exhaust gas stream. This is done to separate coarse dust/powder fractions and to reduce the temperature of the exhaust gas so that it lies within the operating range (≤ 150 °C) of downstream exhaust gas treatment systems. The disadvantages that go hand in hand with gas-powder two-phase exhaust gas could be prevented by using a dust separator that removes the dust/powder from the exhaust gas flow before it enters the heat recovery system. However, this approach is inefficient and ineffective because high-temperature dust separators are very cost-intensive, and sufficient separation efficiency can only be achieved at high gas velocities. This would cause high energy and exergy losses due to the increased pumping work that would be required. Even if this approach would be economically sensible, the thermal inertia of industrial-scale waste heat recovery systems would still limit the maximum waste heat utilization rate to less than 45 % (Ja'fari et al. 2023). Technical constraints like minimum partial loads or maximum ramping speeds prevent steam generators from keeping up with the highly fluctuating availability of industrial waste heat.

A convenient solution to overcome these issues is to add flexibility not only to the steam system but also to the exhaust gas system, more precisely between the waste heat source and the energy conversion equipment. For this purpose, a particular TES system must store high-temperature heat and be robust against highly fluctuating waste heat streams and gas-powder two-phase exhaust gases. The following paragraphs provide an overview of different types of TES and their advantages/disadvantages. A particular focus is put on PBTES systems, their most important performance indicators, and their distinguished suitability for waste heat recovery in the iron and steel industry.

2.2 Thermal energy storage

TES systems are a type of energy storage that store heat (thermal energy), which can be released at a later time. Therefore, the leading utility of TES systems is to overcome the temporal mismatch between the supply and the demand of thermal energy. As the development of TES systems is at an early stage, not many large-scale industrial TES systems are in operation. The International Renewable Energy Agency (IRENA) estimated the globally installed TES capacity at the end of 2019 to be 234 GWh (IRENA 2020). Potential application areas of TES systems in the near future are concentrated solar power (CSP) plants, other conventional power plants (fossil and renewable), and industrial waste heat recovery. In modern CSP plants, TES systems could be integrated to shift electricity generation from diurnal to nocturnal hours and to increase the flexibility of the plant's power output. Similarly, using TES systems, conventional baseload power plants (biomass, nuclear, ...) could profit from increased power output flexibility. Steam generators could operate at full capacity (maximum efficiency) while the electricity generation – decoupled by the TES – follows the demand. As mentioned before, the amount of industrial waste heat is enormous and primarily unused due to the temporal

RESEARCH SUMMARY

mismatch between heat supply and heat demand. TES systems can utilize this waste heat potential by closing the gap between excess heat availability and process heat demand. The three most essential parts of a TES system is/are typically the storage tank(s), which hold(s) the storage material, the storage material, and the heat transfer fluid (HTF). For a TES technology to be competitive, these parts need to meet specific requirements:

- Low capital and operational costs of the storage tank and the auxiliary equipment.
- Low investment costs of the storage material.
- Thermal, chemical, and mechanical stability of the storage material for many charging/discharging cycles.
- High volumetric and gravimetric energy density of the storage material.
- Suitable thermal conductivity of the storage material (some technologies require a low, others a high thermal conductivity).
- High heat transfer coefficients between the storage material and the heat transfer fluid (leads to high power rates of the whole system).

This list does not include specific requirements for the HTF because the type and composition of the HTF are primarily determined by the excess heat source. In most cases, the HTF used to charge/discharge a TES is either a liquid medium (thermal oil, molten salt, water, ...) or some type of exhaust gas from power plants or industrial processes. According to the physical mechanisms exploited to store thermal energy, TES systems can be categorized into sensible heat TES, latent heat TES, and thermo-chemical energy storage.

TES systems that store thermal energy by increasing the temperature of the storage material are called sensible heat TES. Theoretically, the storage material in a sensible heat TES can be any type of solid, liquid, or gaseous substance. However, most sensible heat TES use a solid or liquid medium as storage material. This is due to the high volumetric energy density of condensed materials. In addition, the thermal expansion of gases is usually much higher than that of liquids or solids, which would make storage tanks more expensive and complex. The amount of thermal energy that is stored in a sensible heat TES can be calculated as

$$E = m \int_{T_{\text{init}}}^{T_{\text{final}}} c(T) dT \quad (1)$$

where m is the total mass of the storage material, $c(T)$ is the specific heat capacity of the storage material, T_{init} is the initial temperature and T_{final} is the final temperature of the storage material.

TES systems that utilize heat consumed/released during the phase transition of a phase change material (PCM) are called latent heat TES. In theory, any phase transition

RESEARCH SUMMARY

process, including melting/solidification, evaporation/condensation, etc., can store latent heat. In practice, however, latent heat TES applications are limited to solid/liquid phase transitions. This is because of the comparatively high phase change enthalpy and low volumetric change of the solid/liquid phase transition (Zhang et al. 2018). Neglecting the sensible heat of the solid and the liquid phase, the amount of thermal energy that is stored in a latent heat TES can be calculated as

$$E = m w_l \Delta h_{s/l}(T^*) \quad (2)$$

where m is the total mass of the storage material (PCM), w_l is the mass fraction of the liquid PCM phase, and $\Delta h_{s/l}(T^*)$ is the PCM's latent heat of fusion at its melting temperature T^* . The primary benefit of latent heat TES is their relatively high volumetric and gravimetric energy storage density. This is due to the comparatively high amount of energy converted during a phase transition. Furthermore, latent heat TES can reach high exergy efficiencies due to the narrow range of temperature at which thermal energy is stored. On the other hand, however, latent heat TES are marked by low power rates and high PCM costs. Since the PCM in a discharged latent heat TES is solid, thermal conduction is the only heat transfer mechanism in this state. This has a negative impact on the heat transfer coefficient between the HTF and the PCM, which consequently limits the maximum power rates that latent heat TES can reach. Although there are multiple approaches to solve these issues (encapsulation (Palacios et al. 2023), snowflake-shaped heat exchanger tubes (Scharinger-Urschitz et al. 2020), ...), state-of-the-art latent heat TES systems still cannot compete with the simplicity and cost-effectiveness of sensible heat TES systems.

TES systems for which the charging/discharging process involves a reversible chemical reaction of the storage material are called thermo-chemical energy storage. The amount of thermal energy stored in a thermo-chemical energy storage can be calculated as

$$E = m \xi_p \Delta H_R (T^\circ) \quad (3)$$

where m is the total mass of the storage material inside the storage tank, ξ_p is the extent of reaction, which is the ratio of the amount of reaction products to the total amount of educts and products in the storage system, and $\Delta H_R (T^\circ)$ is the enthalpy of reaction at the reaction temperature T° . In contrast to sensible and latent heat TES systems, thermo-chemical energy storage systems are still in an early stage of development. Significant issues that remain difficult to manage are reaction kinetics (Birkelbach 2020), long-term stability of reactants (Chen et al. 2018), reversibility of reactions and reactor design (Sunku Prasad et al. 2019).

Based on the requirements of TES systems listed in this section, a specific type of sensible heat TES – a PBTES – is found to be the most suitable technology to be implemented for waste heat recovery in the iron and steel industry. This choice is justified by the variety of beneficial properties of PBTES systems from both an economic and a technological point of view. The following paragraphs provide detailed information about PBTES systems and their advantages, highlighting their suitability for waste heat recovery in the iron and steel industry.

2.3 Packed bed thermal energy storage

A PBTES is a particular type of TES that utilizes rocks or any other kind of solids (slag, gravel, glass spheres, porcelain spheres, ceramic spheres, alumina spheres, ...) as storage material and a fluid (gaseous or liquid (Bai et al. 2022)) medium as HTF (Gautam et al. 2020a,b). A PBTES consists of a single non-pressurized storage tank filled with the selected storage material. Typically, the grain size of the storage material particles is in the order of 0.01 m to 0.1 m (Esence et al. 2017). In order to transfer heat to and from the TES, the HTF is in direct contact with the storage material by passing through the gaps between the packed bed particles. Depending on the flow direction of the HTF that passes through the packed bed, PBTES systems can be categorized into horizontal flow systems (Slimani et al. 2023; Soprani et al. 2019) and vertical flow systems (Knobloch et al. 2022; Yang et al. 2019). Figure 2 is a schematic sketch of a vertical flow PBTES, which additionally depicts the most important physical effects that underlie the general functionality and the major benefits of PBTES systems.

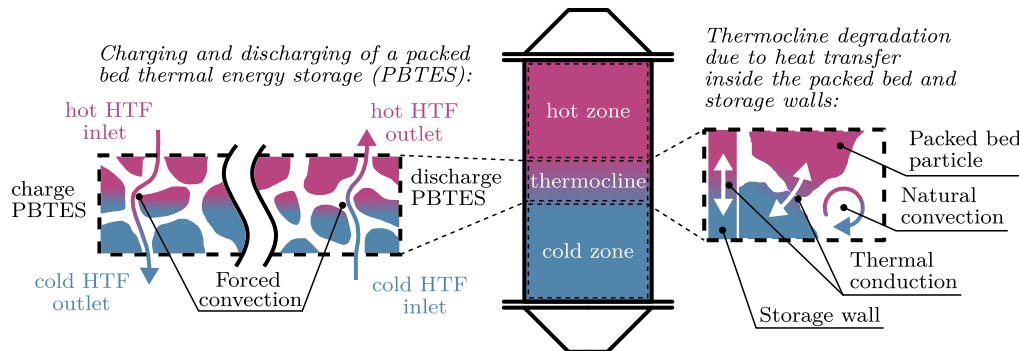


Figure 2: Schematic setup of a vertical flow PBTES with illustrations of the direct-contact heat transfer during charging and discharging and the physical effects that cause thermocline degradation. Adapted from Esence et al. (2017).

In a partially charged vertical flow PBTES, the packed bed is divided into a hot and a cold zone located on top of each other. To charge the storage, hot HTF enters the packed bed in the hot zone and delivers heat to the storage material by passing through the packed bed. The cooled HTF leaves the packed bed at the cold zone. To discharge the storage, this process is reversed by switching the flow direction of the HTF. In discharging mode, cold HTF enters the packed bed at the cold zone, extracts heat by passing through the packed bed, and hot HTF leaves the packed bed at the hot zone (Yang et al. 2019). Due to the direct-contact heat transfer between the HTF and the storage material, PBTES systems do not require heat exchanger tubes in which the HTF would flow. This does not only enhance the heat transfer between the storage material and the HTF (Kalantari et al. 2022), but it also reduces investment and maintenance costs (Cui et al. 2020; Wang et al. 2015). Besides economic advantages, one of TES systems' most critical performance indicators is energy efficiency.

Energy efficiency Generally, energy efficiency is defined as the ratio of useful energy output to total energy input. In contrast to continuous processes, the exact definition of energy efficiency for discontinuous processes is slightly more intricate and application-specific. In the context of TES systems, energy efficiency is defined for a whole charging-standby-discharging cycle as the ratio of energy that can be recovered during discharging to the energy expended during charging. Mathematically, this can be written as

$$\eta_E = \frac{\sum_{k \in \mathcal{R}} \delta Q_{\text{htf},k}}{\underbrace{\sum_{k \in \mathcal{C}} \delta Q_{\text{htf},k}}_{\text{Heat delivered during charging}} + \underbrace{\sum_{k \in \mathcal{C}} \delta Q_{\text{sat},k}}_{\text{Saturation losses during charging}} + \underbrace{\sum_{k \in (\mathcal{C} \cup \mathcal{R})} \delta W_{p,k}}_{\text{Pumping work}}} \quad (4)$$

where $k \in \mathcal{C}$ represents the set of samples (time steps) k during charging, $k \in \mathcal{R}$ represents the set of samples (time steps) k during discharging and $k \in (\mathcal{C} \cup \mathcal{R})$ represents the set of samples (time steps) k during both charging and discharging. The numerator of Equation (4) is the amount of thermal energy that is recovered during discharging ($k \in \mathcal{R}$) and the denominator is the amount of energy that is expended during charging ($k \in \mathcal{C}$) and discharging ($k \in (\mathcal{C} \cup \mathcal{R})$). The energy expended during charging is the sum of the thermal energy delivered to the TES via the HTF, the saturation losses during charging, and the amount of work needed to overcome the pressure drop of the packed bed during charging and discharging. Saturation losses are heat losses due to rising exhaust gas temperatures during the charging process of a PBTES. In a well-designed PBTES, these losses are minimal for the whole operating range and only occur when the TES reaches a fully charged state. Considering Equation (4), there are multiple strategies/options to optimize the energy efficiency of TES systems.

- **Maximize the amount of heat that is recovered during discharging and minimize the amount of energy that has to be supplied during charging:** This can be achieved by optimizing the geometry and the thermal insulation of the storage tank to minimize heat losses to the surrounding during charging, standby, and discharging phases.
- **Minimize the saturation losses during charging:** Saturation losses can be reduced by establishing a rapid temperature transition between the storage's hot and cold zones and by operating the storage in short partial cycles. Both strategies prevent the temperature of the exhaust HTF from being higher than the surrounding temperature during charging. This is probably the most important aspect when it comes to optimizing the energy efficiency of a PBTES.
- **Minimize the work that is needed to pump the HTF through the packed bed:** This can only be done by reducing the superficial flow velocity of the HTF inside the packed bed, which has a negative impact on the heat transfer between the HTF and the storage material and hence on the maximum power rate that

the storage can reach. In terms of energy efficiency, this aspect plays a minor role because the work expended to overcome the pressure drop caused by the packed bed dissipates inside the packed bed in the form of heat, increasing the amount of heat that can be recovered during discharging.

Thermal stratification and thermocline degradation In a well-designed PBTES, an effect called thermal stratification (Oró et al. 2013) is exploited to maximize its efficiency. Thermal stratification means that the hot and the cold zones in a partially charged storage are separated by a thin volume slice in which the whole temperature gradient is concentrated. The resulting shape of the temperature profile inside the storage is also called thermocline. Although the thermocline in a well-designed PBTES is relatively thin and stable, effects like thermal conduction in the storage tank's walls, thermal conduction, and convection inside and in-between the storage material lead to an effect called thermocline degradation (Figure 2). This effect describes the expansion of the thermocline during the operation of a stratified TES, and it is one of the most critical aspects when designing an efficient PBTES system (Bruch et al. 2014, 2017). Ideally, the thermocline inside a stratified TES is as thin as possible (Stekli et al. 2013) since there will be considerably less saturation losses during the charging process of the PBTES. This benefits the energy and the exergy efficiency of a PBTES (Knobloch et al. 2022; Soprani et al. 2019).

Exergy efficiency Exergy also considers the temperature level at which a certain amount of heat is available, and it is often used as a key performance indicator for high-temperature TES systems. Analogously to the energy efficiency, the exergy efficiency of a PBTES can be defined as

$$\eta_B = \frac{\sum_{k \in \mathcal{R}} \delta B_{\text{htf},k}}{\underbrace{\sum_{k \in \mathcal{C}} \delta B_{\text{htf},k}}_{\text{Exergy delivered during charging}} + \underbrace{\sum_{k \in \mathcal{C}} \delta B_{\text{sat},k}}_{\text{Exergy losses during charging}} + \underbrace{\sum_{k \in (\mathcal{C} \cup \mathcal{R})} \delta W_{\text{p},k}}_{\text{Exergy spent in form of work}}}. \quad (5)$$

where the numerator is the amount of exergy that is recovered during discharging ($k \in \mathcal{R}$) and the denominator is the amount of exergy that is expended during charging ($k \in \mathcal{C}$) and discharging ($k \in (\mathcal{C} \cup \mathcal{R})$). Similar to Equation (4), the denominator is the sum of the exergy that is delivered to the storage in the form of heat during charging, the amount of exergy that is lost due to saturation losses during charging, and the amount of exergy that is spent in the form of pumping work during charging and discharging. As with Equation (4), there are multiple strategies/options to optimize the exergy efficiency of a PBTES in Equation (5). In this case, however, the importance of each strategy is different.

- **Maximize the amount of exergy that is recovered during discharging and minimize the amount of exergy that has to be supplied during charging:**

As with the energy efficiency, this can be achieved by optimizing the geometry and the thermal insulation of the storage tank. Additionally, the amount of the exergy recovered during discharging can be maximized by maintaining a thin thermocline and, therefore, a high discharging temperature throughout the whole process (Okello et al. 2014). Furthermore, reducing the minimum temperature difference between the storage material and the HTF during charging and discharging is advantageous for the storage's exergy efficiency. This can be achieved by increasing the superficial velocity of the HTF and, hence, the turbulence inside the storage, which contradicts the third bullet point.

- **Minimize the saturation losses during charging:** The strategy to reduce saturation losses remains the same. However, regarding exergy efficiency, the effect of saturation losses is small. This is because saturation losses are mostly low-temperature heat with low exergy content. Therefore, the reduction of saturation losses does not have a significant impact on the exergy efficiency.
- **Minimize the work needed to pump the HTF through the packed bed:** This can only be achieved by reducing the superficial flow velocity of the HTF inside the packed bed. In this case, however, this aspect plays a much more significant role. As the work dissipating into heat entails a lot of exergy losses, the reduction of pumping work can significantly increase the exergy efficiency of a PBTES.

Because of the beneficial properties of PBTES systems for both short- and medium-term thermal energy storage, many research articles that focus on PBTES systems have been published in recent years. Especially considering their utilization in CSP plants, a variety of comprehensive studies are available (Geissbühler et al. 2019a,b). Depending on the case of the application, there are two basic operating modes of PBTES systems: the static mode and the dynamic mode.

The static mode refers to the operation of a PBTES, which is on standby for a considerable amount of time between charging and discharging. Since PBTES are typically used in the dynamic operating mode, only a few studies investigated the static operation of PBTES systems. Numerical analyses were carried out by Mertens et al. (2014) and Rodrigues et al. (2021). Both conclude, that exergy losses during long standby periods are caused by heat losses to the surrounding and by thermocline degradation. Similar results were found by Okello et al. (2014) and Yang et al. (2019), who experimentally investigated the standby process of air-based solid PBTES for high-temperature applications.

The dynamic operating mode refers to the cyclic operation of a PBTES, which is constantly charged and discharged without intermediate standby periods. Esence et al. (2017) published a review on PBTES systems in which they also summarized the most important articles that investigate the dynamic operating mode, especially the partial cycle operation, of PBTES systems. Zanganeh et al. (2012) studied an industrial scale PBTES and found that the long-term efficiency of a PBTES in partial cycle operation is determined by its stabilized state, which can be controlled by operating parameters. Similar experiments were conducted by Al-Azawii et al. (2023), Bruch et al. (2014, 2017)

and Cascetta et al. (2015) who found that, particularly for short cycles, the effect of thermocline degradation reduces the effective storage capacity of the TES. Marti et al. (2018) and Trevisan et al. (2021) conducted studies in which they used multi-objective optimization techniques to find optimal storage parameters (tank diameter/height ratio, storage material particle size, HTF mass flow rate, ...) intending to minimize investment costs and to maximize the exergy efficiency. These studies highlight the high thermal performance of well-designed and well-operated PBTES systems and promote their utilization as short-term TES systems. Based on the information provided in this section (Section 2.3), the main advantages of PBTES systems, especially for industrial waste heat recovery, are of both economic and technological nature.

Low investment costs Since PBTES systems can use slag, a by-product from the iron and steel industry, as storage material and are made of a single non-pressurized storage tank, the investment costs for building a PBTES are very low compared to other types of TES. Due to the direct contact heat transfer, no heat exchanger tubes are inside the storage, reducing initial material costs.

Low maintenance costs The fact that there are no heat exchanger tubes also reduces maintenance costs that would have to be expended for the repair/replacement of damaged heat transfer equipment. This is especially crucial in an environment where the HTF is contaminated with high amounts of aggressive powder.

Excellent heat transfer between the HTF and the storage material The direct-contact heat transfer between the HTF and the storage material leads to an enhanced heat transfer between these two mediums. This effect has a positive impact on the maximum power rate and the exergy efficiency of the storage.

Thermal stratification As PBTES systems benefit from thermal stratification, the maximum energy and exergy efficiency that a TES of this type can reach is comparatively high.

Low effective thermal conductivity of the packed bed The low effective thermal conductivity of packed beds benefits the long-term exergy efficiency and thermocline degradation of PBTES systems. This is because of the small, point-like contact areas between the packed bed particles.

Suitable for storing high-temperature heat Depending on the selected storage material and the tank material, PBTES systems can be used to store high-temperature heat at up to 1000 °C.

Robust against aggressive HTF Another beneficial aspect of the direct-contact heat transfer is that PBTES systems are potentially robust against HTF contaminated with high amounts of aggressive powder. This is because they do not contain heat transfer equipment that is sensible to these challenging operating conditions.

2.4 Gas-powder two-phase flow in packed beds

A major challenge affecting industrial waste heat recovery systems is the high amount of powder transported with industrial exhaust gases (Section 2.1). The so-called gas-powder two-phase flow is not only very abrasive but also adhesive. Hence, it tends to damage

RESEARCH SUMMARY

and deposit on heat exchanging equipment, which is both uncondusive for its durability and long-term efficiency. Although packed beds are robust against abrasion, gas-powder two-phase flow that passes through a packed bed can lead to an increasing powder hold-up and pressure drop during the operation. Problems that may arise when operating a PBTES with gas-powder two-phase flow are:

- **Increased pressure drop during long-term operation:** An elevated pressure drop due to powder hold-up in the packed bed can lead to an increased pressure drop and, hence, a reduction of the system's exergy efficiency or even a clogging of the storage tank.
- **Nonuniform powder accumulation inside the packed bed:** Uneven powder hold-up inside the packed bed can reduce the maximum energy storage capacity of the TES due to random flow channel formation of the HTF passing through the packed bed.

Despite a wide variety of publications that investigated the powder hold-up and pressure drop inside packed beds in the context of pulverized coal injection into blast furnaces (Ding et al. 2005; Dong et al. 2004a,b; Gupta et al. 2022; Kiochiro et al. 1991; Takahashi et al. 2011; Zhou et al. 2021), there is no study available that considers the same topics in the context of PBTES systems. Conditions and physical effects in a blast furnace are fundamentally different from those in a PBTES. Therefore, the results found in the context of pulverized coal injection into blast furnaces are limited in their transferability.

3 Motivation

According to the most recent study concerning industrial waste heat (Bianchi et al. 2019), the theoretical waste heat potential in the EU's industry in 2014 was 918 TWh. If this amount of energy was re-used to compensate heat that would otherwise be generated by burning natural gas, 170 t of CO₂ emissions would be avoided each year. However, due to the intermittent availability of industrial waste heat, the utilization rate in state-of-the-art industrial waste heat recovery systems is below 45 % (Ja'fari et al. 2023). Therefore, this dissertation aims to improve the utilization rate of industrial waste heat recovery systems by providing additional flexibility via TES integration.

The problem with conventional waste heat recovery systems (Keplinger et al. 2018) is that the entire flexibility is concentrated in the steam system. While this decouples the steam generation from the fluctuating steam and heat demand, it does not decouple the waste heat source from the steam generation equipment. A solution to this issue is to add flexibility to the exhaust part of the waste heat recovery system as well. Because of their ability to store high-temperature heat at high power rates and efficiencies, PBTES systems are particularly useful in providing flexibility at comparatively low costs. In their paper on selecting TES options for industrial waste heat recovery, Manente et al. (2022) concluded that integrating a PBTES into an industrial energy system improves the waste heat utilization rate. Likewise, Miró et al. (2016) stated that TES systems have great potential to overcome the intermittency of industrial excess heat availability. In their studies on using TES systems for industrial waste heat recovery, Ortega-Fernández et al. (2019) and Slimani et al. (2023) numerically investigated the economic benefits and efficiencies of their approaches. Ortega-Fernández et al. (2019) considered two parallel vertical flow PBTES to increase the waste heat utilization rate from an electric arc furnace, whereas Slimani et al. (2023) investigated a horizontal flow PBTES for the same use case. In both studies, the challenges that arise from using high-temperature gas-powder two-phase exhaust gas as HTF were identified and addressed by placing a gas-to-gas heat exchanger between the electric arc furnace and the PBTES. However, this approach not only increases investment costs, maintenance costs, and the complexity of the entire system but also negatively impacts the thermal efficiency of the waste heat recovery system.

Therefore, a novel approach is proposed for direct waste heat utilization in the iron and steel industry. Specifically, this dissertation considers the direct use of industrial exhaust gases as HTF in a PBTES filled with steel slag as storage material. Since most steel-making processes produce slag as a by-product, this is a convenient and cost-effective material to use as storage material in a PBTES. Using steel slag as storage material is further justified by its beneficial heat transfer properties. The partly porous and irregular shape of the slag particles leads to an increased internal surface of the packed bed and an improved heat transfer coefficient between the HTF and the storage material. Both effects contribute to an enhanced heat transfer between storage material and the HTF. Furthermore, the irregular shape of the slag particles facilitates a random uniform packing of the packed bed particles. This prevents the formation of random flow channels

of the HTF flowing through the packed bed.

To estimate the potential of the proposed PBTES integration, a planned waste heat recovery system of an electric arc furnace at *voestalpine Stahl Donawitz GmbH*¹ is selected as use case. A process flow diagram of the main parts of this energy system, including the proposed PBTES integration, is depicted in Figure 3. Instead of just recovering a fraction of the waste heat in a steam generator, this proposed PBTES-enhanced system is designed to recover most of the available waste heat. This is facilitated by integrating a PBTES in parallel to the steam generator. During phases of waste heat oversupply, the amount of heat that exceeds the capacity (max. design capacity or max. ramping speed) of the steam generator is stored in the PBTES. In phases in which the heat from the waste heat source is below the capacity (min. design capacity or max. ramping speed) of the steam generator, this gap is substituted with heat recovered from the PBTES.

A unit commitment model of the proposed energy system is used to quantify the improvement in the waste heat utilization rate that this PBTES integration enables. This mixed integer linear programming model was developed by Kasper et al. (2024) and solves a unit commitment problem to maximize the achievable revenue from electricity and district heating sales. The problem was solved for the planned reference energy system without PBTES integration and for the proposed PBTES-enhanced energy system. For the planned reference energy system, the results revealed an average utilization rate of 45% (Figure 4a), which is in line with values from the literature (Ja'fari et al. 2023). In this case, the decisive constraints of the unit commitment problem are the maximum ramping speed and the minimum power rate of the steam generator. Since the availability of waste heat is highly volatile, the steam generator is frequently forced to shut down. It cannot follow the high gradients of the waste heat source because of the minimum power rate and maximum ramping speed constraints. The optimization results considering the proposed PBTES-enhanced energy system reveal an average waste heat utilization rate

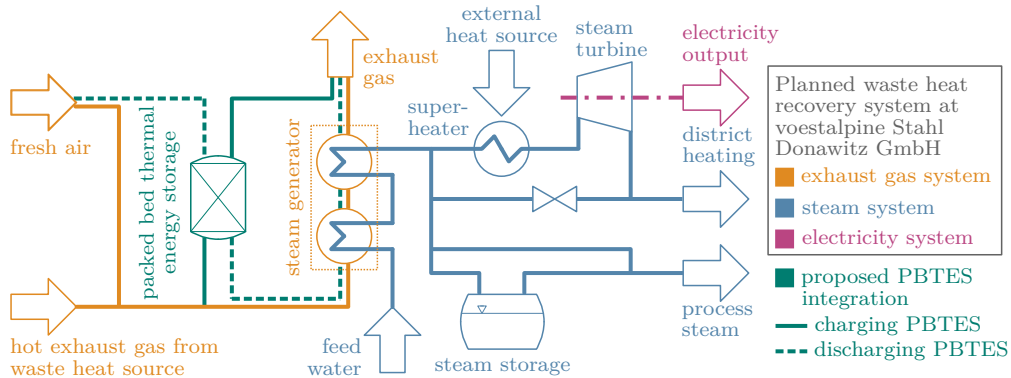


Figure 3: *Process flow diagram of the proposed waste heat recovery system with PBTES integration. Adapted from Kasper et al. (2024).*

¹*voestalpine Stahl Donawitz GmbH* is an Austrian company specialized on the production of high-quality steel with a clear ambition to carbon-neutral steel production in 2050.

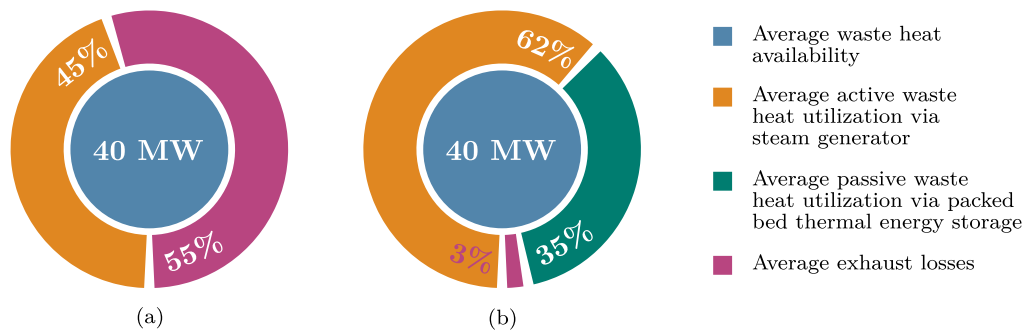


Figure 4: Optimization results of the unit commitment model for (a) the planned energy system without PBTES integration and (b) the proposed PBTES-enhanced energy system.

of 97% (Figure 4b). This increase of the waste heat utilization rate can be attributed to the flexibility added to the exhaust gas system by integrating a PBTES.

The results in Figure 4 show that the PBTES integration not only increases the overall waste heat utilization rate but also enhances the amount of waste heat that can be actively recovered by the steam generator (orange segments in Figure 4) without intermittent storage in the PBTES. This is due to the flexibility that the PBTES has added which mitigates the impact of the maximum ramping speed and the minimum power rate constraints on the operating behavior of the steam generator. By absorbing heat in periods of high waste heat availability and releasing heat in periods of low waste heat availability, the PBTES can close gaps and flatten the course of the available excess heat. This prevents frequent shutdowns of the steam generator and allows the steam generator to follow the gradients of the upstream system (waste heat source + PBTES). Therefore, integrating a PBTES increases the waste heat utilization and reduces the thermo-mechanical load on downstream energy conversion equipment. Furthermore, a PBTES charged with high-temperature gas-powder two-phase flow may also act as a separator for powder particles before they reach and potentially damage downstream heat transfer components. The downside of this aspect is that a continuously rising powder hold-up inside the packed bed will have a negative impact on the storage's thermal efficiency and long-term operation.

While the operation of PBTES systems with clean, single-phase HTF has already been successfully tested on pilot-scale plants (Bai et al. 2022; Bruch et al. 2014; Knobloch et al. 2022; Zanganeh et al. 2012), operating a PBTES with gas-powder two-phase industrial exhaust gases has not been studied yet. When charging a PBTES with gas-powder two-phase flow, the impact of powder hold-up and pressure drop on the long-term storage operation must also be considered. A continuously rising powder hold-up and pressure drop will not only reduce the storage's exergy efficiency. It may also require specific operating strategies that are contrary to the optimal operating strategy regarding thermal efficiency. Usually, in CSP plants or combined with compressed air energy storage, PBTES systems are charged from the top and discharged from the bottom since this

minimizes the thermocline degradation and yields the best thermal efficiency. Although discharging the storage with clean single-phase HTF may reduce the powder hold-up, a continuously increasing accumulation of powder particles will likely lead to a clogging of the storage. It may be better to charge a PBTES from the bottom and to discharge it from the top to prevent this from happening. This strategy could facilitate the removal of powder hold-up and a series connection of multiple storage units in large-scale industrial energy systems. However, to the best of the author's knowledge, there are no studies that investigate the powder hold-up and pressure drop of a PBTES charged with gas-powder two-phase HTF and discharged with clean single-phase HTF. Furthermore, the impact of charging a PBTES from the bottom and discharging it from the top on its thermal efficiency has never been studied.

3.1 Research objective

This dissertation mainly focuses on the thermal efficiency and long-term operation of a PBTES charged with high-temperature gas-powder two-phase exhaust gas from a steel-making process. According to the potential challenges stated in this section, the overall research objective comprises multiple aspects. One goal is to quantify the powder hold-up and the pressure drop of a PBTES charged with gas-powder two-phase flow. Specifically, the evolution of the packed bed's pressure drop and the amount of powder accumulating during long-term operation is an important aspect. These insights will allow us to make statements about the frequency of maintenance, the necessity for powder removal mechanisms, and the degradation of the storage's thermal efficiency due to an increased pressure drop. Furthermore, the identification of regions with an increased accumulation of powder particles is essential to assess the impact of powder hold-up on the storage's thermal storage capacity (random flow channel formation). This may also support the selection of suitable powder removal mechanisms and the evaluation of operation strategies and HTF flow configurations that facilitate the removal of powder hold-up.

Another critical aspect of the research objective is the thermal efficiency of a PBTES operated in an industrial environment. Specifically, the impact of the HTF flow direction on the thermal efficiency of a PBTES is of interest. The goal is to evaluate whether charging a PBTES from the bottom and discharging it from the top significantly impacts the degradation of the thermocline and, thus, the thermal efficiency of the storage. Quantifying key performance indicators such as energy and exergy efficiency will allow us to assess the suitability of the PBTES system to reliably increase the flexibility and efficiency of industrial waste heat recovery systems.

4 Research approach

Multiple experimental studies were conducted to investigate the impact of charging a PBTES with high-temperature gas-powder two-phase flow on its overall performance and operation. The experiments were performed on two separate test rigs to avoid the superimposition of thermal effects and effects caused by the gas-powder two-phase flow. The decision to use two separate test rigs was also made because of safety concerns (dust explosions) and to establish suitable conditions for the utilized measuring devices. A medium-scale high-temperature test rig was designed to investigate the thermal performance of a PBTES for different operating conditions and HTF flow configurations. A separate small-scale cold model was built to explore the powder hold-up and pressure drop of a PBTES that is charged with gas-powder two-phase flow and discharged with clean single-phase HTF. The high-temperature test rig was operated with clean single-phase air, and the cold model was operated at ambient temperature only. To obtain transferable results between the two test rigs, both were filled with the same type of steel slag (for details, see Table 1) as storage material and were designed with a similar height-to-diameter ratio of ≈ 3.5 . The powder used for the cold model experiments consists of metal dust that was collected from the exhaust gases of a steel-making process (for details, see Table 1). The dimensions of both storage tanks, properties of the thermal insulation of the high-temperature test rig, and information on the sensor equipment used for the test rigs are summarized in Table 1.

High-temperature test rig		Cold model test rig	
Tank diameter	0.35 m (bottom) 0.65 m (top)	Tank diameter	0.238 m
Tank height	2.05 m	Tank height	0.78 m
Tank volume	0.405 m ³ (holds 981 kg of slag)	Tank volume	0.034 m ³
Insulation	0.1 m ceramic wool $\lambda = 0.055 \text{ W m}^{-1} \text{ K}^{-1}$	Packed bed height	0.7 m
	0.08 m rock wool $\lambda = 0.04 \text{ W m}^{-1} \text{ K}^{-1}$	Packed bed volume	0.031 m ³
		Packed bed mass	68.5 kg
Temperature sensors	four-wire RTD PT100 class AA ($\pm 0.6 \text{ }^\circ\text{C}$)	Pressure sensors	piezoresistive sensors ($\pm 0.06 \text{ \% FS}$)
Mass flow sensor	hot-wire anemometer ($\pm 4 \text{ \% RD}$)		
Storage material		Powder material	
Particle size	0.016 m to 0.032 m	Type of material	metal dust from the iron and steel industry
Sauter-diameter	0.0194 m	Particle size	0.2 μm to 600 μm $\approx 95\%$ Iron(III) oxide
Particle density	3800 kg m ⁻³	Composition	(Fe ₂ O ₃) + 5% of other transition metal oxides
Void fraction	0.42		
Bulk density	2200 kg m ⁻³		
Spec. heat capacity	750 J kg ⁻¹ K ⁻¹		

Table 1: *Test rig geometries, sensor equipment, and material properties of the cold model and high-temperature experimental setup. Adapted from Schwarzmayr et al. (2023a, 2024b).*

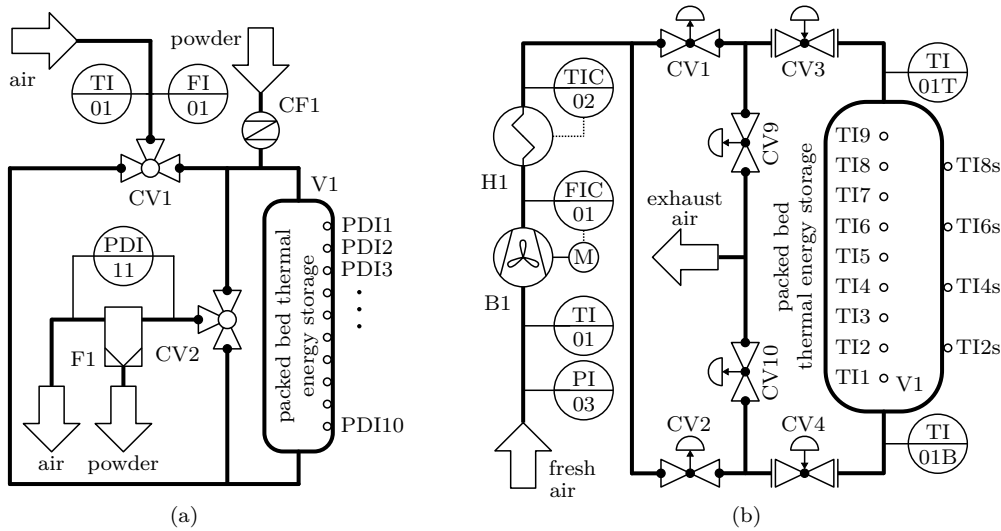


Figure 5: Process flow and instrumentation diagrams of the (a) small-scale cold model test rig and the (b) medium-scale high-temperature test rig. Adapted from Schwarzmayr et al. (2023a, 2024b).

The cold model test rig was designed for an accurate measurement of the pressure drop of a packed bed through which gas-powder two-phase flow passes in one direction and, subsequently, clean air passes in the opposite direction. For this purpose, the cold model's storage tank is equipped with 10 piezoresistive differential pressure sensors (PDI1, PDI2, ..., PDI10 in Figure 5a), which are evenly distributed over the height of the packed bed. These sensors allow for a detailed measurement of the course of the pressure drop inside the packed bed to detect regions with an increased accumulation of powder particles. In addition, the test rig was designed in a way that the mass balance of the powder that passes through the packed bed can be calculated. The three main components of the cold model test rig are the storage tank (V1 in Figure 5a), the cell feeder (CF1 in Figure 5a), and the powder filter (F1 in Figure 5a). Through the cell feeder, designed by Reitingner (2023), the powder material can be dispersed into the airflow to provide the required gas-powder two-phase flow. The powder filter was designed to capture the powder, which is transported by the fluid flow that exits the storage tank. The amount of powder that accumulates inside the packed bed can be calculated as the difference between the amount of powder fed into the fluid flow by the cell feeder and the amount of powder separated by the powder filter.

To simulate a charging process with a gas-powder two-phase flow, clean air is directed through the cell feeder before it passes through the cold model from the top to the bottom and exits the system through a powder filter. The powder added by the cell feeder accumulates inside the packed bed or the powder filter. To simulate a subsequent discharging process with single-phase HTF, clean air passes through the contaminated packed bed from the bottom to the top and exits the experimental setup through the powder filter. The packed bed's pressure drop course was recorded and correlated to the

calculated powder hold-up during post-processing and data analysis for all experiments. Empirical equations for the packed bed pressure drop from the literature (Ergun 1952; Molerus 1982) were used for data validation and analysis. It is essential to mention that the results from these investigations are transferable to large-scale devices only if all similarity criteria (*Reynolds-* and *Euler-*number) are met (see Publication 2).

It was found that when charging a PBTES with gas-powder two-phase flow 98 % of the powder mass that the HTF transports accumulate inside the packed bed. When discharging a powder-contaminated PBTES with clean single-phase HTF, the HTF does not entrain detectable amounts of powder from the packed bed. This means, that the powder hold-up inside a packed bed does not change during discharging. Furthermore, most of the powder that deposits inside the storage is concentrated near the surface where the HTF enters the packed bed. This was detected by a disproportional increase of the pressure drop in this layer of the packed bed (green bars in Figure 6a). Together with *Molerus'* equation (Molerus 1982), the recorded pressure drop data was used to estimate the void fraction at different vertical positions inside the packed bed. These calculations revealed a nonuniform reduction of the packed bed void fraction along the vertical axis of the storage tank (orange bars in Figure 6a). In the top layer (0.08 m, 11 % of the packed bed's total height) of the packed bed – where the HTF enters – the void fraction was reduced significantly more compared to the rest of the storage volume. This indicates that most of the powder hold-up is concentrated in this region. These results were confirmed by a visual investigation of the packed bed, which further indicated an even distribution of the powder hold-up in the radial direction of the storage tank (see Figure 6b and c). Therefore, there is no risk of random flow channel formation that would reduce the storage capacity of the PBTES. In Publication 2, it was concluded that an efficient strategy to keep the powder hold-up in a PBTES below a specific value is inevitable. Since most of the powder accumulates near the surface where the HTF enters

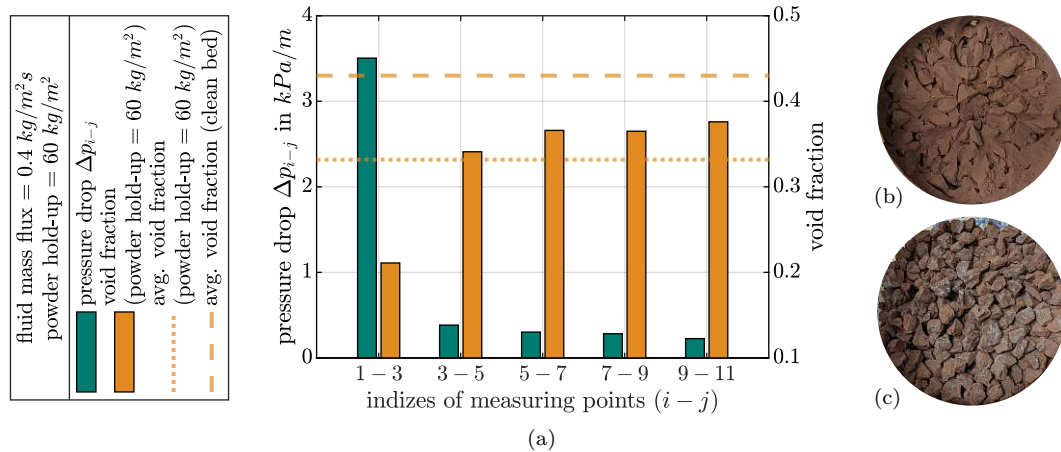


Figure 6: *Experimental results from Publication 2: (a) Pressure drop and void fraction; (b) Powder hold-up in the top layer; (c) Powder hold-up in the remaining layers. Adapted from Schwarzmayr et al. (2024b).*

RESEARCH SUMMARY

the packed bed, it was suggested that the storage should be charged from the bottom and discharged from the top. In this way, the powder would accumulate at the bottom surface of the packed bed, where it can be easily removed via periodic knocking/trembling mechanisms.

The medium-scale high-temperature test rig was used to study the thermal efficiency of a PBTES for different operating conditions and HTF flow configurations. Experiments were conducted for two different operating conditions, namely the standby and the partial cycle operation, and two different HTF flow configurations, the forward (FWD) and the reverse (REV) mode. In the context of this work, the FWD mode refers to charging the storage from the top and discharging it from the bottom. The REV mode refers to charging the storage from the bottom and discharging it from the top. These experiments aimed to quantify the impact of the HTF flow direction on the test rig's thermocline degradation and exergy efficiency. For an exact measurement of the thermal state of the storage material (especially the position and shape of the thermocline), the test rig is equipped with multiple PT100 temperature sensors (TI01B, TI1, TI2, ..., TI9, TI01T). Additionally, eight temperature sensors ($2 \times$ TI2s, ..., $2 \times$ TI8s) were placed on the storage tank's lateral surface between the steel vessel and the insulation material to enable an accurate estimation of the heat losses to the surroundings.

Experiments with various standby periods were carried out to investigate the impact of the HTF flow direction on the thermal efficiency of a PBTES in standby operation. The results of all these experiments are published in Publication 1 and shown in Figure 7a. In the first set of experiments, the storage was charged for 2 h and fully discharged after a standby period of 0.5 h for both the FWD- and the REV-mode. For these experiments, an energy efficiency of 92 % and an exergy efficiency of 83 % were measured, and no significant difference between the FWD- and the REV-mode could be detected. In a second set of experiments, the test rig was again charged for 2 h and fully discharged afterward for both the FWD- and the REV-mode. This time, however, the test rig was discharged not until after a standby period of 22 h. The analysis of these experiments indicated a significantly faster degradation of the standby efficiency of the storage that was operated in REV-mode. The energy and exergy efficiency of the storage that was charged in FWD-mode were 74 % and 55 %, respectively. In the experiments in which the storage was operated in REV-mode, the energy and exergy efficiencies were observed to be 70 % and 45 %, respectively. The comparison of these results indicates that, for long standby periods, the thermal performance of a PBTES operated in REV-mode is notably lower compared to a PBTES operated in FWD-mode. To quantify what "long" means in this context, the entropy generation rate was calculated for all experiments using the second law of thermodynamics. These evaluations indicated a significantly higher entropy generation rate during the experiments in which the storage was operated in REV-mode. In the first minutes of the standby periods, the entropy generation rate is the same for both the FWD- and the REV-mode. In contrast to the FWD-mode, the rate of entropy generation in the REV-mode was observed to rise afterwards until it reached a maximum after approximately 7 h. These observations indicate that it takes at least 7 h until the accelerated thermocline degradation in the REV-mode significantly impacts the thermal

performance of the PBTES. Therefore, it was concluded that operating a PBTES in standby operation and REV-mode is only recommended if standby periods are below 7 h. Otherwise, a significant degradation of the thermal performance has to be expected.

Since the operating conditions of a PBTES in industrial waste heat recovery systems will most likely be short partial cycles, the impact of the HTF flow direction on the thermal performance of a PBTES in partial cycle operation was also investigated. Partial cycle experiments for both the FWD- and the REV-mode with cycle durations between 40 min to 60 min were carried out until the test rig reached a steady state operation mode. The results of these experiments are documented in Publication 3 and shown in Figure 7b. They indicate that thermocline degradation has a detectable impact on the long-term efficiency of a PBTES in partial cycle operation regardless of the HTF flow direction. The energy and exergy efficiency of a PBTES in steady state partial cycle operation were lower by 5 % points and 3 % to 4 % points respectively, compared to the first cycle. The increased losses in the steady-state partial cycle operation are mainly caused by saturation losses at the end of the charging periods. Efficiencies when operating the test rig in REV-mode were slightly lower than in FWD-mode. This can be attributed to increased heat losses to the surroundings via the metal grating that supports the packed bed and an adverse surface-to-volume ratio at the bottom of the packed bed. In contrast to the standby experiments, no additional deterioration of the storage performance caused by thermocline degradation could be observed for the partial cycle experiments. Therefore, in Publication 3, it was concluded that thermocline degradation has no significant impact on the steady-state partial cycle operation and long-term performance of a PBTES that is operated in REV-mode. The experimental results presented in this section enable the analysis of the interactions between the powder hold-up and the thermal performance of a PBTES operated with gas-powder two-phase exhaust gas. They provide reference values for economic assessments, payback period estimations, and essential system parameters for the design- and operational optimization of a PBTES in an industrial environment.

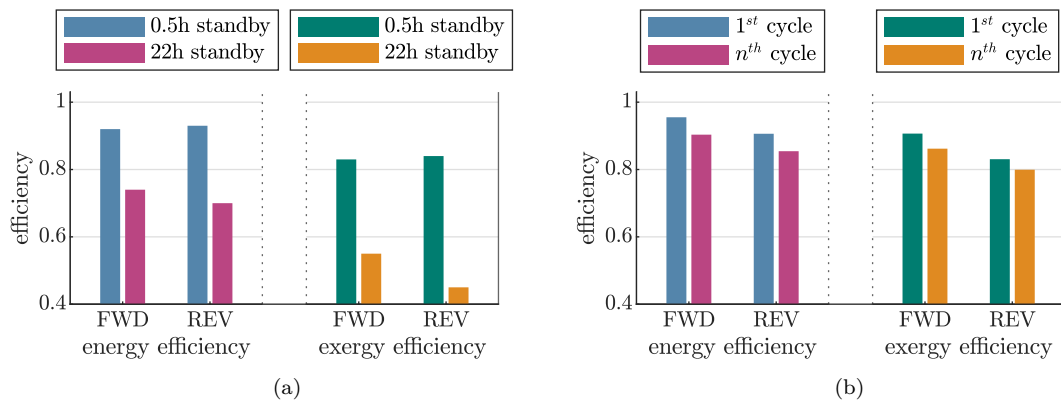


Figure 7: Results from Publication 1 and 3: Impact of the HTF flow direction on the efficiency of a PBTES in (a) standby and (b) partial cycle operation. Adapted from Schwarzmayr et al. (2023a, 2024a).

RESEARCH SUMMARY

These insights will support the improvement of PBTES design for this particular use case and thus advance PBTES systems towards their deployment for waste heat recovery in the iron and steel industry.

However, there are still implementation barriers considering system integration and storage management. Since any TES system is part of an industrial energy system is subject to fluctuating excess heat availability and process heat demand, efficient and resilient operation planning is essential. This topic was covered in collaboration with colleagues in a research project called *5DIndustrialTwin* as part of this dissertation. This project was funded by the Austrian Research Promotion Agency (Project number 881140) and was dedicated to the development of a digital twin platform for industrial energy systems. The purpose of this digital twin platform is to enable an efficient, flexible, and reliable operation of a PBTES. This development was a multi-step process involving the formulation of the digital twin platform using a five-dimensional modeling approach (Publication 6), its implementation on the medium-scale test rig that was used for the experimental investigations in the present dissertation (Publication 4) and its testing and evaluation (Publication 7). Based on the requirements of industrial energy systems, the digital twin platform was designed to provide a framework for specialized services in different domains. With its five dimensions that consist of the physical entity, the virtual entity, the connection dimension, the data dimension, and the service dimension the developed digital twin platform reinforces the bi-directional interaction between specialized services in the physical and virtual space. A message-oriented middleware (Thoma et al. 2023) was used to reinforce the bi-directional flow of information between the other four dimensions of the digital twin. Ontologies (Steindl et al. 2020) – a concept from information science – were employed for a machine-readable representation of domain knowledge and other data in the data dimension. To ensure a hitch-free operation of all tasks and services within the digital twin, a workflow engine (Steindl et al. 2021) that executes workflows that are formulated according to business process modeling notation form the centerpiece of the service dimension. As a first step of evaluation, the digital twin platform was implemented on the medium-scale PBTES test rig (see Section 4) and tested by using an online soft sensor modeling service. The methodology and results are published in Publication 4 and demonstrate the bi-directional interaction between the five dimensions of the digital twin platform. The second and final step of the evaluation, which included techno-economic assessments employing an industrial use case from the iron and steel industry, is published in Publication 7. Along with a description of the industrial use case, this publication provides detailed documentation of essential services, including online model adaption (Publication 5), operational optimization and approximation of non-linear operating behavior (Publications 8 and 9). The entirety of these publications (4, 5, 6, 7, 8 and 9) emphasizes the benefits of digital twin technologies for the efficient operation of industrial energy systems.

5 Conclusion and outlook

The present dissertation investigated the thermal efficiency and long-term operation of packed bed thermal energy storage (PBTES) systems for waste heat recovery in the iron and steel industry. Since the intermittent availability of excess heat is one of the primary reasons for a low waste heat utilization rate in the industry sector, thermal energy storage (TES) systems can contribute to overcoming this issue. It was shown that a well-conceived integration of PBTES systems into industrial energy systems can provide the necessary flexibility to match waste heat availability with process heat demand. The PBTES integration proposed in this dissertation does not only increase the maximum waste heat utilization rate from 45 % to theoretically 97 %. It also relieves the dynamic load on critical system components, which reduces investment costs and extends their operational lifetime.

One major challenge that the direct utilization of industrial exhaust gases as heat transfer fluid (HTF) entails is the composition of industrial exhaust gases and its impact on the optimal operation strategy of the storage system. This topic was experimentally studied using a cold model test rig. The experimental results indicate that 98 % of the powder mass that is transported by the gas-powder two-phase HTF deposits inside the storage, and most of it is concentrated near the surface where the HTF enters the packed bed. Discharging with clean HTF does not reduce the powder hold-up or the pressure drop inside the packed bed. The radial distribution of powder hold-up inside the packed bed is uniform, and no random formations of HTF flow channels through the packed bed occur. Additional studies using a high-temperature test rig were carried out to evaluate the thermal performance of a PBTES for different operating conditions and HTF flow directions. The results reveal that overall, the energy and exergy efficiency are lower due to accelerated thermocline degradation when the storage is charged from the bottom and discharged from the top. However, in partial cycle operation and standby operation with short standby periods, the energy and exergy efficiency losses are insignificant. For a PBTES in steady-state partial cycle operation that is charged from the bottom and discharged from the top, the energy and exergy efficiency are lower by less than 4 % points and 5 % points respectively compared to a PBTES with the opposite HTF flow direction.

It is essential to mention that the results presented in this work are limited to the conditions at which they were generated. Effects of gas-powder two-phase flow on the powder hold-up and pressure drop of a PBTES and effects of different operating strategies on the thermal behavior of a PBTES were investigated separately. The decision for separate experiments was taken in order to facilitate accurate measurements and because of safety concerns. To quantify the powder hold-up and pressure drop in a PBTES charged with gas-powder two-phase flow a cold model test rig was used. The results obtained from these experiments are therefore only applicable if all similarity criteria (including *Reynolds*- and *Euler*-number) are met. The thermal performance for different HTF flow directions was investigated using a medium-scale high-temperature test rig operated with clean air and a comparatively high surface-to-volume ratio. The energy and exergy

RESEARCH SUMMARY

efficiencies expected from an industrial-scale storage with a lower surface-to-volume ratio are notably higher than the ones presented in this work. Furthermore, the impact of results from the cold model study on the thermal behavior of a PBTES can only be evaluated on a conceptual level at this point. Further research and development will be necessary to fully confirm these deductions.

Still, the scientific findings summarized in this dissertation provide evidence for the suitability and thermal performance of PBTES systems for waste heat recovery in the iron and steel industry. The proposed PBTES integration can increase the flexibility of the whole system which reduces the fluctuating thermal load on steam generators so that they can be designed for a comparatively narrow operating range. In this dissertation, it was shown that the energy and exergy efficiency of a PBTES in partial cycle operation are not noticeably affected by the flow direction of the HTF and are greater than 87 % and 81 % respectively. These insights provide flexibility regarding the design and integration of PBTES systems into industrial energy systems. If required by structural and operational constraints, PBTES systems can be charged from the bottom and discharged from the top to facilitate the series connection of multiple tanks and the removal of powder hold-up.

While a continuous powder accumulation occurs during perfusion with the gas-powder two-phase flow, the powder hold-up in the storage tank is not entrained by clean HTF flowing through the packed bed. This signifies that a PBTES can decrease the exposure of downstream heat conversion equipment to gas-powder two-phase flow. Therefore, the proposed PBTES integration protects heat transfer equipment from erosion due to powder particles transported by the exhaust gases and prevents the build-up of powder layers on the heat exchanger surfaces. This positively impacts the durability and long-term efficiency of steam generators and reduces the initial and running costs of the whole waste heat recovery system. All in all, it can be concluded that integrating a PBTES into waste heat recovery systems enhances the overall energy conversion efficiency and the waste heat utilization rate of the whole system and reduces investment costs and running costs (maintenance, replacements, ...) of downstream energy conversion equipment.

Although the results and conclusions emphasize the potential of PBTES systems to enhance the waste heat utilization rate in industrial energy systems, PBTES systems are not yet advanced enough to be deployed and operated in an industrial environment. There are still open questions and barriers that need to be approached to continue the development of PBTES systems for waste heat recovery in the iron and steel industry. The remaining issues are the continuous accumulation of powder inside a PBTES operated with gas-powder two-phase gas and the up-scaling and transferability of experimental results to industrial-scale systems. A continuously rising powder accumulation negatively impacts the long-term performance of the PBTES, which may require frequent maintenance of the packed bed material. Therefore, managing powder hold-up in a PBTES should be the focus of prospective investigations. Different strategies – some of which have already been identified in the present work – to keep the powder hold-up in a PBTES below a certain level and to prevent frequent shut-downs should be tested and evaluated in future experiments. Furthermore, the conclusions drawn considering the impact of powder hold-up on the thermal performance of a PBTES need to be validated via experimental

RESEARCH SUMMARY

studies on a prototype test rig. Future research could also focus on optimizing the design of PBTES systems (storage geometry, novel HTF flow configurations, thermal insulation, type of storage material, particle size of storage material, ...) so that the main benefits of PBTES systems (cost-effectiveness, internal heat transfer, thermal stratification, ...) can be exploited as effectively as possible.

The results of this dissertation show that the optimal utilization of waste heat is of high importance, even though the majority of emission savings in the iron and steel industry will be achieved through electrification and hydrogen-based technologies. Integrating a PBTES increases the total efficiency of waste heat recovery systems and reduces operational costs, contributing to the decarbonization of the energy-intensive industry. The iron and steel industry's greenhouse gas emissions can be reduced significantly by substituting heat from burning fossil fuels with waste heat from hot exhaust gases. The results summarized in this dissertation provide a first glance at the potential of PBTES systems to increase the flexibility and efficiency of waste heat recovery systems in the iron and steel industry.

References

- Al-Azawii, M. M. S., S. F. H. Alhamdi, S. Braun, J.-F. Hoffmann, N. Calvet, and R. Anderson (Aug. 2023). “Thermocline in packed bed thermal energy storage during charge-discharge cycle using recycled ceramic materials - Commercial scale designs at high temperature”. en. In: *Journal of Energy Storage* 64, p. 107209. ISSN: 2352-152X. DOI: 10.1016/j.est.2023.107209
- Bai, Y., L. Wang, L. Lin, X. Lin, L. Peng, and H. Chen (July 2022). “A performance analysis of the spray-type packed bed thermal energy storage for concentrating solar power generation”. en. In: *Journal of Energy Storage* 51, p. 104187. ISSN: 2352-152X. DOI: 10.1016/j.est.2022.104187
- Bianchi, G., G. P. Panayiotou, L. Aresti, S. A. Kalogirou, G. A. Florides, K. Tsamos, S. A. Tassou, and P. Christodoulides (2019). “Estimating the waste heat recovery in the European Union Industry”. In: *Energy, Ecology and Environment* 4.5, pp. 211–221. ISSN: 2363-8338. DOI: 10.1007/s40974-019-00132-7
- Birkelbach, F. (2020). “Non-parametric kinetic modeling of gas-solid reactions for thermochemical energy storage”. en. Accepted: 2020-09-17T10:45:21Z Journal Abbreviation: Nicht-parametrische Modellierung der Kinetik von Gas-Feststoffreaktionen für thermochemische Energiespeicherung. Thesis. Technische Universität Wien. DOI: 10.34726/hss.2020.82863
- Birkelbach, F., L. Kasper, P. Schwarzmayr, and R. Hofmann (2023a). *Modeling Partial Cycle Behavior of a Thermal Storage in Milp: Comparison of Heuristics for Approximating Non-Linear Operating Behavior*. submitted to Journal of Energy Storage. DOI: 10.2139/ssrn.4656763
- Birkelbach, F., L. Kasper, P. Schwarzmayr, and R. Hofmann (2023b). “Operation Planning with Thermal Storage Units Using MILP: Comparison of Heuristics for Approximating Non-Linear Operating Behavior”. In: *36th Int. Conf. on Eff., Cost, Opt., Sim. and Env. Imp. of En. Sys. (ECOS 2023)*. Las Palmas De Gran Canaria, Spain: ECOS 2023, pp. 1345–1350. DOI: 10.52202/069564-0122
- Bruch, A., J. F. Fourmigué, and R. Couturier (July 2014). “Experimental and numerical investigation of a pilot-scale thermal oil packed bed thermal storage system for CSP power plant”. en. In: *Solar Energy* 105, pp. 116–125. ISSN: 0038-092X. DOI: 10.1016/j.solener.2014.03.019
- Bruch, A., S. Molina, T. Esence, J. F. Fourmigué, and R. Couturier (Apr. 2017). “Experimental investigation of cycling behaviour of pilot-scale thermal oil packed-bed thermal storage system”. en. In: *Renewable Energy* 103, pp. 277–285. ISSN: 0960-1481. DOI: 10.1016/j.renene.2016.11.029
- C3S (2023). *July 2023 sees multiple global temperature records broken | Copernicus*. URL: <https://climate.copernicus.eu/july-2023-sees-multiple-global-temperature-records-broken> (visited on 10/07/2023)

- Cascetta, M., G. Cau, P. Puddu, and F. Serra (Oct. 2015). “Experimental investigation of a packed bed thermal energy storage system”. en. In: *Journal of Physics: Conference Series* 655.1. Publisher: IOP Publishing, p. 012018. ISSN: 1742-6596.
DOI: 10.1088/1742-6596/655/1/012018
- Chen, X., Z. Zhang, C. Qi, X. Ling, and H. Peng (Dec. 2018). “State of the art on the high-temperature thermochemical energy storage systems”. In: *Energy Conversion and Management* 177, pp. 792–815. ISSN: 0196-8904.
DOI: 10.1016/j.enconman.2018.10.011
- Cui, Z., Q. Du, J. Gao, R. Bie, and D. Li (June 2020). “Development of a direct contact heat exchanger for energy and water recovery from humid flue gas”. en. In: *Applied Thermal Engineering* 173, p. 115214. ISSN: 1359-4311.
DOI: 10.1016/j.applthermaleng.2020.115214
- Ding, Y., Z. Wang, D. Wen, M. Ghadiri, X. Fan, and D. Parker (Sept. 2005). “Solids behaviour in a gas–solid two-phase mixture flowing through a packed particle bed”. en. In: *Chemical Engineering Science* 60.19, pp. 5231–5239. ISSN: 0009-2509.
DOI: 10.1016/j.ces.2005.04.052
- Dong, X. F., D. Pinson, S. J. Zhang, A. B. Yu, and P. Zulli (Nov. 2004a). “Gas–powder flow and powder accumulation in a packed bed: I. Experimental study”. en. In: *Powder Technology* 149.1, pp. 1–9. ISSN: 0032-5910.
DOI: 10.1016/j.powtec.2004.09.040
- Dong, X. F., S. J. Zhang, D. Pinson, A. B. Yu, and P. Zulli (Nov. 2004b). “Gas–powder flow and powder accumulation in a packed bed: II. Numerical study”. en. In: *Powder Technology* 149.1, pp. 10–22. ISSN: 0032-5910.
DOI: 10.1016/j.powtec.2004.09.039
- Ergun, S. (1952). “Fluid flow through packed columns”. In: *Chemical Engineering Progress* 48.2, pp. 89–94.
- Esence, T., A. Bruch, S. Molina, B. Stutz, and J.-F. Fourmigué (Sept. 2017). “A review on experience feedback and numerical modeling of packed-bed thermal energy storage systems”. en. In: *Solar Energy* 153, pp. 628–654. ISSN: 0038-092X.
DOI: 10.1016/j.solener.2017.03.032
- European Commission (2023). *Causes of climate change*.
URL: https://climate.ec.europa.eu/climate-change/causes-climate-change_en (visited on 09/05/2023)
- First Dog on the Moon (July 2023). “The northern hemisphere is on fire! The temperature records being broken are record-breaking!” In: *The Guardian*. ISSN: 0261-3077.
URL: <https://www.theguardian.com/commentisfree/2023/jul/19/the-northern-hemisphere-is-on-fire-the-temperature-records-being-broken-are-record-breaking> (visited on 08/02/2023)
- Forman, C., I. K. Muritala, R. Pardemann, and B. Meyer (May 2016). “Estimating the global waste heat potential”. en. In: *Renewable and Sustainable Energy Reviews* 57, pp. 1568–1579. ISSN: 1364-0321.
DOI: 10.1016/j.rser.2015.12.192
- Gautam, A. and R. P. Saini (Sept. 2020a). “A review on sensible heat based packed bed

solar thermal energy storage system for low temperature applications”. en. In: *Solar Energy* 207, pp. 937–956. ISSN: 0038-092X.

DOI: 10.1016/j.solener.2020.07.027

Gautam, A. and R. P. Saini (Feb. 2020b). “A review on technical, applications and economic aspect of packed bed solar thermal energy storage system”. en. In: *Journal of Energy Storage* 27, p. 101046. ISSN: 2352-152X.

DOI: 10.1016/j.est.2019.101046

Geissbühler, L., A. Mathur, A. Mularczyk, and A. Haselbacher (Jan. 2019a). “An assessment of thermocline-control methods for packed-bed thermal-energy storage in CSP plants, Part 1: Method descriptions”. en. In: *Solar Energy* 178, pp. 341–350. ISSN: 0038-092X.

DOI: 10.1016/j.solener.2018.12.015

Geissbühler, L., A. Mathur, A. Mularczyk, and A. Haselbacher (Jan. 2019b). “An assessment of thermocline-control methods for packed-bed thermal-energy storage in CSP plants, Part 2: Assessment strategy and results”. en. In: *Solar Energy* 178, pp. 351–364. ISSN: 0038-092X.

DOI: 10.1016/j.solener.2018.12.016

Gupta, G. S., S. Lakshminarasimha, and M. Shrenik (Feb. 2022). “Quantitative Measurement of Powder Holdups in the Packed Beds”. en. In: *Transactions of the Indian Institute of Metals* 75.2, pp. 381–395. ISSN: 0975-1645.

DOI: 10.1007/s12666-021-02431-2

IEA (Oct. 2013). *From hidden fuel to world’s first fuel? - News*.

URL: <https://www.iea.org/news/from-hidden-fuel-to-worlds-first-fuel> (visited on 09/08/2023)

IEA (May 2019). *Emissions savings – Multiple Benefits of Energy Efficiency – Analysis*. URL: <https://www.iea.org/reports/multiple-benefits-of-energy-efficiency/emissions-savings> (visited on 09/08/2023)

IEA (2022). *Coal in Net Zero Transitions: Strategies for Rapid, Secure and People-centred Change*. International Energy Agency. ISBN: 978-92-64-90003-5.

URL: <https://doi.org/10.1787/5873f7bb-en>

IEA (2023a). *CO₂ Emissions in 2022*. Paris: International Energy Agency.

URL: <https://www.iea.org/reports/co2-emissions-in-2022>

IEA (2023b). *World electricity final consumption by sector, 1974-2019*.

URL: <https://www.iea.org/data-and-statistics/charts/world-electricity-final-consumption-by-sector-1974-2019> (visited on 09/07/2023)

IPCC (2018). *Global Warming of 1.5°C: IPCC Special Report on Impacts of Global Warming of 1.5°C above Pre-industrial Levels in Context of Strengthening Response to Climate Change, Sustainable Development, and Efforts to Eradicate Poverty*. Cambridge: Cambridge University Press.

DOI: 10.1017/9781009157940

“Human Influence on the Climate System” (2021a). In: *Climate Change 2021 – The Physical Science Basis: Working Group I Contribution to the Sixth Assessment*

Report of the Intergovernmental Panel on Climate Change. Ed. by IPCC. Cambridge: Cambridge University Press, pp. 423–552. ISBN: 978-1-00-915788-9.

DOI: 10.1017/9781009157896.005

“Weather and Climate Extreme Events in a Changing Climate” (2021b). In: *Climate Change 2021 – The Physical Science Basis: Working Group I Contribution to the Sixth Assessment Report of the Intergovernmental Panel on Climate Change*. Ed. by IPCC. Cambridge: Cambridge University Press, pp. 1513–1766. ISBN: 978-1-00-915788-9.

DOI: 10.1017/9781009157896.013

IRENA (2020). *Innovation outlook: Thermal energy storage*. Abu Dhabi: International Renewable Energy Agency. ISBN: 978-92-9260-279-6.

Ja’fari, M., M. I. Khan, S. G. Al-Ghamdi, A. J. Jaworski, and F. Asfand (Dec. 2023). “Waste heat recovery in iron and steel industry using organic Rankine cycles”. In: *Chemical Engineering Journal* 477, p. 146925. ISSN: 1385-8947.

DOI: 10.1016/j.cej.2023.146925

Kalantari, H., L. Amiri, and S. A. Ghoreishi-Madiseh (2022). “Analysis of the performance of direct contact heat exchange systems for application in mine waste heat recovery”. en. In: *International Journal of Energy Research* 46.1. _eprint: <https://onlinelibrary.wiley.com/doi/pdf/10.1002/er.6734>, pp. 290–307. ISSN: 1099-114X.

DOI: 10.1002/er.6734

Kasper, L., F. Birkelbach, P. Schwarzmayr, G. Steindl, D. Ramsauer, and R. Hofmann (Jan. 2022). “Toward a Practical Digital Twin Platform Tailored to the Requirements of Industrial Energy Systems”. In: *Applied Sciences* 12.14. Number: 14 Publisher: Multidisciplinary Digital Publishing Institute, p. 6981. ISSN: 2076-3417.

DOI: 10.3390/app12146981

Kasper, L., P. Schwarzmayr, F. Birkelbach, F. Javernik, M. Schwaiger, and R. Hofmann (Jan. 2024). “A digital twin-based adaptive optimization approach applied to waste heat recovery in green steel production: Development and experimental investigation”. In: *Applied Energy* 353, p. 122192. ISSN: 0306-2619.

DOI: 10.1016/j.apenergy.2023.122192

Keplinger, T., M. Haider, T. Steinparzer, A. Patrejko, P. Trunner, and M. Haselgrübler (May 2018). “Dynamic simulation of an electric arc furnace waste heat recovery system for steam production”. en. In: *Applied Thermal Engineering* 135, pp. 188–196. ISSN: 1359-4311.

DOI: 10.1016/j.applthermaleng.2018.02.060

Kiochiro, S., S. Masakata, I. Shin-ichi, T. Reijiro, and Y. Jun-ichiro (1991). “Pressure Loss and Hold-up Powders for Gas-Powder Two Phase Flow in Packed Beds”. In: *ISIJ International* 31.5, pp. 434–439.

DOI: doi.org/10.2355/isijinternational.31.434

Knobloch, K., Y. Muhammad, M. S. Costa, F. M. Moscoso, C. Bahl, O. Alm, and K. Engelbrecht (June 2022). “A partially underground rock bed thermal energy storage with a novel air flow configuration”. en. In: *Applied Energy* 315, p. 118931. ISSN: 0306-2619.

- DOI: 10.1016/j.apenergy.2022.118931
- Manente, G., Y. Ding, and A. Sciacovelli (July 2022). “A structured procedure for the selection of thermal energy storage options for utilization and conversion of industrial waste heat”. en. In: *Journal of Energy Storage* 51, p. 104411. ISSN: 2352-152X.
DOI: 10.1016/j.est.2022.104411
- Marti, J., L. Geissbühler, V. Becattini, A. Haselbacher, and A. Steinfeld (Apr. 2018). “Constrained multi-objective optimization of thermocline packed-bed thermal-energy storage”. en. In: *Applied Energy* 216, pp. 694–708. ISSN: 0306-2619.
DOI: 10.1016/j.apenergy.2017.12.072
- Mertens, N., F. Alobaid, L. Frigge, and B. Epple (Dec. 2014). “Dynamic simulation of integrated rock-bed thermocline storage for concentrated solar power”. en. In: *Solar Energy* 110, pp. 830–842. ISSN: 0038-092X.
DOI: 10.1016/j.solener.2014.10.021
- Miró, L., J. Gasia, and L. F. Cabeza (Oct. 2016). “Thermal energy storage (TES) for industrial waste heat (IWH) recovery: A review”. In: *Applied Energy* 179, pp. 284–301. ISSN: 0306-2619.
DOI: 10.1016/j.apenergy.2016.06.147
- Molerus, O. (1982). “Kohärente Darstellung des Druckverlustverhaltens von Festbetten und des Ausdehnungsverhaltens homogener Flüssigkeits-/Feststoff-Wirbelschichten”. de. In: *Fluid-Feststoff-Strömungen: Strömungsverhalten feststoffbeladener Fluide und kohäsiver Schüttgüter*. Ed. by O. Molerus. Berlin, Heidelberg: Springer, pp. 8–38. ISBN: 978-3-642-50215-6.
DOI: 10.1007/978-3-642-50215-6_2
- NASA (2023a). *Carbon Dioxide Concentration | NASA Global Climate Change*. en.
URL: <https://climate.nasa.gov/vital-signs/carbon-dioxide> (visited on 11/16/2023)
- NASA (2023b). *Climate Change Evidence: How Do We Know?*
URL: <https://climate.nasa.gov/evidence> (visited on 09/05/2023)
- NASA (2023c). *Global Warming*. en. Text.Article. Publisher: NASA Earth Observatory.
URL: <https://earthobservatory.nasa.gov/features/GlobalWarming> (visited on 11/16/2023)
- Okello, D., O. J. Nydal, and E. J. K. Banda (Oct. 2014). “Experimental investigation of thermal de-stratification in rock bed TES systems for high temperature applications”. en. In: *Energy Conversion and Management* 86, pp. 125–131. ISSN: 0196-8904.
DOI: 10.1016/j.enconman.2014.05.005
- Oró, E., A. Castell, J. Chiu, V. Martin, and L. F. Cabeza (Sept. 2013). “Stratification analysis in packed bed thermal energy storage systems”. en. In: *Applied Energy* 109, pp. 476–487. ISSN: 0306-2619.
DOI: 10.1016/j.apenergy.2012.12.082
- Ortega-Fernández, I. and J. Rodríguez-Aseguinolaza (Mar. 2019). “Thermal energy storage for waste heat recovery in the steelworks: The case study of the REslag project”. en. In: *Applied Energy* 237, pp. 708–719. ISSN: 0306-2619.
DOI: 10.1016/j.apenergy.2019.01.007
- Palacios, A., M. E. Navarro-Rivero, B. Zou, Z. Jiang, M. T. Harrison, and Y. Ding

(Nov. 2023). “A perspective on Phase Change Material encapsulation: Guidance for encapsulation design methodology from low to high-temperature thermal energy storage applications”. In: *Journal of Energy Storage* 72, p. 108597. ISSN: 2352-152X. DOI: 10.1016/j.est.2023.108597

Panayiotou, G. P., G. Bianchi, G. Georgiou, L. Aresti, M. Argyrou, R. Agathokleous, K. M. Tsamos, S. A. Tassou, G. Florides, S. Kalogirou, and P. Christodoulides (Sept. 2017). “Preliminary assessment of waste heat potential in major European industries”. en. In: *Energy Procedia*. Proceedings of 1st International Conference on Sustainable Energy and Resource Use in Food Chains including Symposium on Heat Recovery and Efficient Conversion and Utilisation of Waste Heat ICSEF 2017, 19-20 April 2017, Windsor UK 123, pp. 335–345. ISSN: 1876-6102.

DOI: 10.1016/j.egypro.2017.07.263

Papapetrou, M., G. Kosmadakis, A. Cipollina, U. La Commare, and G. Micale (June 2018). “Industrial waste heat: Estimation of the technically available resource in the EU per industrial sector, temperature level and country”. en. In: *Applied Thermal Engineering* 138, pp. 207–216. ISSN: 1359-4311.

DOI: 10.1016/j.applthermaleng.2018.04.043

Reitinger, A. (2023). “Construction of a test rig for the characterization of gas-powder two-phase flow in packed bed thermal energy storage systems”. en. Accepted: 2023-05-30T08:43:58Z Journal Abbreviation: Konstruktion eines Kaltmodells für die Charakterisierung einer Gas-Feststoff zweiphasenströmung in einem vertikalen Festbettregenerator. Thesis. Wien.

DOI: 10.34726/hss.2023.103589

Rodrigues, F. A. and M. J. de Lemos (2021). “Stratification and energy losses in a standby cycle of a thermal energy storage system”. In: *International Journal of Energy for a Clean Environment* 22, pp. 1–32.

Scharinger-Urschitz, G., P. Schwarzmayr, H. Walter, and M. Haider (Dec. 2020). “Partial cycle operation of latent heat storage with finned tubes”. In: *Applied Energy* 280, p. 115893. ISSN: 0306-2619.

DOI: 10.1016/j.apenergy.2020.115893

Schwarzmayr, P., F. Birkelbach, L. Kasper, and R. Hofmann (2022). “Development of a Digital Twin Platform for Industrial Energy Systems”. In: *Accelerated Energy Innovations and Emerging Technologies*. Vol. 25. Cambridge, USA: Energy Proceedings. DOI: 10.46855/energy-proceedings-9974

Schwarzmayr, P., F. Birkelbach, H. Walter, and R. Hofmann (May 2023a). “Standby efficiency and thermocline degradation of a packed bed thermal energy storage: An experimental study”. In: *Applied Energy* 337, p. 120917. ISSN: 0306-2619.

DOI: 10.1016/j.apenergy.2023.120917

Schwarzmayr, P., F. Birkelbach, H. Walter, and R. Hofmann (Sept. 2023b). “Study on the Standby Characteristics of a Packed Bed Thermal Energy Storage: Experimental Results and Model Based Parameter Optimization”. In: American Society of Mechanical Engineers Digital Collection.

DOI: 10.1115/POWER2023-108578

- Schwarzmayr, P., F. Birkelbach, H. Walter, and R. Hofmann (Apr. 2024a). “Exergy efficiency and thermocline degradation of a packed bed thermal energy storage in partial cycle operation: An experimental study”. In: *Applied Energy* 360, p. 122895. ISSN: 0306-2619.
DOI: 10.1016/j.apenergy.2024.122895
- Schwarzmayr, P., F. Birkelbach, H. Walter, F. Javernik, M. Schwaiger, and R. Hofmann (Jan. 2024b). “Packed bed thermal energy storage for waste heat recovery in the iron and steel industry: A cold model study on powder hold-up and pressure drop”. In: *Journal of Energy Storage* 75, p. 109735. ISSN: 2352-152X.
DOI: 10.1016/j.est.2023.109735
- Slimani, H., Y. Filali Baba, H. Ait Ousaleh, A. Elharrak, F. El Hamdani, H. Bouzekri, A. Al Mers, and A. Faik (Mar. 2023). “Horizontal thermal energy storage system for Moroccan steel and iron industry waste heat recovery: Numerical and economic study”. en. In: *Journal of Cleaner Production* 393, p. 136176. ISSN: 0959-6526.
DOI: 10.1016/j.jclepro.2023.136176
- Soprani, S., F. Marongiu, L. Christensen, O. Alm, K. D. Petersen, T. Ulrich, and K. Engelbrecht (Oct. 2019). “Design and testing of a horizontal rock bed for high temperature thermal energy storage”. en. In: *Applied Energy* 251, p. 113345. ISSN: 0306-2619.
DOI: 10.1016/j.apenergy.2019.113345
- Sprecher, M., H. B. Lungen, B. Stranzinger, H. Rosemann, and W. Adler (2019). *Abwärmepotenziale in Anlagen integrierter Hüttenwerke der Stahlindustrie*. Umweltbundesamt.
URL: <https://www.umweltbundesamt.de/publikationen/abwaermenutzungspotenziale-in-anlagen-integrierter>
- Steindl, G. and W. Kastner (June 2020). “Ontology-Based Model Identification of Industrial Energy Systems”. In: *2020 IEEE 29th International Symposium on Industrial Electronics (ISIE)*. ISSN: 2163-5145, pp. 1217–1223.
DOI: 10.1109/ISIE45063.2020.9152386
- Steindl, G. and W. Kastner (Jan. 2021). “Semantic Microservice Framework for Digital Twins”. en. In: *Applied Sciences* 11.12. Number: 12 Publisher: Multidisciplinary Digital Publishing Institute, p. 5633. ISSN: 2076-3417.
DOI: 10.3390/app11125633
- Stekli, J., L. Irwin, and R. Pitchumani (2013). “Technical Challenges and Opportunities for Concentrating Solar Power With Thermal Energy Storage”. In: *Journal of Thermal Science and Engineering Applications* 5.2. ISSN: 1948-5085.
DOI: 10.1115/1.4024143
- Sunku Prasad, J., P. Muthukumar, F. Desai, D. N. Basu, and M. M. Rahman (Nov. 2019). “A critical review of high-temperature reversible thermochemical energy storage systems”. In: *Applied Energy* 254, p. 113733. ISSN: 0306-2619.
DOI: 10.1016/j.apenergy.2019.113733
- Takahashi, H., H. Kawai, T. Kondo, and M. Sugawara (2011). “Permeation and Blockage of

Fine Particles Transported by Updraft through a Packed Bed”. In: *ISIJ International* 51.10, pp. 1608–1616.

DOI: 10.2355/isijinternational.51.1608

Thoma, M. and G. Steindl (Sept. 2023). “Integrating Constrained MQTT Devices into IoT Platforms for Smart Local Energy Communities”. In: *2023 IEEE 28th International Conference on Emerging Technologies and Factory Automation (ETFA)*. ISSN: 1946-0759, pp. 1–4.

DOI: 10.1109/ETFA54631.2023.10275366

Trevisan, S., Y. Jemmal, R. Guedez, and B. Laumert (Apr. 2021). “Packed bed thermal energy storage: A novel design methodology including quasi-dynamic boundary conditions and techno-economic optimization”. en. In: *Journal of Energy Storage* 36, p. 102441. ISSN: 2352-152X.

DOI: 10.1016/j.est.2021.102441

Wang, W., H. Li, S. Guo, S. He, J. Ding, J. Yan, and J. Yang (July 2015). “Numerical simulation study on discharging process of the direct-contact phase change energy storage system”. en. In: *Applied Energy* 150, pp. 61–68. ISSN: 0306-2619.

DOI: 10.1016/j.apenergy.2015.03.108

Yang, B., F. Bai, Y. Wang, and Z. Wang (Mar. 2019). “Study on standby process of an air-based solid packed bed for flexible high-temperature heat storage: Experimental results and modelling”. en. In: *Applied Energy* 238, pp. 135–146. ISSN: 0306-2619.

DOI: 10.1016/j.apenergy.2019.01.073

Zanganeh, G., A. Pedretti, S. Zavattoni, M. Barbato, and A. Steinfeld (Oct. 2012). “Packed-bed thermal storage for concentrated solar power – Pilot-scale demonstration and industrial-scale design”. In: *Solar Energy* 86.10, pp. 3084–3098. ISSN: 0038-092X.

DOI: 10.1016/j.solener.2012.07.019

Zhang, N., Y. Yuan, X. Cao, Y. Du, Z. Zhang, and Y. Gui (2018). “Latent Heat Thermal Energy Storage Systems with Solid–Liquid Phase Change Materials: A Review”. In: *Advanced Engineering Materials* 20.6, p. 1700753. ISSN: 1527-2648.

DOI: 10.1002/adem.201700753

Zhou, H., X. Tian, M. Kou, S. Wu, and Y. Shen (Nov. 2021). “Numerical study of fine particles behaviors in a packed bed with lateral injection using CFD-DEM”. en. In: *Powder Technology* 392, pp. 317–324. ISSN: 0032-5910.

DOI: 10.1016/j.powtec.2021.07.019

Publications

The present dissertation is based on three peer-reviewed research articles published in scientific journals. Each manuscript presents results from experimental studies that contribute to this dissertation. In addition to these journal publications, two papers were presented at international conferences. This chapter provides these publications' full-length articles as well as a synopsis that contextualizes them.

1	Standby efficiency and thermocline degradation of a packed bed thermal energy storage: An experimental study	36
2	Packed bed thermal energy storage for waste heat recovery in the iron and steel industry: A cold model study on powder hold-up and pressure drop	45
3	Exergy efficiency and thermocline degradation of a packed bed thermal energy storage in partial cycle operation: An experimental study	54
	Contributions to international conferences	66
4	Development of a Digital Twin Platform for Industrial Energy Systems .	66
5	Study on the Standby Characteristics of a Packed Bed Thermal Energy Storage: Experimental Results and Model-Based Parameter Optimization	67

Beyond the core journal publications and the contributions to international conferences listed above, several further studies related to this dissertation were published in collaboration with colleagues. For each of these co-author publications, the abstract and a summary that links them to the contents of this dissertation are provided in this chapter.

	Co-author publications	68
6	Toward a Practical Digital Twin Platform Tailored to the Requirements of Industrial Energy Systems	68
7	A digital twin-based adaptive optimization approach applied to waste heat recovery in green steel production: Development and experimental investigation	69
8	Operation planning with thermal storage units using MILP: comparison of heuristics for approximating non-linear operating behaviour	70
9	Modeling Partial Cycle Behavior of a Thermal Storage in MILP: Comparison of Heuristics for Approximating Non-Linear Operating Behavior	71

Publication 1

Standby efficiency and thermocline degradation of a packed bed thermal energy storage: An experimental study

published in Applied Energy in collaboration with Felix Birkelbach, Heimo Walter, and René Hofmann.

In this study, the standby efficiency and the thermocline degradation of a packed bed thermal energy storage (PBTES) were experimentally investigated for different heat transfer fluid (HTF) flow directions. These investigations were motivated by special operational requirements (amongst other things, the conclusions from Publication 2) for a PBTES operated in an industrial environment. It was found that for standby periods lasting only a few hours, the thermocline degradation and the flow direction of the HTF in the preceding charging process do not affect the standby efficiency of a PBTES. However, for standby periods longer than 7 h, an accelerated thermocline degradation and a faster decrease of the standby efficiency occur if the PBTES was charged from the bottom. While the energy and exergy efficiency for a short standby period (0.5 h) are the same for both HTF flow directions during charging, for a standby period of 22 h they are lower by 5 % points and 18 % points if the storage is charged from the bottom respectively. Therefore, it was concluded that for a PBTES designed for long standby periods (multiple hours), an operating mode charged from the top is preferred.

Author contribution: Conceptualization, Methodology, Validation, Formal Analysis, Investigation, Data Curation, Writing - Original Draft, Visualization.

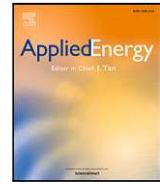
P. Schwarzmayr, F. Birkelbach, H. Walter, and R. Hofmann (May 2023a). "Standby efficiency and thermocline degradation of a packed bed thermal energy storage: An experimental study". In: Applied Energy 337, p. 120917. ISSN: 0306-2619.

DOI: 10.1016/j.apenergy.2023.120917



Contents lists available at ScienceDirect

Applied Energy

journal homepage: www.elsevier.com/locate/apenergy

Standby efficiency and thermocline degradation of a packed bed thermal energy storage: An experimental study

Paul Schwarzmayr^{*}, Felix Birkelbach, Heimo Walter, René Hofmann

Institute for Energy Systems and Thermodynamics, TU Wien, Getreidemarkt 9, Vienna, 1060, Austria

ARTICLE INFO

Keywords:

Packed bed
Thermal energy storage
Standby mode
Stratification
Thermocline degradation
Energy/exergy efficiency

ABSTRACT

The waste heat potential from industrial processes is tremendous and if it can be utilized it may significantly contribute to the mitigation of climate change. A packed bed thermal energy storage system is a low-cost storage technology that can be employed to enable the utilization of waste heat from industrial processes. This system can be used to store excess heat and release this energy when it is needed at a later time. To ensure the efficient operation of a packed bed thermal energy storage, its characteristics in standby mode need to be studied in great detail. In the present study, the standby efficiency and thermocline degradation of a lab-scale packed bed thermal energy storage in standby mode is experimentally investigated for different flow directions of the heat transfer fluid during the preceding charging period. Results show that for long standby periods, the standby efficiency is significantly affected by the flow direction of the heat transfer fluid. The maximum entropy generation rate for a 22 h standby process with the flow direction of the heat transfer fluid from the bottom to the top in the preceding charging process is twice as high as for the same process with reversed flow direction. Energy efficiency is 5% higher whilst exergy efficiency is even 18% higher in the process with reversed flow direction.

1. Introduction

The recovery of waste heat in the energy intensive industry has great potential to contribute to the mitigation of climate change. More than two thirds ($\approx 70\%$) of the industry sectors' energy demand is for heat [1]. For some sectors up to one half of this heat consumption is discharged as waste heat as stated by Papapetrou et al. [2], who estimated the available waste heat potential for the EU per industrial sector, temperature level and country. A similar study was conducted by Panayiotou et al. [3] who made an assessment of the waste heat potential in major European industries. In their study on the estimation of globally available waste heat, Forman et al. [4] concluded that 72% of the global primary energy consumption is dissipated during conversion. Especially in the iron and steel industry heat is often wasted because of temporal discrepancies of heat demand and supply. Thermal energy storage (TES) technologies can be used to improve the efficiency of these discontinuous batch processes by closing the gap between heat demand and supply. Manente et al. [5] studied the integration of TES systems into industrial energy processes and found that the integration of a TES, either of sensible or latent type [6], results in an enhanced energy efficiency and an increased process output.

A simple but highly efficient type of TES is a packed bed thermal energy storage (PBTES). Comprehensive reviews on PBTES systems were compiled by Gautam et al. [7,8] and Baoshan et al. [9]. Interesting

studies on novel design and air flow configurations of PBTES systems were conducted by Soprani et al. [10] and Knobloch et al. [11]. PBTES systems are sensible TES systems which use a packed bed of rocks or other suitable solids as storage material. To charge a PBTES, hot heat transfer fluid (HTF), in most cases air, passes through the bed, delivering heat to the storage material. For the recovery of stored heat the flow direction inside the storage is reversed and cold HTF is used to extract heat from the storage material. Since the HTF is in direct contact with the packed bed, a vast surface area is provided for the heat transfer inside the storage. This leads to very high power rates, a high temperature stratification inside the packed bed and therefore an overall enhancement of the system's efficiency. Temperature stratification means that the storage volume is separated into a hot and a cold section. These two sections are separated by a thin volume slice – the thermocline – where the whole temperature gradient is concentrated. During the charging process, hot HTF pushes the thermocline towards one end of the storage, expanding the hot section. During the discharging process, cold HTF pushes the thermocline in the opposite direction. For the characterization of thermoclines the authors refer to the work of Orò et al. [12], in which methods to describe stratification in TES are discussed. In theory, the discharging temperature of a PBTES is exactly as high as the charging temperature for the whole process when the thermocline is ideal. In reality, irreversible effects like heat

^{*} Corresponding author.

E-mail addresses: paul.schwarzmayr@tuwien.ac.at (P. Schwarzmayr), rene.hofmann@tuwien.ac.at (R. Hofmann).

<https://doi.org/10.1016/j.apenergy.2023.120917>

Received 2 December 2022; Received in revised form 7 February 2023; Accepted 23 February 2023

Available online 2 March 2023

0306-2619/© 2023 The Author(s). Published by Elsevier Ltd. This is an open access article under the CC BY license (<http://creativecommons.org/licenses/by/4.0/>).

Nomenclature**Acronyms**

ASU	Air supply unit
EU	European Union
FWD	Forward
HTF	Heat transfer fluid
LD	Linz-Donawitz
PBTES	Packed bed thermal energy storage
REV	Reverse
RTD	Resistance temperature detector
TES	Thermal energy storage

Roman symbols

A	Surface area in m^2
B	Exergy in J
\dot{B}	Exergy flow rate in W
c	Specific heat capacity of storage material $J kg^{-1} K^{-1}$
c_p	Specific heat capacity at constant pressure for HTF in $J kg^{-1} K^{-1}$
h	Specific enthalpy in $J kg^{-1}$
k	Heat transfer coefficient in $W m^{-2} K^{-1}$
M	Momentum of energy in J m
m	Mass of storage material in kg
\dot{m}	Mass flow rate of HTF in $kg s^{-1}$
MIX	MIX number
n	Number of vertical volume sections $n = 9$
Q	Heat in J
\dot{Q}	Heat flow rate from/to HTF or surrounding in W
S	Entropy in $J K^{-1}$
\dot{S}	Entropy flow rate in $W K^{-1}$
T	Temperature in K
t	Time in s
U	Internal energy in J

Greek symbols

λ	Thermal conductivity in $W m^{-1} K^{-1}$
η	Efficiency

Subscripts

amb	Ambient
b	Exergy
$charge$	Charge
e	Energy
exp	Experimental
gen	Generation
HTF	Heat transfer fluid
i	Volume element index
in	Inlet

lat	Lateral
mix	Mixed
out	Outlet
Q	Heat
$recover$	Recover
ref	Reference ($T_{ref} = 295.15 K$)
rel	Relative
s	Surface
str	Stratified
sys	System
t/b	Top/bottom

were drawn by Stekli et al. [14], who point out that the biggest techno-economic challenge of thermocline TES systems is thermocline degradation. An experimental study on multiple consecutive charging/discharging cycles was carried out by Bruch et al. [15,16] on a PBTES with rocks as storage material and thermal oil as HTF. Bruch et al. concluded that for a well-designed and well-operated PBTES in dynamic operation, i.e. consecutive charging/discharging cycles, thermocline degradation is negligible. However, Okello et al. [17] found that if the heat stored in a stratified storage is to be used after some time (12–24 h), a significant degradation of the thermocline and therefore significant exergy losses can be observed as the system tries to reach thermodynamic equilibrium.

Studies associated with static operation, i.e. the standby mode, of TES systems such as the paper from Okello et al. are rare. Mertens et al. [18] numerically investigated a PBTES for concentrated solar power (CSP) applications, also considering the standby mode. Xu et al. [19] carried out numerical studies on the standby mode of a PBTES with molten salt as HTF. The most recent publications considering the static operation of a PBTES are from Rodrigues et al. [20], Gavino et al. [21] and Yang et al. [22]. Rodrigues et al. numerically investigated the destratification after a charging process also considering laminar natural convection including the local thermal non-equilibrium assumption. The study from Yang et al. includes numerical investigations with experimental validation on both the dynamic and static operation of a pilot-scale PBTES test rig. Both studies only investigated the standby process after charging a TES from the top. Given that a hot section and a cold section coexist in the storage, buoyancy effects and therefore natural convection may occur in the tank. Hence, a vertical flow direction of the HTF and charging the TES from the top will always be the first choice [13] in order to minimize destratification, especially during considerably long standby periods.

However, there are scenarios in which it is much more convenient to charge a PBTES from the bottom and discharge it from the top in order to meet certain design criteria [23]. At industrial scale the maximum height of a PBTES is limited to approximately 16 m because of mechanical reasons [13] which furthermore limits the maximum storage capacity of a single storage. A possible solution for that is, to build several smaller storage tanks and connect them to each other in series or parallel. One way for a series connection of multiple tanks is to connect the bottom of the first tank to the bottom of the second tank, the top of the second tank to the top of the third tank and so on. This configuration reduces the pipe length between two tanks and is therefore the most energy- and cost-efficient approach. However, it also means that half of the storage tanks are charged from the top and discharged from the bottom and the other half are charged from the bottom and discharged from the top. At this point, the impact of the HTF flow direction during the preceding charging process on the thermocline degradation and the standby efficiency of a PBTES is of high interest. To the best of the authors' knowledge, no studies that aim to compare the standby efficiency and the thermocline

losses to the surrounding, thermal conduction and natural convection inside the packed bed lead to a degradation of the thermocline and therefore to a reduced efficiency of the storage. An extensive review on experience feedback and numerical modeling of PBTES systems was compiled by Esence et al. [13], in which they point out the importance of maintaining high temperature stratification in a PBTES in order to maximize exergy efficiency and storage capacity. Similar conclusions

degradation of a PBTES that was charged from the top with a PBTES that was charged from the bottom exist. In order to close this research gap, the present study investigates the standby process of a PBTES for both scenarios. The results include numerical reference values of entropy generation inside the packed bed as well as energy- and exergy efficiencies of the storage. These values allow the comparison of both scenarios and the quantification of the impact of the HTF flow direction during the preceding charging process on the standby efficiency and the thermocline degradation of a PBTES.

Section 2 of this paper includes a presentation of the experimental setup used for the investigations as well as a description of the utilized measurement equipment, the sensor layout and the measurement control. In Section 3, the first and second law of thermodynamics are used for data analysis so that the internal effects in a PBTES during a standby period can be quantified. In the end of Section 3 the impact of measurement errors on the calculated quantities is presented and briefly discussed. The experimental data and the derived results are debated in Section 4. An interpretation of the entropy generation equation along with reference values for energy and exergy efficiencies under different operational conditions are given and comprehensively discussed. Finally, Section 5 provides a summary of the main results as well as a conclusion considering the consequences and the potential of the novel insights collected in this work.

2. Material and methods

The experimental setup for the present investigations consists of a lab-scale PBTES test rig filled with slag as storage material. The specific slag utilized for the experiments is a by-product from a steel producing process called the Linz-Donawitz(LD)-process and consists of irregular shaped, porous rocks (see Fig. 1).



Fig. 1. PBTES test rig at the laboratory of TU Wien: with thermal insulation (left), storage material (center), without thermal insulation (right).

The geometric shape of this LD-slag enhances the heat transfer between the HTF and the storage material and results in an even and homogeneous perfusion of the packed bed. The storage tank is a vertically standing, conical steel vessel filled with storage material. In order to minimize heat losses to the surrounding the TES is insulated with multiple layers of ceramic wool, rock wool and aluminum sheeting. Fig. 1 shows the test rig before and after installing the thermal

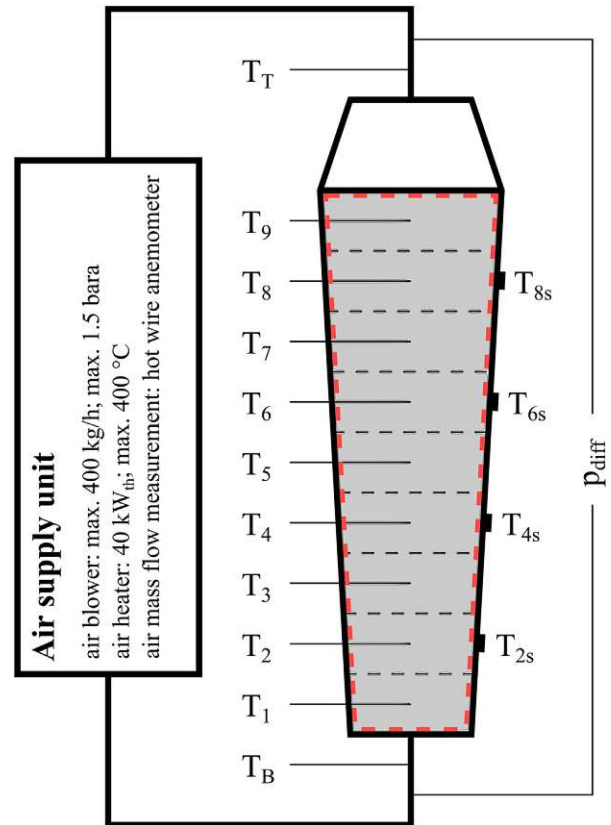


Fig. 2. Storage instrumentation and discretization.

insulation. The test rig is connected to an air supply unit (ASU) that provides air with temperatures from 20 °C to 400 °C and a mass flow from 100 kg h⁻¹ to 400 kg h⁻¹.

Additionally, the experimental setup is equipped with several temperature and differential pressure sensors. In Fig. 2 a simplified P&ID-diagram including the relevant equipment for the present investigations is depicted. For detailed information about the sensor layout and the process control system the authors refer to their previous work [24]. Four-wire resistance temperature detectors (RTD) class AA (or 1/3 DIN) PT100 sensors are utilized for the temperature measurements. The test rig is equipped with two PT100 temperature sensors (T_T and T_B), that measure the HTF temperature at the in-/outlet of the storage vessel as well as nine PT100 temperature sensors (T_1, T_2, \dots, T_9) inside the packed bed and eight PT100 temperature sensors ($2 \times T_{s2}, 2 \times T_{s4}, 2 \times T_{s6}, 2 \times T_{s8}$) on the lateral surface of the storage between the steel vessel and the first layer of insulation. For data analysis the storage volume is vertically discretized into nine sections as it is shown in Fig. 2. Each of these sections is equipped with a temperature sensor located at the center axis of the storage volume. The eight sensors on the lateral surface of the TES are mounted in pairs opposite of each other in every second section of the TES. To simplify matters, only one sensor of each pair is shown in Fig. 2. Measurements for the HTF mass flow, humidity and the temperature of the surrounding are provided by the ASU. For a measured value of 300 °C, the measurement error of the temperature sensors including all steps of signal conversion do not exceed ± 0.6 °C. The mass flow of the HTF is measured with a hot-wire anemometer with a maximum measurement error of 4% with respect to the measured value. Details on the test rig geometry, properties of the storage material and operational parameters used for the experiments are given in Table 1.

Table 1
Summary of parameters: Test rig geometry, data/properties of storage material, operational parameters.

Test rig	
Storage type	Vertical PBTES
Tank material	P295
Tank diameter	350 mm (bottom), 500 mm (middle), 650 mm (top)
Tank height	2050 mm
Storage volume	0.405 m ³
Thermal insulation	100 mm of ceramic wool ($\lambda = 0.055 \text{ W m}^{-1} \text{ K}^{-1}$),
	80 mm of rock wool ($\lambda = 0.04 \text{ W m}^{-1} \text{ K}^{-1}$),
	0.1 mm of aluminum sheeting
Storage material	
Type of storage material	LD-slag (irregular shaped, partly porous) CaO (24–49%), SiO ₂ (6–37%),
Composition of storage material	Fe, O _y (10–36%), MgO (0–13%),
	Al ₂ O ₃ (0–7%), Cr ₂ O ₃ (0–0.55%)
Grain size	16 mm to 32 mm
Particle density	3800 kg m ⁻³
Porosity	0.42
Bulk density	2200 kg m ⁻³
Specific heat capacity	900 J kg ⁻¹ K ⁻¹
Operating parameters	
Mass of storage material	891 kg
Air mass flow	200 kg h ⁻¹
Charging temperature	300 °C
Recovery temperature	20 °C
Mean superficial air velocity	1 m s ⁻¹

For the investigations carried out in this work, experiments for different standby times are conducted. The experiments start with an empty storage (temperatures inside the storage between 20 °C to 25 °C) before it is charged for 2 h. As soon as the charging process is completed, the TES remains in standby for various periods of time (0.5 h and 22 h). Subsequently the stored heat is recovered. The cut-off temperature for the discharging process is set at 70 °C. This procedure is repeated for both scenarios: charging the TES from the top, which will be referred to as forward-case (FWD-case) and charging the TES from the bottom, which will be referred to as reversed-case (REV-case).

3. Theory and calculations

To characterize stratification and standby efficiency of a PBTES, several methods and parameters have been proposed over the past few years [12]. The most suitable parameter for a TES with a conical storage tank and therefore an uneven distribution of the storage mass along the vertical axis is the *MIX* number. This dimensionless number was defined by Andersen et al. [25] and is based on the momentum of energy. The *MIX* number can be calculated with

$$MIX = \frac{M_{str} - M_{exp}}{M_{str} - M_{mix}} \quad (1)$$

where M_{exp} is the momentum of energy derived from experimental data, M_{str} is the momentum of energy for a perfectly stratified storage and M_{mix} is the momentum of energy of a perfectly mixed storage. Both M_{str} and M_{mix} are calculated for the TES, storing the same amount of energy as derived from the experimental data. For a perfectly stratified storage the *MIX* number equals 0, for a perfectly mixed storage the *MIX* number equals 1. For details on the calculation procedure of the *MIX* number the authors refer to [12].

In order to quantify the impact of the charging direction of a PBTES on the thermocline degradation and the standby efficiency, data analysis is conducted in a specific way, so that effects due to heat losses to the surrounding and effects due to heat transfer inside the packed bed can be examined separately. This is elegantly achieved by making use of the entropy generation equation (Eq. (2)), i.e. the expression of the second law of thermodynamics for closed systems. The left side of

this equation represents the change in system entropy. The right side is the sum of the entropy introduced into the system due to heat crossing the system boundary and the entropy generated within the system.

If this equation is applied to a system with suitable system boundaries, the entropy generation term δS_{gen} is solely influenced by irreversible effects due to heat transfer inside the packed bed. For the present work, a system with boundaries that enclose nothing more than the packed bed itself is chosen (marked by the red dashed line in Fig. 2). Hereby, only irreversible effects caused by heat transfer inside the packed bed contribute to the entropy generation term and irreversibilities due to heat transfer to the surrounding are not included. The entropy generation equation for the chosen system can be written as

$$\sum_{i=1}^n dS_{sys,i}(t) = \frac{\delta Q_{t/b}(t)}{T_{t/b}(t)} + \sum_{i=1}^n \frac{\delta Q_{lat,i}(t)}{T_i(t)} + \delta S_{gen} \quad (2)$$

where dS_{sys} is the change in system entropy, $\delta Q_{t/b}$ and δQ_{lat} represent heat crossing the system boundary at a temperature of $T_{t/b}$ and T_i respectively and δS_{gen} stands for the entropy generation inside the system. The change in system entropy (left side of Eq. (2)) can be calculated from the measured temperature data using the equation of state

$$dS_{sys,i}(t) = m_i \int_{T_i(t)}^{T_i(t+dt)} \frac{c(T)}{T} dT \quad (3)$$

where m_i is the mass of the storage material in each of the nine sections of the test rig, c is the specific heat capacity of the storage material and T is the absolute temperature in Kelvin. For the next term in Eq. (2) which represents the entropy introduced into the system due to heat crossing the system boundary, the heat losses to the surrounding need to be calculated. With a suitable correlation for the Nusselt number for natural convection on a vertically standing cylinder [26], the lateral heat loss rate to the surrounding for each of the nine sections of the TES can be calculated by

$$\dot{Q}_{lat,i}(t) = k A_{lat,i} (T_{amb} - T_{s,i}) \quad (4)$$

where \dot{Q}_{lat} is the heat flow rate through the lateral surface of the test rig, k is the heat transfer coefficient of the test rig's wall, A_{lat} is the lateral surface of the test rig, T_{amb} is the temperature of the ambient air surrounding the test rig and T_s is the temperature between the steel vessel and the first layer of thermal insulation. The heat transfer coefficient k in Eq. (4) is calculated from geometry data, the heat transfer coefficient to the surrounding and thermo-physical properties of the insulation material (see Table 1). The thermal conductivity of the insulation material is assumed to be constant for the whole temperature range. For $T_{s,i}$ the measurements of the temperature sensors between the steel vessel and the first layer of insulation are used.

Considering the standby process of the TES, where the only heat crossing the system boundary are heat losses to the surrounding, the energy balance for the packed bed can be written as

$$\sum_{i=1}^n dU_{sys,i}(t) = \delta Q_{t/b}(t) + \sum_{i=1}^n \delta Q_{lat,i}(t). \quad (5)$$

where dU_{sys} is the change in the system's internal energy, which equals the sum of all heat losses. This equality allows the calculation of the heat losses through the top and the bottom surface of the packed bed $\delta Q_{t/b}$. Finally, Eq. (2) can be rearranged to calculate the entropy generation inside the system.

An alternative way to make statements about the impact of the charging direction on the thermocline degradation and the standby efficiency is to calculate energy and exergy round-trip efficiencies in the FWD- and REV-case and to compare them. Therefore characteristic parameters like the thermal power rate of the storage and the stored/recovered thermal energy for the charging and discharging processes need to be calculated. The power rate can be determined by

the energy balance for the HTF flow passing through the packed bed and can be expressed as

$$\dot{Q}(t) = \dot{m}(t) \int_{T_{in}(t)}^{T_{out}(t)} c_p(T) dT \quad (6)$$

where \dot{Q} is the heat flow rate to/from the HTF, \dot{m} is the mass flow rate of the HTF passing through the packed bed, c_p is the specific heat capacity of the HTF at isobaric conditions and T_{in} and T_{out} are the temperatures of the HTF entering and exiting the storage tank. The stored/recovered energy U is defined as the integral of the heat flow rate over a certain interval of time:

$$U(t) = \int_{t_0}^t \dot{Q}(t) dt \quad (7)$$

The stored/recovered exergy B can be determined analogous to Eq. (7) by substituting \dot{Q} with \dot{B} . The rate of exergy in-/output is calculated using another expression of the second law of thermodynamics applied to the HTF flow passing through the packed bed by

$$\dot{B}(t) = \dot{Q}(t) - T_{ref} \dot{m}(t) \int_{T_{in}}^{T_{out}} \frac{c_p(T)}{T} dT \quad (8)$$

where \dot{B} is the rate of exergy in-/output and T_{ref} is the reference temperature for the entropy. Finally, the energy efficiency η_e and the exergy efficiency η_b can be calculated as the ratios of the recovered quantities $U_{recovered}$ and $B_{recovered}$ to the stored quantities U_{charge} and B_{charge} .

$$\eta_e = \frac{U_{recovered}}{U_{charge}}, \quad \eta_b = \frac{B_{recovered}}{B_{charge}} \quad (9)$$

3.1. Uncertainty analysis

The law of error propagation is used to estimate the impact of measurement errors on the derived quantities. For calculations where only measurements from temperature sensors are brought into the equation, the resulting uncertainties are insignificant compared to the measured values (<1%). Calculations where the HTF mass flow is involved show slightly higher errors in the calculated quantities. In Eq. (10) the law of error propagation applied to the energy balance in Eq. (6) is given. The error in the heat flow rate $\delta\dot{Q}$ can be calculated by using the formula

$$\delta\dot{Q}^2 = \left(\frac{\partial\dot{Q}}{\partial\dot{m}}\right)^2 \delta\dot{m}^2 + \left(\frac{\partial\dot{Q}}{\partial h_{in}}\right)^2 \delta h_{in}^2 + \left(\frac{\partial\dot{Q}}{\partial h_{out}}\right)^2 \delta h_{out}^2 \quad (10)$$

where

$$\delta h = c_p(T) \delta T \quad (11)$$

and h_{in} and h_{out} are the specific enthalpies of the HTF entering and exiting the storage tank. With the maximum errors of the measurement devices ($\delta\dot{m} = \pm 8 \text{ kg h}^{-1}$ and $\delta T = \pm 0.6^\circ\text{C}$), errors in the heat flow rate $\delta\dot{Q}$ and the exergy in-/output rate $\delta\dot{B}$ are well below 4% with respect to the measured values. The error of the calculated heat flow rate is illustrated in Fig. 6 in Section 4. These uncertainties do not have an impact on the quality of the results in the present work.

4. Results and discussion

The data collected in the experiments and described at the end of Section 2 are used to make qualitative and quantitative statements on the standby efficiency and the thermocline degradation of the examined PBTES test rig. Fig. 3 shows the degradation of the thermocline inside the test rig after charging the TES for 2 h from the top (FWD-case; upper graph) and from the bottom (REV-case; lower graph).

The thermocline immediately after the charging process (standby time equals zero) is represented by the solid blue lines. The o-markers show the vertical positions of the temperature sensors. For both flow directions the thermoclines have a similar shape after charging. The slight shift in the positions of the thermoclines is due to the slightly

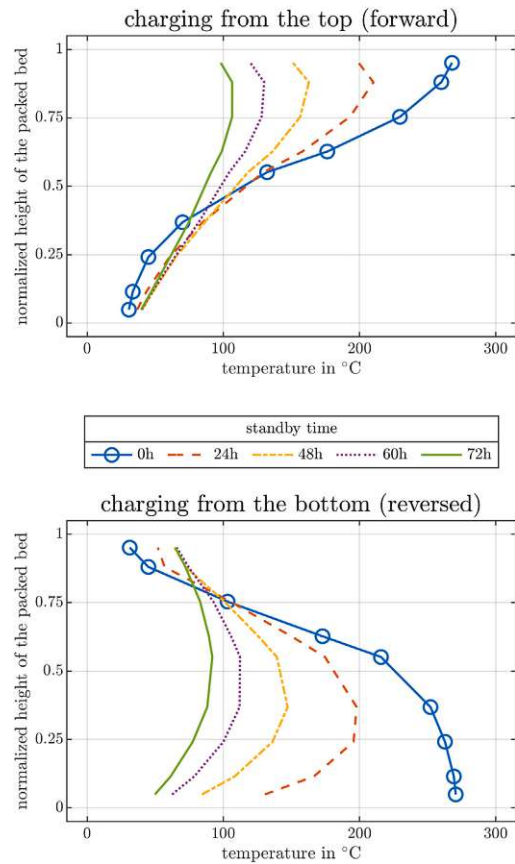


Fig. 3. Thermocline degradation for charging from the top (upper graph) and charging from the bottom (lower graph) during a standby period.

uneven mass distribution of the storage material as a result of the conical shape of the storage vessel.

After some time in standby mode, the temperature in the storage decreases and the thermoclines start to degrade as it is shown in Fig. 3. In the FWD-case, the thermocline flattens and retains its shape within the whole standby period. The slight bend in the thermocline at the hot end (top) of the packed bed is due to heat losses through the top surface. In the REV-case, the thermocline flattens as well but, in addition it significantly changes its shape. Likewise, a bend at the hot end of the thermocline can be observed, which is due to heat losses through the bottom surface of the packed bed. In this case, however, the bend is much more accentuated, owing to the fact that in the first case (FWD-case), the thermocline is self-stabilizing due to buoyancy effects, which it is not in the second case (REV-case). In the FWD-case the heat losses through the top surface are partially compensated by heat transfer to the top as a result of natural convection, whilst there are no effects that could possibly compensate the heat losses through the bottom surface in the REV-case. In addition to the differences in this specific bend, a faster degradation of the thermocline can be noticed in the REV-case. In contrast to the FWD-case, the temperature at the cold end (top) of the packed bed rises and the maximum temperature inside the storage moves towards the cold end.

In Fig. 4 the MIX number in the FWD-case and the REV-case for a standby period of 96 h is illustrated. In both cases the MIX number is ≈ 0.08 at the beginning of the standby process. In the FWD-case the MIX number slightly increases in the first half of the standby period and levels out at a value of ≈ 0.13 , which indicates a very stable thermal stratification throughout the whole standby period. A

completely different behavior can be observed in the REV-case. There, the MIX number rises for the whole standby period until it reaches the maximum value of 1 after 96 h which indicates a fully mixed storage. These observations suggest that natural convection in the packed bed may have a noticeable impact on the standby mode of a PBTES.

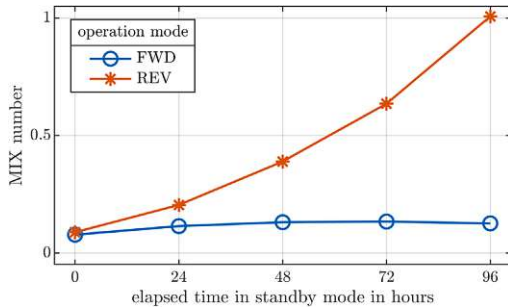


Fig. 4. Comparison of the MIX number in the FWD- and the REV-case for a standby period of 96 h.

For the quantification of these effects the entropy generation equation in Eq. (2) is used. The result of these evaluations are visualized in Fig. 5. This graph includes the three terms from Eq. (2) plotted as separate curves for a standby period of the test rig after 2 h of charging for both, the FWD- and the REV-case. Blue lines with o-markers show the rate of change in system entropy \dot{S}_{sys} , red lines with *-markers show the entropy flow rates due to the heat flow rate across the system boundary \dot{S}_Q and the green lines with □-markers show the entropy generation rate inside the system \dot{S}_{gen} . The x-axis represents the elapsed time in standby mode. Notice that the absolute values of \dot{S}_{sys} and \dot{S}_Q are higher in the REV-case. This is because of the higher heat losses to the surrounding due to a higher surface-to-volume ratio in the bottom half of the storage. Nevertheless, these additional heat losses do not have an impact on the results and conclusions drawn in the present work, as it will be discussed later in this section.

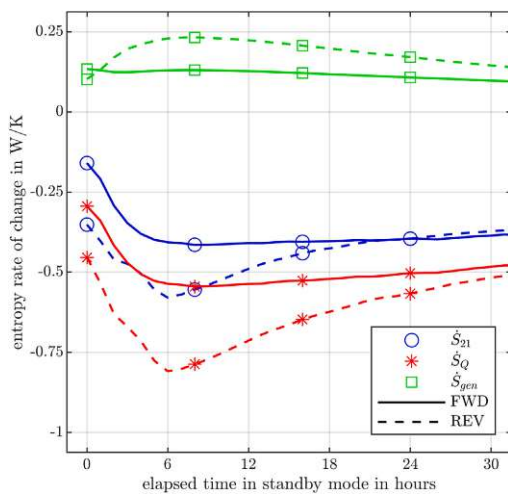


Fig. 5. Entropy generation for a standby period of 30 h.

Of much higher interest is the fact, that there is a significant difference in the entropy generation rate \dot{S}_{gen} . As explained in Section 3, this term is solely influenced by irreversible effects inside the packed bed, which could be heat transfer due to conduction, heat transfer due to natural convection and heat transfer due to radiation. Heat transfer due

to radiation is negligible because of the vanishingly small temperature differences inside the packed bed. In the FWD-case the hot zone in the storage is above the cold zone which makes the effects of natural convection equally insignificant. Therefore, the entropy generation in the FWD-case is only caused by irreversible effects due to heat conduction in the solid storage material. Because the thermal conduction is not affected by buoyancy forces, the entropy generation due to heat conduction will be the same in the REV-case. Considering Fig. 5 these assumptions appear to be true within the first few minutes of the standby period. However, in the REV-case, the entropy generation term increases until it reaches a maximum with two times the value of the FWD-case after about 7 h in standby. This extra entropy production can only be explained by irreversible effects caused by heat transfer due to natural convection inside the packed bed. In addition, it can be determined, that it takes the system about 7 h to establish a fully developed air circulation inside the packed bed.

These results are also supported by the evaluation of the efficiencies defined in Eq. (9). If one considers the ratio η_b/η_c , where η_b is the exergy round-trip efficiency and η_c the energy round-trip efficiency, the value of this ratio would equal 1 for both, the FWD- and the REV-case, if no irreversible effects like heat transfer were present inside the system, even if heat losses to the surrounding were different for both cases. It would be less than 1, but still the same value for both cases, if irreversible effects were present to the same extent, again, even if heat losses to the surrounding were different. However, if the value of this ratio is different in the FWD-case and the REV-case, more irreversible effects occur in the case with the smaller ratio (η_b/η_c). And that is exactly what is found in the evaluation of the measured data (see Table 2). The argumentation of why these additional irreversibilities can only be caused by heat transfer due to natural convection is the same as before.

Table 2
Energy- and exergy efficiencies for experiments with different charging directions (FWD and REV) and standby times (0.5 h and 22 h).

		FWD	REV	$\Delta\eta_{rel}$
0.5 h	η_c	0.92	0.93	$\approx 0\%$
	η_b	0.83	0.84	$\approx 0\%$
	η_b/η_c	0.90	0.90	
22 h	η_c	0.74	0.70	$\approx 5\%$
	η_b	0.55	0.45	$\approx 18\%$
	η_b/η_c	0.74	0.64	

Now that it has been shown that the influence of natural convection on the standby efficiency of a PBTES depends on the HTF flow direction in the preceding charging period, some important metrics that can be derived from the data are presented and discussed in the following paragraphs. In Fig. 6 the normalized energy in-/output rate is plotted over the normalized stored/recovered energy for different experiments. The energy input rate and the stored energy at the end of the charging process are used for the normalization of the calculated quantities. All experiments start with an empty storage (stored energy equals zero) and an energy input rate of zero. This starting point is marked with a black circle in Fig. 6. During the following charging process the test rig shows similar behaviors for every experiment (black solid line with arrow markers). After 2 h of charging the HTF flow is stopped and the storage is switched to the standby mode. The recovery of the stored heat (discharging) is started after 0.5 h in standby for one half of the experiments and after 22 h in standby for the other half. Considering an ideal storage with zero heat losses to the surrounding and without thermocline degradation the discharging curve would continue following the solid black line, regardless of the standby time. In practice, however, the discharging behavior of the storage is different. The discharging curves deriving from the measured data of the experiments are plotted as colored lines in Fig. 6. It can be observed, that the longer the standby period between charging and discharging the storage, the

less energy can be recovered. In the experiments, where the storage is switched to the discharging mode after only 0.5 h of standby time – which is the minimum standby time that can be realized due to the thermal inertia of the ASU – the energy efficiency is remarkably high (92%) and very similar to the observations of Bruch et al. [16]. Furthermore, even 87% of the theoretically possible maximum energy output rate is reached in the experiments with 0.5 h of standby time. These results are similar for both, the FWD-case (dotted blue line) and the REV-case (dashed red line) experiments. In the other experiments with much longer time periods in standby mode, the results for both cases begin to diverge. When the discharging process is started after 22 h in standby mode, the energy efficiency in the FWD-case (dashed green line) is observed to be 74% in contrast to 70% in the REV-case (solid yellow line). Similar discrepancies apply to the energy output rate. 65% and 62% of the theoretically possible maximum energy output rate are reached in the FWD- and REV-case respectively.

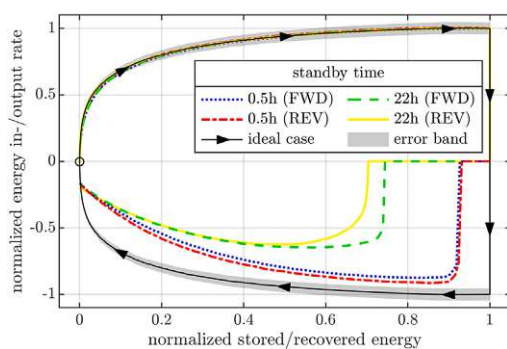


Fig. 6. Energy in-/output rate over stored/recovered energy.

The exergy efficiencies are generally lower than the energy efficiencies due to entropy generation inside the packed bed caused by finite heat transfer between the storage material and the HTF, which can be seen in Fig. 7. For a standby time of 0.5 h the exergy efficiency is already as low as 83%. Which again is similar for both, the FWD-case (dotted blue line) and the REV-case (dashed red line) experiments. In experiments with longer time periods in standby mode exergy efficiencies of 55% and 45% can be observed in the FWD- (dashed green line) and the REV-case (solid yellow line) respectively. These results are summarized in Table 2.

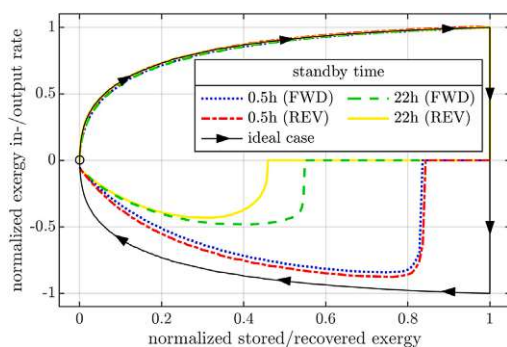


Fig. 7. Exergy in-/output rate over stored/recovered exergy.

It can be observed that for a standby time of 0.5 h the efficiencies for both, the FWD- and the REV-case are nearly the same. This means, that both cases can be seen as equivalent and no additional losses have to be expected, even if the flow direction of the HTF in the preceding charging process is from the bottom to the top. In contrast, losses in the energy efficiency of 5% and losses in the exergy efficiency of 18% are

observed for a standby time of 22 h and the same operational parameters. Finally, it should be mentioned that the calculated efficiencies apply to a PBTES system with similar geometry, insulation and storage temperatures as described in Section 2 and Table 1. The results and conclusions drawn in this work are representative for all types of TES that utilize a packed bed as storage material and a gas as HTF. However, one has to be aware that for a PBTES, where one of these parameters is significantly different, the system's efficiencies may differ from the ones presented in this work.

5. Conclusion

This study examines the standby efficiency of a packed bed thermal energy storage for different flow directions of the heat transfer fluid in the preceding charging process. The test rig used for the experimental investigations is a lab-scale packed bed thermal energy storage with a vertical flow of the heat transfer fluid. The storage tank is filled with LD-slag in the form of irregular shaped, porous rocks with a particle size of 16 mm to 32 mm as storage material and it uses air as heat transfer fluid.

The results reveal that if the heat stored in a packed bed thermal energy storage is recovered immediately after the charging process, an energy efficiency of 92% and an exergy efficiency of 83% can be reached. This applies to both scenarios: charging the storage from the top and from the bottom. In this case, the fluid flow direction in the preceding charging process does not have an impact on the system's energy and exergy efficiency. However, the efficiencies and thermocline degradation during a long standby period of the storage significantly depend on the flow direction of the heat transfer fluid in the preceding charging process. If the flow direction in the preceding charging process is from the bottom to the top, the entropy generation in the packed bed and thus exergy losses due to irreversible effects during the standby period are twice as high compared to the forward flow direction. This difference is attributed to natural convection. In contrast to energy and exergy efficiencies of 74% and 55% when charging the storage from the top and discharging it from the bottom, significantly lower values of 70% and 45% could be observed when charging the storage from the bottom and discharging it from the top. Furthermore, it could be shown that it takes 7 h until a fully developed air circulation is established inside the packed bed of the analyzed system. Considering a storage system with a maximum standby time well below 7 h, the fluid flow direction in the preceding charging process does not have an impact on this storage's standby efficiency. However, if a system is designed for much longer standby periods, charging the storage from the top will lead to significantly higher energy and exergy efficiencies. The consequence of charging the storage from the bottom instead of charging it from the top is a decrease in energy and exergy efficiency of 5% and 18% for a 22 h standby period.

The results presented in this work provide detailed information about the efficiency of a packed bed thermal energy storage that can be used as a basis of economic assessments and payback period calculations. Therefore, this study contributes to the development of thermal energy storage systems aiming for their deployment in order to make use of the industry sectors' enormous waste heat potential.

CRedit authorship contribution statement

Paul Schwarzmayr: Conceptualization, Methodology, Validation, Formal analysis, Investigation, Data curation, Writing – original draft, Visualization. **Felix Birkelbach:** Conceptualization, Methodology, Formal analysis, Writing – review & editing. **Heimo Walter:** Conceptualization, Methodology, Formal analysis, Writing – review & editing, Visualization, Supervision. **René Hofmann:** Conceptualization, Validation, Writing – review & editing, Supervision, Funding acquisition.

Declaration of competing interest

The authors declare that they have no known competing financial interests or personal relationships that could have appeared to influence the work reported in this paper.

Data availability

Data will be made available on request.

Acknowledgments

The authors acknowledge funding support of this work through the research project *5DIndustrialTwin* as part of the Austrian Climate and Energy Fund's initiative Energieforschung (e!MISSION) 6th call (KLIEN/FFG project number 881140). Furthermore, the authors acknowledge TU Wien Bibliothek for financial support through its Open Access Funding programme.

References

- [1] Jouhara H, Olabi AG. Editorial: Industrial waste heat recovery. *Energy* 2018;160:1–2. <http://dx.doi.org/10.1016/j.energy.2018.07.013>.
- [2] Papapetrou M, Kosmadakis G, Cipollina A, La Commare U, Micale G. Industrial waste heat: Estimation of the technically available resource in the EU per industrial sector, temperature level and country. *Appl Therm Eng* 2018;138:207–16. <http://dx.doi.org/10.1016/j.applthermaleng.2018.04.043>.
- [3] Panayiotou GP, Bianchi G, Georgiou G, Aresti L, Argyrou M, Agathokleous R, Tsamos KM, Tassou SA, Florides G, Kalogirou S, Christodoulides P. Preliminary assessment of waste heat potential in major European industries. *Energy Procedia* 2017;123:335–45. <http://dx.doi.org/10.1016/j.egypro.2017.07.263>.
- [4] Forman C, Muritala IK, Pardemann R, Meyer B. Estimating the global waste heat potential. *Renew Sustain Energy Rev* 2016;57:1568–79. <http://dx.doi.org/10.1016/j.rser.2015.12.192>.
- [5] Manente G, Ding Y, Sciacovelli A. A structured procedure for the selection of thermal energy storage options for utilization and conversion of industrial waste heat. *J Energy Storage* 2022;51:104411. <http://dx.doi.org/10.1016/j.est.2022.104411>.
- [6] Scharinger-Urschitz G, Schwarzmayr P, Walter H, Haider M. Partial cycle operation of latent heat storage with finned tubes. *Appl Energy* 2020;280:115893. <http://dx.doi.org/10.1016/j.apenergy.2020.115893>.
- [7] Gautam A, Saini RP. A review on sensible heat based packed bed solar thermal energy storage system for low temperature applications. *Sol Energy* 2020;207:937–56. <http://dx.doi.org/10.1016/j.solener.2020.07.027>.
- [8] Gautam A, Saini RP. A review on technical, applications and economic aspect of packed bed solar thermal energy storage system. *J Energy Storage* 2020;27:101046. <http://dx.doi.org/10.1016/j.est.2019.101046>.
- [9] Xie B, Baudin N, Soto J, Fan Y, Luo L. Thermocline packed bed thermal energy storage system: a review. In: Jeguirim M, editor. *Renewable energy production and distribution. Advances in renewable energy technologies*, Vol. 1, Academic Press; 2022, p. 325–85. <http://dx.doi.org/10.1016/B978-0-323-91892-3.24001-6>.
- [10] Soprani S, Marongiu F, Christensen L, Alm O, Petersen KD, Ulrich T, Engelbrecht K. Design and testing of a horizontal rock bed for high temperature thermal energy storage. *Appl Energy* 2019;251:113345. <http://dx.doi.org/10.1016/j.apenergy.2019.113345>.
- [11] Knobloch K, Muhammad Y, Costa MS, Moscoso FM, Bahl C, Alm O, Engelbrecht K. A partially underground rock bed thermal energy storage with a novel air flow configuration. *Appl Energy* 2022;315:118931. <http://dx.doi.org/10.1016/j.apenergy.2022.118931>.
- [12] Oró E, Castell A, Chiu J, Martín V, Cabeza LF. Stratification analysis in packed bed thermal energy storage systems. *Appl Energy* 2013;109:476–87. <http://dx.doi.org/10.1016/j.apenergy.2012.12.082>.
- [13] Esence T, Bruch A, Molina S, Stutz B, Fourmigué J-F. A review on experience feedback and numerical modeling of packed-bed thermal energy storage systems. *Sol Energy* 2017;153:628–54. <http://dx.doi.org/10.1016/j.solener.2017.03.032>.
- [14] Stekli J, Irwin L, Pitchumani R. Technical Challenges and Opportunities for Concentrating Solar Power With Thermal Energy Storage. *J Therm Sci Eng Appl* 2013;5(2). <http://dx.doi.org/10.1115/1.4024143>.
- [15] Bruch A, Fourmigué JF, Couturier R. Experimental and numerical investigation of a pilot-scale thermal oil packed bed thermal storage system for CSP power plant. *Sol Energy* 2014;105:116–25. <http://dx.doi.org/10.1016/j.solener.2014.03.019>.
- [16] Bruch A, Molina S, Esence T, Fourmigué JF, Couturier R. Experimental investigation of cycling behaviour of pilot-scale thermal oil packed-bed thermal storage system. *Renew Energy* 2017;103:277–85. <http://dx.doi.org/10.1016/j.renene.2016.11.029>.
- [17] Okello D, Nydal OJ, Banda EJK. Experimental investigation of thermal de-stratification in rock bed TES systems for high temperature applications. *Energy Convers Manage* 2014;86:125–31. <http://dx.doi.org/10.1016/j.enconman.2014.05.005>.
- [18] Mertens N, Alobaid F, Frigge L, Eppe B. Dynamic simulation of integrated rock-bed thermocline storage for concentrated solar power. *Sol Energy* 2014;110:830–42. <http://dx.doi.org/10.1016/j.solener.2014.10.021>.
- [19] Xu C, Wang Z, He Y, Li X, Bai F. Parametric study and standby behavior of a packed-bed molten salt thermocline thermal storage system. *Renew Energy* 2012;48:1–9. <http://dx.doi.org/10.1016/j.renene.2012.04.017>.
- [20] Rodrigues FA, de Lemos MJ. Stratification and energy losses in a standby cycle of a thermal energy storage system. *Int J Energy A Clean Environ* 2021;22:1–32.
- [21] Gaviño D, Cortés E, García J, Calderón-Vásquez I, Cardemil J, Estay D, Barraza R. A discrete element approach to model packed bed thermal storage. *Appl Energy* 2022;325:119821. <http://dx.doi.org/10.1016/j.apenergy.2022.119821>.
- [22] Yang B, Bai F, Wang Y, Wang Z. Study on standby process of an air-based solid packed bed for flexible high-temperature heat storage: Experimental results and modelling. *Appl Energy* 2019;238:135–46. <http://dx.doi.org/10.1016/j.apenergy.2019.01.073>.
- [23] Cabeza LF, Martorell I, Miró L, Fernández AI, Barreneche C, Cabeza LF, Fernández AI, Barreneche C. 1 - Introduction to thermal energy storage systems. In: Cabeza LF, editor. *Advances in thermal energy storage systems*. Woodhead publishing series in energy, 2nd ed.. Woodhead Publishing; 2021, p. 1–33. <http://dx.doi.org/10.1016/B978-0-12-819885-8.00001-2>.
- [24] Schwarzmayr P, Birkelbach F, Kasper L, Hofmann R. Development of a digital twin platform for industrial energy systems. In: *Accelerated energy innovations and emerging technologies*, Vol. 25. Cambridge, USA: Energy Proceedings; 2022. <http://dx.doi.org/10.46855/energy-proceedings-9974>.
- [25] Andersen E, Furbo S, Fan J. Multilayer fabric stratification pipes for solar tanks. *Sol Energy* 2007;81(10):1219–26. <http://dx.doi.org/10.1016/j.solener.2007.01.008>.
- [26] Merker GP. *Konvektive Wärmeübertragung. Wärme- und stoffübertragung*, Berlin, Heidelberg: Springer Berlin Heidelberg; 1987. <http://dx.doi.org/10.1007/978-3-642-82890-4>.

Publication 2

Packed bed thermal energy storage for waste heat recovery in the iron and steel industry: A cold model study on powder hold-up and pressure drop

published in the Journal of Energy Storage in collaboration with Felix Birkelbach, Heimo Walter, Florian Javernik, Michael Schwaiger and René Hofmann.

In this paper, the impact of using gas-powder two-phase exhaust gas as heat transfer fluid (HTF) in a packed bed thermal energy storage (PBTES) on the powder hold-up and pressure drop of the packed bed was studied. These investigations were motivated by the idea of using a PBTES to improve the efficiency of waste heat recovery systems in the iron and steel industry. The results of this cold model study indicate that 98 % of the powder transported by industrial exhaust gas used to charge a PBTES accumulates inside the packed bed. Moreover, single-phase HTF during subsequent discharging does not entrain detectable amounts of powder from the contaminated packed bed. This means that the HTF that exits the PBTES carries 98 % less powder than the initial industrial gas-powder two-phase exhaust gas. Measuring the increase of the pressure drop over the height of the packed bed revealed that in a contaminated packed bed, the pressure drop is caused almost entirely by a thin layer at the surface of the packed bed where the gas-powder two-phase flow enters during charging. This indicates that the majority of the powder hold-up is concentrated in this layer. To facilitate the removal of the powder hold-up, it was recommended to charge the PBTES from the bottom and to remove the accumulated powder from the bottom surface using periodic knocking/trembling mechanisms. These conclusions were the motivation for the investigation of the thermal performance of a PBTES under these exact operating conditions (charging a PBTES from the bottom) in Publications 1 and 3.

Author contribution: Conceptualization, Methodology, Validation, Formal Analysis, Investigation, Data Curation, Writing - Original Draft, Visualization.

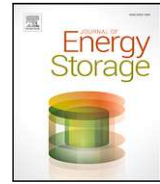
P. Schwarzmayr, F. Birkelbach, H. Walter, F. Javernik, M. Schwaiger, and R. Hofmann (Jan. 2024b). "Packed bed thermal energy storage for waste heat recovery in the iron and steel industry: A cold model study on powder hold-up and pressure drop". In: Journal of Energy Storage 75, p. 109735. ISSN: 2352-152X.

DOI: 10.1016/j.est.2023.109735



Contents lists available at ScienceDirect

Journal of Energy Storage

journal homepage: www.elsevier.com/locate/est

Research papers



Packed bed thermal energy storage for waste heat recovery in the iron and steel industry: A cold model study on powder hold-up and pressure drop

Paul Schwarzmayr^{a,*}, Felix Birkelbach^a, Heimo Walter^a, Florian Javernik^b,
Michael Schwaiger^b, René Hofmann^a

^a Institute for Energy Systems and Thermodynamics, TU Wien, Getreidemarkt 9, Vienna, 1060, Austria

^b voestalpine Stahl Donawitz GmbH, Kerpelystraße 199, Leoben, 8700, Austria

ARTICLE INFO

Keywords:

Packed bed thermal energy storage
Gas-powder two phase flow
Powder hold-up
Pressure drop
Exergy efficiency
Iron/steel industry

ABSTRACT

Waste heat recovery in the energy intensive industry is one of the most important measures for the mitigation of climate change. The present study examines the integration of a packed bed thermal energy storage for waste heat recovery in the iron and steel industry. Along with the highly fluctuating availability of excess heat the main difficulty of waste heat recovery in industrial processes is the high amount of powder that is transported by the hot exhaust gases. Therefore, the experimental investigations in this study focus on the powder hold-up and pressure drop in a packed bed thermal energy storage that is operated with a gas-powder two phase exhaust gas as heat transfer fluid. The ultimate goal is, to assess its suitability and robustness under such challenging operational conditions. The results indicate, that 98 % of the powder that is introduced into the system with the heat transfer fluid during charging accumulates in the packed bed. Remarkably, most of the powder hold-up in the packed bed is concentrated near the surface at which the heat transfer fluid enters the packed bed. When reversing the flow direction of the heat transfer fluid to discharge the storage with a clean single phase gas, this gas is not contaminated with the powder that has been accumulated in previous charging periods. The entirety of these findings reinforces the suitability of packed bed thermal energy storage systems for waste heat recovery in the energy intensive industry.

1. Introduction

The waste heat potential from the industry sector is enormous and its exploitation can lead to substantial primary energy savings. The biggest challenge of waste heat recovery is, that the utilization of only a fraction of the theoretical waste heat potential (approx. one third in 2014) is economically feasible. This is mainly because of techno-economic constraints like minimum temperature requirements, discontinuous waste heat availability, technology costs, or even the lack of suitable technologies. A comprehensive review considering the implementation of thermal energy storage (TES) systems for industrial waste heat recovery is provided by Miró et al. [1]. In a similar study Manente et al. [2] stated, that one of the most suitable types of TES for industrial waste heat recovery is a packed bed thermal energy storage (PBTES). Since PBTES systems use a non-pressurized steel vessel as storage tank, rocks or some other type of solids as storage material and a gaseous medium as heat transfer fluid (HTF) they are extremely cost efficient and require little maintenance.

Contrary to the maturity of PBTES systems for their integration into concentrated solar power (CSP) plants [3,4] studies on their utilization as industrial waste heat recovery systems are rare. The biggest difference between integrating a PBTES into an industrial waste heat recovery system and into a CSP plant is the composition of the HTF. In a CSP plant a PBTES system is charged and discharged with clean air whereas in an industrial waste heat recovery system the HTF will be some kind of gas-powder two phase exhaust gas. In their studies on the utilization of a PBTES for waste heat recovery in industrial processes Ortega-Fernández et al. [5] and Slimani et al. [6] dealt with this issue by placing a high temperature dust filter and a gas-to-gas heat exchanger between the industrial waste heat source and the TES so that the TES can be operated with clean air. However, this approach is far from optimal, because the filtration of high temperature gas is difficult and expensive and the exergy efficiency of gas-to-gas heat exchangers is low. Additionally the lifetime of these heat exchangers would be short due to the abrasiveness of the gas-powder two phase exhaust gas. Therefore, the authors of the present study consider the

* Corresponding author.

E-mail addresses: paul.schwarzmayr@tuwien.ac.at (P. Schwarzmayr), michael.schwaiger@voestalpine.com (M. Schwaiger), rene.hofmann@tuwien.ac.at (R. Hofmann).

<https://doi.org/10.1016/j.est.2023.109735>

Received 31 July 2023; Received in revised form 23 October 2023; Accepted 12 November 2023

2352-152X/© 2023 The Author(s). Published by Elsevier Ltd. This is an open access article under the CC BY license (<http://creativecommons.org/licenses/by/4.0/>).

Nomenclature	
Acronyms	
CSP	Concentrated solar power
HTF	Heat transfer fluid
LD	Linz–Donawitz
PBTES	Packed bed thermal energy storage
TES	Thermal energy storage
Roman symbols	
\bar{d}	Sauter diameter in m
Eu	<i>Euler</i> -number
L	Packed bed height in m
Δp	Pressure drop in Pa
$\Delta \hat{p}$	Relative pressure drop
p	Pressure in Pa
r_0	Characteristic length of a non-spherical packed bed particle in m
Re	<i>Reynolds</i> -number
v	Superficial fluid velocity in m s^{-1}
Greek symbols	
δ_0	Characteristic length for the fluid flow path in m
η	Dynamic viscosity of the fluid in Pa s
Φ_D	Shape factor for non-spherical packed bed particles
ψ	Fractional void volume in $\text{m}^3 \text{m}^{-3}$
ρ	Mass density of the fluid in kg m^{-3}
Subscripts	
f	Fluid
i	Index of pressure measuring point
j	Index of pressure measuring point
n	Sample number
p	(packed bed) Particle

direct use of high temperature gas-powder two phase exhaust gas from industrial processes as HTF for charging a PBTES. A schematic view of the proposed waste heat recovery system is depicted in Fig. 1. This approach drastically decreases investment (no high temperature filtration, no additional heat exchanger) and maintenance costs (filter, heat exchanger) of the whole system. In order to make assessments on the suitability and robustness of a PBTES system in such a setting this study examines the behavior of a PBTES system that is operated with a gas-powder two phase exhaust gas as HTF.

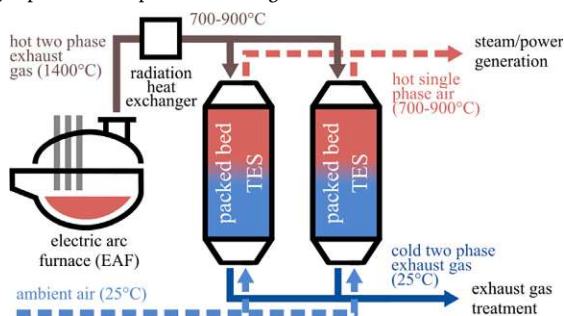


Fig. 1. Integration of PBTES systems for the waste heat recovery from industrial exhaust gas.

The first studies that consider gas-powder two phase flows in packed beds date back to the early 1990s and were conducted to investigate the behavior of coal powder that is injected into a blast furnace. In the most recent study from Gupta et al. [7] the authors state that despite the variety of publications considering this topic [8–12], the literature reveals that consistency is lacking and that the behavior of gas-powder two phase flow in packed beds is still not fully understood yet. Additionally, the application of experimental results that were generated in the context of pulverized coal injection into a blast furnace to a PBTES that is operated with a gas-powder two phase HTF is impracticable. Operational conditions that prevail in a blast furnace are fundamentally different to the conditions in a PBTES. Probably the biggest difference is, that in a blast furnace the powder (pulverized coal) undergoes a chemical reaction either with the gaseous part of the flowing fluid (burning) or the packed bed particles (reduction of iron ore) whereas in a PBTES the interactions between the packed bed and the HTF are limited to heat transfer, momentum transfer and adhesion. In a blast furnace coal powder with a narrow particle size distribution and a median particle size of $75 \mu\text{m}$ is laterally injected into the bottom of the packed bed. In a PBTES that is operated with a gas-powder two phase HTF the gas-powder flow enters the packed bed through the top surface. Furthermore, the particle size distribution of metal dust from a steel producing processes is much wider with a median particle size of less than $10 \mu\text{m}$. Therefore, the authors of this study decide to build upon existing research on gas-powder two phase flows in packed beds that was conducted in the context of coal powder injection into blast furnaces and to apply and extend this area of research towards PBTES systems that are operated with a gas-powder two phase HTF.

The remainder of this paper includes a presentation of the test rig that is designed and erected for the experimental investigations in Section 2. Additionally, properties and other information about the materials that are used for the packed bed and the powder are summarized in Section 2. Section 3 delineates the data analysis procedure and empirical pressure drop equations that are used for measurement data validation. Section 4 includes the presentation of all the results from the experiments as well as an interpretation of these results with the ultimate goal to assess the suitability of PBTES systems for waste heat recovery in the iron and steel industry.

2. Material and methods

2.1. Experimental setup

To investigate the powder hold-up and pressure drop in a PBTES when it is operated with a gas-powder two phase HTF, a lab-scale cold model test rig of a vertical PBTES is used. Fig. 2 shows a P&ID of the cold model test rig with all its components and instrumentation. The storage tank itself is a vertical acrylic glass cylinder with a height to diameter ratio of approximately 3 and is filled with 68.5 kg of storage material. The storage material and the powder for the experiments were chosen in a way, that the operational conditions are comparable with an industrial scale PBTES. As storage material slag, a by-product from the iron and steel industry, is used. In addition to the extremely low costs, the suitability of slag as storage material for a PBTES is justified by its good heat transfer properties due to its geometric shape. The irregular shaped and partly porous rocks that the slag is composed of lead to a uniform random packing, hence an even perfusion, and a high volume-specific surface of the packed bed, hence an improved heat transfer between HTF and storage material. More details about the storage tank's geometry and properties of the storage material are summarized in Table 1. For the experiments the storage tank is equipped with 11 pressure measuring points (PT1, PT2, ..., PT11) that are evenly distributed over the height of the packed bed. Piezoresistive pressure sensors are used to record the pressure differences between each of the pressure measuring points in the storage tank. Before the experiments the piezoresistive sensors are calibrated to an accuracy of

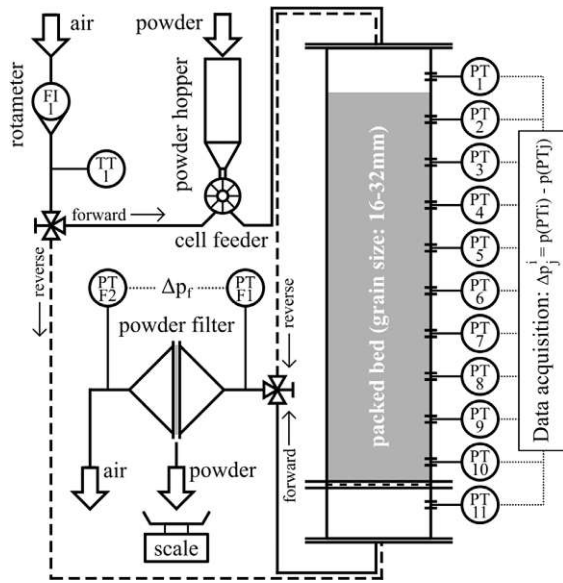


Fig. 2. Experimental test rig.

$\pm 0.06\%$ of full scale. The flow rate of the HTF (dry, clean and cold ambient air provided by an air supply unit) into the system is controlled with a rotameter flow meter.

To simulate a charging process of the PBTES cold model with a gas-powder two phase flow the initially clean HTF (cold ambient air) is directed to a cell feeder where powder is added before it enters the PBTES storage tank. The feed rate of the powder can be controlled by adjusting the rotational speed of the cell feeder. In order to represent reality as accurately as possible metal dust collected from the exhaust gases of a steel producing process is utilized as powder for the experiments. In Fig. 3, the particle size distribution of the powder is provided. These data are measured with a laser diffraction particle size analyzer (Malvern® Mastersizer 2000 [13]) that is fed with a dry sample dispersion unit (Malvern® Aero S [14]). The particle size distribution of the powder depicted in Fig. 3 is the average of 12 consecutive measurements. The particle size of this type of powder ranges from $0.2 \mu\text{m}$ to $600 \mu\text{m}$ with a median of $8.85 \mu\text{m}$ where the most common sizes are $3.5 \mu\text{m}$ and $350 \mu\text{m}$. Detailed information about the metal dust are provided in Table 1. Downstream of the cell feeder the gas-powder two phase HTF enters the storage tank from the top, passes through the packed bed and leaves the tank at the bottom. Before the HTF exits the system it passes through a powder filter that separates the remaining powder from the HTF flow. The path of the HTF flow for a charging process is indicated with solid lines in Fig. 2.

For the simulation of a discharging process of the PBTES cold model with clean single-phase HTF, air from the rotameter directly enters the storage tank from the bottom, passes through the packed bed and leaves the tank at the top. Again, the air that exits the storage tank is directed through the powder filter before it is released into the environment. The HTF flow path for the discharging process is indicated with dashed lines in Fig. 2.

2.2. Experimental procedure

Before the actual experiments with gas-powder two phase flow, the pressure drop curve of clean HTF passing through the clean packed bed depending on the HTF mass flux is recorded. For these experiments the HTF mass flux is set between $0 \text{ kg m}^{-2} \text{ s}^{-1}$ to $0.6 \text{ kg m}^{-2} \text{ s}^{-1}$. The upper

Table 1

Summary of parameters: Test rig geometry, data/properties of storage material, HTF and powder.

Test rig	
Storage type	vertical PBTES
Diameter of pipes	46 mm
Tank diameter	238 mm
Tank height	780 mm
Tank volume	0.034 m^3
Packed bed height	700 mm
Packed bed volume	0.031 m^3
Packed bed mass	68.5 kg
Packed bed material	
Type of material	slag (irregular shaped, partly porous)
Particle size	16 mm to 32 mm
Sauter-diameter \bar{d}_p	19.4 mm (calculation see [15])
Particle density	3800 kg m^{-3}
Void fraction	0.42
Bulk density	2200 kg m^{-3}
Shape factor (Φ_D)	0.8 [15]
volume-specific heat transfer coefficient	$\approx 11 \times 10^3 \text{ W m}^{-3} \text{ K}^{-1}$
Reynolds-number $Re = \rho_i v \bar{d}_p / (\psi \eta)$	750 to 1000
Euler-number (see Equation (3))	6.8 to 7.3
Heat transfer fluid	
Type of fluid	Air ($T = 294.15 \text{ K}$)
Density	1.205 kg m^{-3}
Dynamic viscosity	$18.23 \times 10^{-6} \text{ Pa s}$
HTF mass flux	0.3 and $0.4 \text{ kg m}^{-2} \text{ s}^{-1}$
Powder content	0.025 kg to 0.045 kg powder per kg air
Powder	
Type of material	metal dust from the iron and steel industry
Particle size	$0.2 \mu\text{m}$ to $600 \mu\text{m}$
Composition	$\approx 95\%$ Iron(III) oxide (Fe_2O_3) + 5% of other transition metal oxides
Powder mass flux	$7.5 \text{ g m}^{-2} \text{ s}^{-1}$ to $13.5 \text{ g m}^{-2} \text{ s}^{-1}$ and $10 \text{ g m}^{-2} \text{ s}^{-1}$ to $18 \text{ g m}^{-2} \text{ s}^{-1}$

limit was chosen because a further increase of the HTF mass flux would increase the pressure drop and the thickness of the thermozone which both mean a low exergy efficiency of the PBTES. Empirical equations from the literature are utilized to reconstruct and validate the measured data.

For the core experiments of this study, the cell feeder is used to produce a gas-powder two phase flow with a relative powder content of 25 g to 45 g powder per kg air which is representative for the powder content of exhaust gas from state-of-the-art steel producing processes (LD-converter and electric arc furnace). This gas-powder two phase flow further passes through the whole system as described in Section 2.1. The increase in pressure drop in the packed bed is measured with the differential pressure sensors PT1, PT2, ..., PT11. The amount of powder hold-up inside the packed bed is determined via a mass

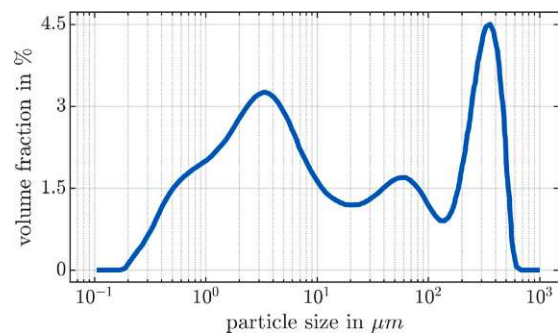


Fig. 3. Particle size distribution of the powder used for the experiments.

balance by measuring the amount of powder that is feed into the HTF flow from the powder hopper and the amount of powder that is separated from the HTF in the powder filter after passing through the packed bed. This mass balance is evaluated periodically by removing the powder filter from its housing to record its mass increase. At each time, the powder filter is cleaned before it is put back into its housing to prevent the exponentially rising pressure drop of the powder filter to impact the behavior of the remaining system. For this purpose, the test rig is equipped with two parallel powder filters so that one filter can be removed and weighed without having to interrupt the experiments. When the pressure drop of the packed bed reaches a certain threshold the charging process with gas powder two phase flow is stopped. For the experiments in this study the pressure threshold is set to 1000 Pa since this is the maximum pressure difference that can be recorded by the measurement equipment. After stopping the charging process, the flow direction of the HTF is reversed to simulate a discharging process of the PBTES with clean HTF. Clean air passes through the packed bed from the bottom to the top and exits the system through the powder filter. The reduction in pressure drop and powder hold-up is measured and determined as before. This whole procedure is repeated for a HTF mass flux of 0.3 and 0.4 kg m⁻² s⁻¹.

The results of these experiments can be transferred and applied to larger devices if certain similarity criteria (*Reynolds*- and *Euler*-number) are satisfied. Values for the *Reynolds*- and *Euler*-number are given in this section and in Table 1.

3. Theory and calculations

For the validation of the measured data empirical equations from the literature are used. According to Kast et al. [15] there are two different ways to model the pressure drop in a fluid passing through a packed bed. The first and simpler option is, to model the packed bed as several pipes connected in parallel which leads to the *Ergun*-equation [16]. With this equation the pressure drop per unit length can be calculated as

$$\frac{\Delta p}{\Delta L} = 150 \frac{(1-\psi)^2}{\psi^3} \frac{\eta v}{\bar{d}_p^2} + 1.75 \frac{1-\psi}{\psi^3} \frac{\rho_f v^2}{\bar{d}_p} \quad (1)$$

where ψ is the fractional void volume in the packed bed, \bar{d}_p is the Sauter-diameter of the packed bed material, η is the dynamic viscosity of the fluid, v is the superficial fluid velocity and ρ_f is the mass density of the fluid. At this point it should be mentioned, that *Ergun*'s-equation is included in this study because it is the most common equation used to calculate the pressure drop in packed beds in the literature. However, one main disadvantage of the modeling approach used by *Ergun* is that the real flow paths of the fluid are only insufficiently considered. Detailed information on the limitations of *Ergun*'s-equation are provided by Kast et al. [15].

A more versatile but also more complex equation for the calculation of the pressure drop per unit length is the *Molerus*-equation. This equation was deduced based on the fluid flow around single packed bed particles and therefore allows a much more detailed modeling of the fluid flow paths within a packed bed with uniform randomly packed particles. By postulating equilibrium between the resistance force exerted by the fluid to each packed bed particle and the force due to the pressure drop in the fluid, *Molerus* [17] found that

$$\frac{\Delta p}{\Delta L} = \frac{3}{4} \frac{\rho_f v^2}{\bar{d}_p} \frac{1-\psi}{\psi^2} \text{Eu}(\Phi_D) \quad (2)$$

where

$$\text{Eu}(\Phi_D) = \frac{24}{\text{Re} \Phi_D^2} \left\{ 1 + 0.685 \left[\frac{r_0}{\delta_0} + 0.5 \left(\frac{r_0}{\delta_0} \right)^2 \right] \right\} + \frac{4}{\sqrt{\text{Re} \Phi_D^{1.5}}} \left[1 + 0.289 \left(\frac{r_0}{\delta_0} \right)^{1.5} \right] + \frac{1}{\Phi_D} \left[0.4 + 0.514 \frac{r_0}{\delta_0} \right]. \quad (3)$$

The *Euler*-number $\text{Eu}(\Phi_D)$ in Eq. (3) is a function of the packed bed particle *Reynolds*-number Re , a factor Φ_D that accounts for the non-spherical shape of the packed bed particles and a length ratio r_0/δ_0 which is characteristic for the geometry of the fluid flow path between the packed bed particles. For a packed bed with a fractional void volume ψ and uniform randomly packed particles the *Reynolds*-number Re and the length ratio r_0/δ_0 can be calculated as

$$\text{Re} = \frac{\rho_f v \bar{d}_p}{\psi \eta} \quad \text{and} \quad \frac{r_0}{\delta_0} = \left[\frac{0.95}{\sqrt[3]{1-\psi}} - 1 \right]^{-1}. \quad (4)$$

3.1. Data processing and uncertainty analysis

For a compact presentation of the most important findings of the present study the measured data from the experiments is processed using Eq. (5). In this equation the pressure measurements from any two pressure measuring points p_i and p_j are used to compute the relative pressure drop between to measuring point $\Delta \hat{p}_{i-j}(n)$.

$$\Delta \hat{p}_{i-j}(n) = \frac{\Delta p_{i-j}(n)}{\Delta p_{i-j}(n=1)} = \frac{p_i(n) - p_j(n)}{p_i(n=1) - p_j(n=1)} \quad (5)$$

The relative pressure drop between two measuring points $\Delta \hat{p}_{i-j}(n)$ is the ratio of the pressure difference of the n^{th} sample $\Delta p_{i-j}(n)$ and the pressure difference of the first sample, i.e. the clean bed, $\Delta p_{i-j}(n=1)$.

To estimate the impact of uncertainties of the measurement devices on the results presented in this study an uncertainty analysis using the law of error propagation is conducted. As mentioned in Section 2.1, piezoresistive sensors with an accuracy of $\pm 0.06\%$ of full scale are used to measure pressure differences between the measuring points in the test rig's packed bed. With a full scale of 2000 Pa (measurement range of ± 1000 Pa) the utilized sensors deliver measurements with an accuracy of ± 1.2 Pa. As the calculation of $\Delta \hat{p}_{i-j}(n)$ in Eq. (6) requires two differential pressure measurements ($\Delta p_{i-j}(n)$ and $\Delta p_{i-j}(n=1)$), the law of error propagation is used to calculate the uncertainty of the relative pressure drop as

$$\delta \Delta \hat{p}_{i-j}(n)^2 = \left(\frac{\delta \Delta p_{i-j}(n)}{\Delta p_{i-j}(n=1)} \right)^2 + \left(- \frac{\Delta p_{i-j}(n) \delta \Delta p_{i-j}(n=1)}{\Delta p_{i-j}(n=1)^2} \right)^2. \quad (6)$$

The relative uncertainty of $\Delta \hat{p}_{1-11}(n)$ and $\Delta \hat{p}_{1-3}(n)$ with respect to the calculated value are well below $\pm 2\%$ and $\pm 8.5\%$ respectively. These uncertainties are insignificant compared to the scattering of the experimental data (see Figs. 6, 9 and 10) and therefore do not have an impact on the quality of the results presented in Section 4.

4. Results and discussion

To guarantee consistency and reproducibility of the measured data, the pressure drop curve of the clean packed bed is recorded three times before the core experiments. Between each of these three measurements the test rig's tank is emptied and refilled again. The results of these experiments are plotted in Fig. 4 as blue circles. It can be seen, that the data is only slightly scattered in vertical direction which indicates reproducibility of the results. Furthermore, empirical equations from *Ergun* and *Molerus* are used to compare the measured data. The parameters used for the *Ergun*- and *Molerus*- equation are documented in Table 1 which are either obtained from data sheets or from the literature [15]. Both equations (dashed lines) fit the experimental data (blue circles and solid blue line) very well as it can be seen in Fig. 4. Thereby it can be confirmed that the test rig used for the experiments in the present study delivers results that are consistent and follow the trend as predicted by the *Ergun* and *Molerus* equations.

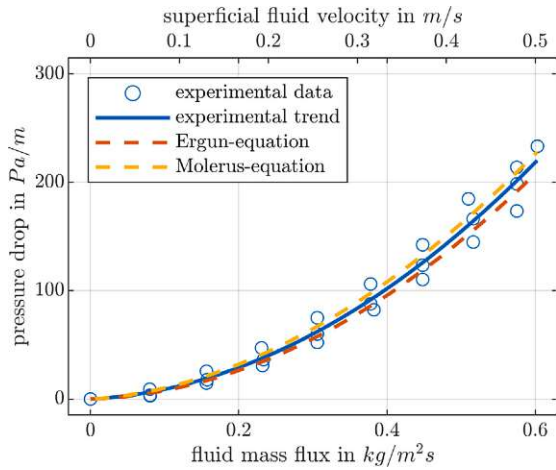


Fig. 4. Pressure drop curve of clean HTF passing through a clean and dusty packed bed.

4.1. Powder hold-up

The amount of powder that accumulates in the packed bed during a charging process (powder hold-up) is determined by measuring the amount of powder that is fed into the system by the cell feeder and the amount of powder that accumulates in the powder filter. The experiments reveal, that for a fluid mass flux of $0.4 \text{ kg m}^{-2} \text{ s}^{-1}$ approximately 98 % of the powder accumulates in the packed bed during a charging process. This means, that the PBTES does not only act as a thermal storage, but also as a dust collector. For an industrial scale PBTES that is operated at high temperatures this means that the HTF that exits the PBTES during a charging process is not only cold but also carries just 2 % of the amount of powder than the HTF that enters the PBTES. Furthermore, discharging the storage with clean air that passes through the contaminated packed bed in the opposite direction does not lead to a reduction of the powder hold-up in the packed bed. This is confirmed by evaluating the powder mass balance during all the discharging phases. Hence, clean air that is used to discharge the PBTES is not contaminated with powder that has been accumulated in the packed bed in a previous charging process.

One of the most interesting observations from the experiments is the axial distribution of pressure drop and powder hold-up in the packed bed which is visualized in Fig. 5. In this plot the left ordinate represents

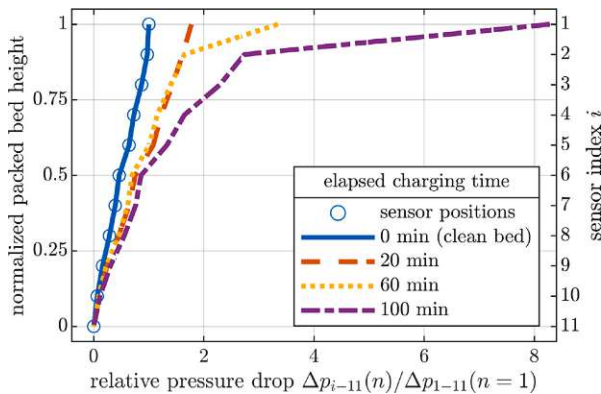


Fig. 5. Vertical/axial distribution of the pressure drop in a packed bed with powder hold-up.

the normalized height of the packed bed and the right ordinate shows the positions of the pressure sensors. On the abscissa, the pressure drop between measuring point i and the bottom of the packed bed relative to the total pressure drop of the clean packed bed is given. The blue solid line with \circ -markers represents the relative pressure drop curve for the clean packed bed. The rest of the lines show the relative pressure drop curve of the packed bed after it was charged with gas-powder two phase flow for different periods of time. While the initial pressure drop curve (0 min) and the pressure drop curve recorded after 20 min of gas-powder two phase flow are linear functions of the packed bed height, the other two curves show different results that suggest a nonuniform distribution of powder hold-up in vertical direction. After 60 min of charging with gas-powder two phase flow (yellow dotted line) one half of the total pressure drop is caused only by the top layer (0.08 m, 11 % of the packed bed's total height) of the packed bed. These observations indicate that most of the powder that accumulates in the packed bed is concentrated at the surface where the two phase HTF enters the packed bed. Similar results are presented in Fig. 6.

This plot shows the relative pressure drop of the upper fifth of the packed bed – where the gas-powder two phase flow enters the packed bed – on the left ordinate ($\Delta\hat{p}_{1-3}$) and the relative pressure drop of the remaining height of the packed bed on the right ordinate ($\Delta\hat{p}_{3-11}$). The amount of powder hold-up in the packed bed is plotted on the abscissa. Both graphs start at a powder hold-up of 0 kg m^{-2} (clean bed) and increase with the powder hold-up in the packed bed. It can clearly be seen that the pressure drop in the upper fifth of the bed rises exponentially whereas the pressure drop in the lower region of the packed bed seems to flatten. At a powder hold-up of 40 kg m^{-2} the pressure drop in the upper fifth already increased by a factor of 8 while the pressure drop in the lower region of the packed bed has not even doubled. These results too suggest, that a large part of the powder that is introduced into a PBTES accumulates near the surface at which the gas-powder two phase flow enter the packed bed. The small portion of the powder that is further transported into the system is distributed inside the packed bed considerably uniform. These results are supported by the data presented in Fig. 7.

The left ordinate and the blue bars in this figure represent the pressure drop between two measuring points i and j . The abscissa indicates the indices of measuring points between which the presented data is measured. On the right ordinate the void fraction of the packed bed is

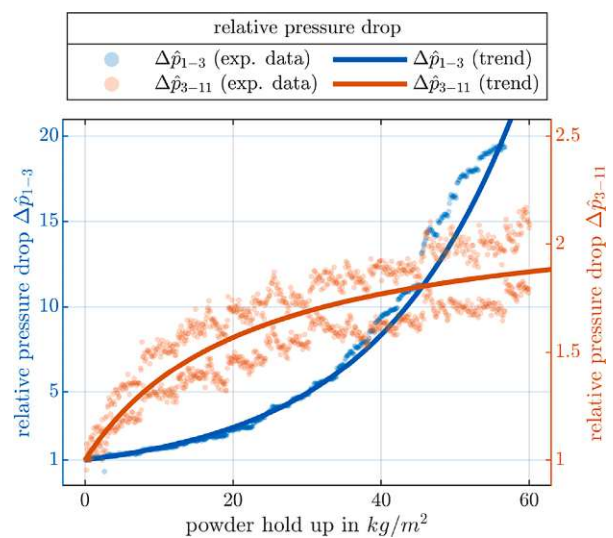


Fig. 6. Pressure drop in a packed bed with powder hold-up at different vertical/axial positions.

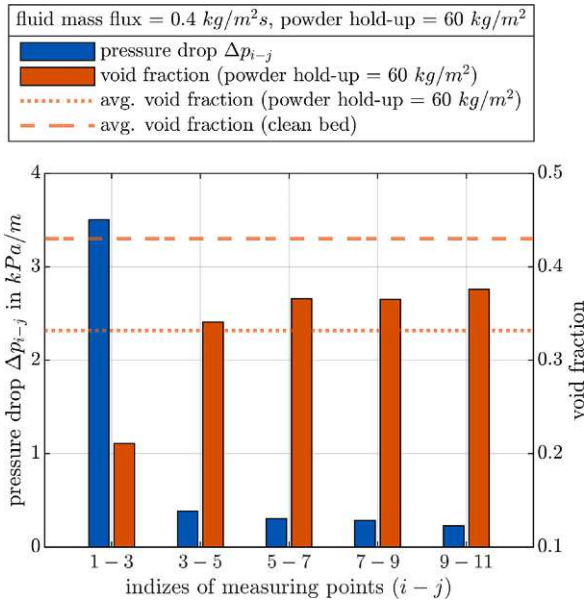


Fig. 7. Pressure drop and void fraction of a PBTES with a fluid mass flux of $0.4 \text{ kg m}^{-2} \text{ s}^{-1}$ and a powder hold-up of 60 kg m^{-2} .

shown. The red dashed line is the average void fraction of the clean bed and the red dotted line is the average void fraction of a contaminated packed bed which is calculated using the measured powder hold-up of 60 kg m^{-2} . Together with the data (pressure drop) presented in Fig. 7 the Molerus Eq. (2) is used to estimate the void fraction inside the packed for different vertical positions. These calculations are validated by comparing them to the total powder hold-up determined by the powder mass balance. The results are presented as red bars in Fig. 7 and indicate, that only the void fraction in the top fifth of the packed bed (between measuring points 1 and 3) is significantly lower than the void fraction of the clean packed bed. In addition to these calculated results Fig. 8 shows the packed bed in the PBTES test rig at three different states. In the left picture a clean packed bed is depicted. The center picture shows the top surface (where the gas-powder two phase flow enters the packed bed) of a packed bed with a powder hold-up of 30 kg m^{-2} . The right picture is taken from the same angle after the top fifth of the packed bed is removed. As was already assumed when interpreting the data in Figs. 5–7, Fig. 8 shows that most of the powder hold-up in the packed bed is concentrated near the top surface of the packed bed. Furthermore the center and right photographs in Fig. 8 show an even radial distribution of the powder hold-up which indicates a uniform perfusion of the packed bed even with a significant amount of powder hold-up. After each experiment the contaminated storage material was removed layer-by-layer and the packed bed was checked for any areas with more powder accumulation than in others. After none of the experiments any irregularities in the uniformity of the powder accumulation could be detected. The detailed examination of the packed bed during and after each experiment suggests that there is no risk of random flow channel formation through the packed bed.

4.2. Influence of powder/fluid mass flux

The trend of the pressure drop for a charging period of 80 min is depicted in Fig. 9. This figure shows the relative pressure drop between the upper- and lowermost pressure measuring points $\Delta \hat{p}_{1-11}$ of the test rig for two powder mass fluxes and a fluid mass flux of $0.4 \text{ kg m}^{-2} \text{ s}^{-1}$. These results show that the pressure drop of a PBTES that is charged with a gas-powder two phase exhaust gas increases exponentially over

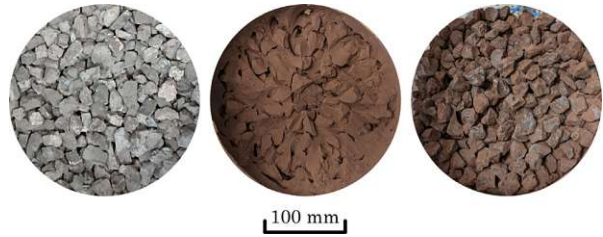


Fig. 8. Photograph of a clean packed bed (left) and a packed bed with a powder hold-up of 60 kg m^{-2} : top view directly after charging (center), top view after charging and after removing the upper fifth of the packed bed (right).

time. After a charging period of 50 min with a powder mass flux of $17 \text{ kg m}^{-2} \text{ s}^{-1}$ an increase of the pressure drop by a factor of up to 4.5 is observed. A reduction of the powder mass flux also leads to a slower increase of the pressure drop, however, no saturation effects could be observed in any of the experiments. This means, that independent of the powder mass flux, powder will continue to accumulate over time which leads to a reduced exergy efficiency of the TES due to the increased pressure drop and eventually a clogging of the packed bed. Hence, frequent maintenance intervals at which the packed bed is cleaned or renewed are necessary. The frequency of maintenance can only be reduced by reducing the powder content of the fluid that passes through the packed bed. This could be realized by using a drop-out box that separates the coarse powder fractions from the HTF before it enters the PBTES.

In Fig. 10 the impact of the fluid mass flux on the trend of the relative pressure drop of the packed bed is shown. It can be seen that a reduction of the fluid mass flux leads to a much faster increase of the relative pressure drop with respect to the powder hold-up in the packed bed. Notice, that in both cases the powder content of the fluid is 0.042 kg powder per kg fluid and the abscissa in Fig. 10 represents the powder hold-up in the packed bed and not the charging time. As a higher fluid mass flux with the same powder content also means a higher powder mass flux, the difference with respect to the charging time would not be as pronounced, but still present. The reason for that is based on the elutriation velocity of the powder particles which is (among other factors) mainly determined by its size. The smaller the

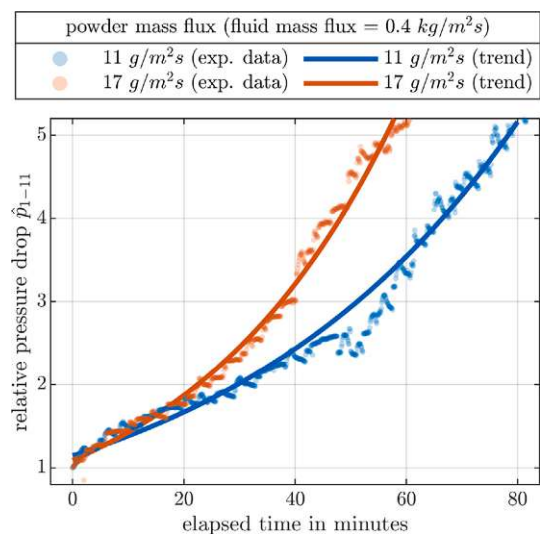


Fig. 9. Impact of the powder mass flux on the pressure drop of a packed bed that is operated with a gas-powder two phase flow.

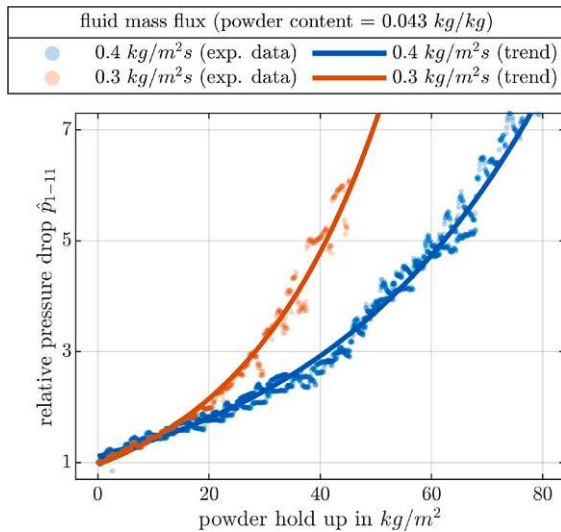


Fig. 10. Impact of the fluid mass flux on the pressure drop of a packed bed that is operated with a gas-powder two phase flow.

particle, the lower its elutriation velocity and vice versa. For the present use-case this means that all powder particles with an elutriation velocity higher than the velocity of the fluid passing through the packed bed will accumulate in the packed bed. Powder particles with an elutriation velocity that is lower than the fluid velocity remain in the fluid flow and pass through the packed bed. Nevertheless, the data in Fig. 10 allows to make some important statements about the preferred operation strategy of a PBTES that is charged with a gas-powder two phase flow. Fig. 10 shows that a powder hold-up of 40 kg m^{-2} increases the pressure drop of a PBTES that is charged with a fluid mass flux of 0.3 and $0.4 \text{ kg m}^{-2} \text{ s}^{-1}$ by a factor of 5 and 3 respectively. This observation combined with the fact that both experiments were conducted with HTF having the same powder content means that the higher the HTF mass flux, i.e. the thermal power rate, at which the PBTES is charged, the slower the decrease of the storage's exergy efficiency due to the increased pressure drop. For the operation of a PBTES that is charged with a gas-powder two phase flow this implies, that high charging power rates should be preferred to reduce the impact of powder hold-up on the pressure drop and hence the systems exergy efficiency.

4.3. Summary and discussion

The proposed integration of a PBTES for the waste heat recovery in the iron and steel industry is attractive because of its simplicity and its energetic and economic benefits. Excess heat from steel producing processes that is available as hot gas-powder two phase exhaust gas can be stored in a PBTES by directly using the exhaust gas as HTF. Due to the considerably uniform distribution of the powder hold-up in radial direction there is little risk of thermal performance degradation (storage capacity, thermal power rate) of the storage caused by random flow channel formation. As clean HTF that is used to discharge the PBTES is not contaminated by powder hold-up in the PBTES, heat recovered from the storage can be used in conventional waste heat boilers or for preheating purposes.

However, the results also show that there still is need for research and development work in order to make PBTES systems suitable for waste heat recovery in the iron and steel industry. The main challenge in this context is to find an operating/maintenance strategy to keep the pressure drop of HTF passing through the packed bed within appropriate bounds. It is important to keep the pressure drop of HTF passing

through the packed bed as low as possible as the exergy efficiency of a PBTES is strongly influenced by the energy needed to pump HTF through the packed bed. Considering the results presented in this study strategies and technologies to reduction of the powder content of the HTF before it enters the PBTES and to reduce the amount of powder hold-up that accumulates in the PBTES are required. The powder content of the HTF can be reduced with existing technologies like gravity separators (drop-out boxes). An interesting approach to reduce the powder hold-up in the packed bed is to switch the flow direction for the charging and discharging process of the PBTES (charging from bottom and discharging from top) and to utilize periodic knocking/trembling mechanisms to clean the packed bed from the accumulated powder hold-up. As the powder hold-up in the PBTES concentrates near the surface at which the HTF enters the packed bed, which, for switched flow directions would be the bottom surface of the bed, the removal of the powder hold-up takes place by gravitation. The limitations and possible challenges this approach could entail include a reduced exergy efficiency of the storage due to thermocline degradation especially during long standby periods. For details considering these effects the authors refer to their previous work [18].

5. Conclusion

The present study examined the suitability of packed bed thermal energy storage systems for the waste heat recovery in the iron and steel industry. Besides extreme temperatures and the highly fluctuating and unpredictable availability of excess heat, the main difficulty of waste heat recovery in industrial processes is the high amount of powder that is transported by the hot exhaust gases. Therefore the focus of this study was the investigation of the behavior/characteristics of a packed bed thermal energy storage that is operated with a gas-powder two phase heat transfer fluid.

A lab-scale test rig of a packed bed thermal energy storage was used to quantify the pressure drop and powder hold-up that have to be expected when a packed bed thermal energy storage is operated with a gas-powder two phase heat transfer fluid.

The investigations revealed that, for the given materials and operational parameters, 98 % of the powder that enters the test rig when it is charged with a gas-powder two phase fluid accumulates in the packed bed. Only the finest fractions (2 %) of the powder remain in the fluid flow passing through the packed bed. Furthermore, reversing the flow direction of the heat transfer fluid and discharging the test rig with a clean single phase fluid does not lead to a reduction of the powder hold-up inside the packed bed. Hence, clean fluid that is used to discharge the test rig is not contaminated with the powder hold-up in the packed bed. Additionally an uneven distribution of the powder hold-up along the fluid flow direction was observed by examining the packed bed after the experiments. These observations are consistent with the pressure drop measurements during the experiments. A large proportion of the powder hold-up is concentrated near the surface at which the fluid flow enters the packed bed. The distribution of powder hold-up in radial direction of the test rig was observed to be uniform and no random flow channel formation could be detected.

Overall, the integration of a packed bed thermal energy storage as waste heat recovery system in the iron and steel industry was found to be suitable and is definitely worth further investigation. Especially the evaluation and development of suitable strategies for the removal of powder hold-up from the storage material should be the main focus in future research projects.

CRedit authorship contribution statement

Paul Schwarzmayr: Conceptualization, Methodology, Validation, Formal analysis, Investigation, Data curation, Writing – original draft, Visualization. **Felix Birkelbach:** Conceptualization, Methodology, Formal analysis, Writing – review & editing. **Heimo Walter:** Conceptualization, Methodology, Formal analysis, Writing – review & editing.

Visualization, Supervision. **Florian Javernik**: Conceptualization, Resources, Writing – review & editing, Project administration, Funding acquisition. **Michael Schwaiger**: Conceptualization, Resources, Writing – review & editing, Project administration, Funding acquisition. **René Hofmann**: Conceptualization, Validation, Writing – review & editing, Supervision, Funding acquisition.

Declaration of competing interest

The authors declare that they have no known competing financial interests or personal relationships that could have appeared to influence the work reported in this paper.

Data availability

Data will be made available on request.

Acknowledgments

The authors acknowledge funding support of this work through the research project *5DIndustrialTwin* as part of the Austrian Climate and Energy Fund's initiative Energieforschung (e!MISSION) 6th call (FFG project number 881140). Furthermore, the authors acknowledge TU Wien Bibliothek, Austria for financial support through its Open Access Funding programme.

References

- [1] L. Miró, J. Gasia, L.F. Cabeza, Thermal energy storage (TES) for industrial waste heat (IWH) recovery: A review, *Appl. Energy* 179 (2016) 284–301, <http://dx.doi.org/10.1016/j.apenergy.2016.06.147>.
- [2] G. Manente, Y. Ding, A. Sciacovelli, A structured procedure for the selection of thermal energy storage options for utilization and conversion of industrial waste heat, *J. Energy Storage* 51 (2022) 104411, <http://dx.doi.org/10.1016/j.est.2022.104411>.
- [3] L. Geissbühler, A. Mathur, A. Mularczyk, A. Haselbacher, An assessment of thermocline-control methods for packed-bed thermal-energy storage in CSP plants, Part 1: Method descriptions, *Sol. Energy* 178 (2019) 341–350, <http://dx.doi.org/10.1016/j.solener.2018.12.015>.
- [4] L. Geissbühler, A. Mathur, A. Mularczyk, A. Haselbacher, An assessment of thermocline-control methods for packed-bed thermal-energy storage in CSP plants, Part 2: Assessment strategy and results, *Sol. Energy* 178 (2019) 351–364, <http://dx.doi.org/10.1016/j.solener.2018.12.016>.
- [5] I. Ortega-Fernández, J. Rodríguez-Aseguinolaza, Thermal energy storage for waste heat recovery in the steelworks: The case study of the REslag project, *Appl. Energy* 237 (2019) 708–719, <http://dx.doi.org/10.1016/j.apenergy.2019.01.007>.
- [6] H. Slimani, Y. Filali Baba, H. Ait Ousaleh, A. Elharrak, F. El Hamdani, H. Bouzekri, A. Al Mers, A. Faik, Horizontal thermal energy storage system for Moroccan steel and iron industry waste heat recovery: Numerical and economic study, *J. Clean. Prod.* 393 (2023) 136176, <http://dx.doi.org/10.1016/j.jclepro.2023.136176>.
- [7] G.S. Gupta, S. Lakshminarasimha, M. Shrenik, Quantitative measurement of powder holdups in the packed beds, *Trans. Indian Inst. Met.* 75 (2) (2022) 381–395, <http://dx.doi.org/10.1007/s12666-021-02431-2>.
- [8] H. Zhou, X. Tian, M. Kou, S. Wu, Y. Shen, Numerical study of fine particles behaviors in a packed bed with lateral injection using CFD-DEM, *Powder Technol.* 392 (2021) 317–324, <http://dx.doi.org/10.1016/j.powtec.2021.07.019>.
- [9] X.F. Dong, S.J. Zhang, D. Pinson, A.B. Yu, P. Zulli, Gas-powder flow and powder accumulation in a packed bed: II: Numerical study, *Powder Technol.* 149 (1) (2004) 10–22, <http://dx.doi.org/10.1016/j.powtec.2004.09.039>.
- [10] X.F. Dong, D. Pinson, S.J. Zhang, A.B. Yu, P. Zulli, Gas-powder flow and powder accumulation in a packed bed: I. Experimental study, *Powder Technol.* 149 (1) (2004) 1–9, <http://dx.doi.org/10.1016/j.powtec.2004.09.040>.
- [11] H. Takahashi, H. Kawai, T. Kondo, M. Sugawara, Permeation and blockage of fine particles transported by updraft through a packed bed, *ISIJ Int.* 51 (10) (2011) 1608–1616, <http://dx.doi.org/10.2355/isijinternational.51.1608>.
- [12] S. Kiochiro, S. Masakata, I. Shin-ichi, T. Reijiro, Y. Jun-ichiro, Pressure loss and hold-up powders for gas-powder two phase flow in packed beds, *ISIJ Int.* 31 (5) (1991) 434–439, <http://dx.doi.org/10.2355/isijinternational.31.434>.
- [13] Mastersizer 3000 - Particle Size Analyzer | Malvern Panalytical.
- [14] Aero S - Dry Powder Dispersion Unit | Malvern Panalytical.
- [15] W. Kast, H. Nirschl, W. Kast, H. Nirschl, W. Kast, H. Nirschl, E.S. Gaddis, E.S. Gaddis, K.-E. Wirth, J. Stichlmair, L1 Einphasige Strömungen, in: *VDI-Wärmeatlas*, in: VDI-Buch, Springer, Berlin, Heidelberg, 2013, pp. 1221–1284, http://dx.doi.org/10.1007/978-3-642-19981-3_74.
- [16] S. Ergun, Fluid flow through packed columns, *Chem. Eng. Prog.* 48 (2) (1952) 89–94.
- [17] O. Molerus, Kohärente Darstellung des Druckverlustverhaltens von Festbetten und des Ausdehnungsverhaltens homogener (Flüssigkeits-/Feststoff-) Wirbelschichten, in: O. Molerus (Ed.), *Fluid-Feststoff-Strömungen: Strömungsverhalten Feststoffbeladener Fluide Und Kohäsiver Schüttgüter*, Springer, Berlin, Heidelberg, 1982, pp. 8–38, http://dx.doi.org/10.1007/978-3-642-50215-6_2.
- [18] P. Schwarzmayr, F. Birkelbach, H. Walter, R. Hofmann, Standby efficiency and thermocline degradation of a packed bed thermal energy storage: An experimental study, *Appl. Energy* 337 (2023) 120917, <http://dx.doi.org/10.1016/j.apenergy.2023.120917>.

Publication 3

Exergy efficiency and thermocline degradation of a packed bed thermal energy storage in partial cycle operation: An experimental study

published in Applied Energy in collaboration with Felix Birkelbach, Heimo Walter and René Hofmann.

In this paper the impact of the HTF flow direction on the exergy efficiency and the thermocline degradation of a PBTES in partial cycle operation was investigated. The results indicate that the energy and exergy efficiency of a PBTES in steady-state operation is lower by 5 % points and 4 % to 7 % points, respectively, compared to the efficiencies in the first cycle. An impact of the HTF flow direction on these values could not be observed. Although the overall energy and exergy efficiency of a PBTES is slightly lower when it is charged from the bottom and discharged from the top, no additional exergy losses due to thermocline degradation could be detected in the experiments of this study. The slightly lower efficiencies measured during the experiments during which the storage was charged from the bottom can be attributed to the elevated heat losses at the bottom of the packed bed. This is due to an increased heat transfer to the surroundings via the metal grating on which the packed bed sits and an adverse surface-to-volume ratio at the bottom of the storage tank. In this paper, it was concluded that for a PBTES in partial cycle operation, the HTF flow direction does not impact its long-term exergy efficiency and thermocline degradation. Therefore, the operating strategy suggested in Publication 2 is suitable for a PBTES used as an industrial waste heat recovery system.

Author contribution: Conceptualization, Methodology, Validation, Formal Analysis, Investigation, Data Curation, Writing - Original Draft, Visualization.

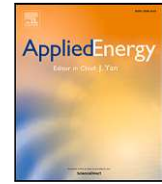
P. Schwarzmayr, F. Birkelbach, H. Walter, and R. Hofmann (Apr. 2024a). "Exergy efficiency and thermocline degradation of a packed bed thermal energy storage in partial cycle operation: An experimental study". In: Applied Energy 360, p. 122895. ISSN: 0306-2619.

DOI: [10.1016/j.apenergy.2024.122895](https://doi.org/10.1016/j.apenergy.2024.122895)



Contents lists available at ScienceDirect

Applied Energy

journal homepage: www.elsevier.com/locate/apenergy

Exergy efficiency and thermocline degradation of a packed bed thermal energy storage in partial cycle operation: An experimental study

Paul Schwarzmayr*, Felix Birkelbach, Heimo Walter, René Hofmann

Institute for Energy Systems and Thermodynamics, TU Wien, Getreidemarkt 9, Vienna, 1060, Austria

ARTICLE INFO

Keywords:

Packed bed thermal energy storage
Waste heat recovery
Energy/exergy efficiency
Thermocline degradation
Partial cycle operation
Iron/steel industry

ABSTRACT

To enable the exploitation of the industry sectors' huge waste heat potential this study investigates the utilization of packed bed thermal energy storage systems for the waste heat recovery in the iron and steel industry. The main goal is to assess the partial cycle operation of a packed bed thermal energy storage with industrial exhaust gas that is contaminated with high amounts of metal powder. A continuously rising accumulation of powder particles inside the packed bed requires the storage to be charged from the bottom in order to facilitate the removal of powder hold-up. Therefore, investigations focus on the dependency of the thermal performance of the storage on the flow direction of heat transfer fluid during charging/discharging. Exergy efficiency and thermocline degradation are evaluated as key performance indicators for different flow directions of the heat transfer fluid using a lab-scale test rig. Results show that, compared to charging from the top, a slightly faster thermocline degradation occurs for a storage that is charged from the bottom. Still, energy and exergy efficiencies in partial cycle operation are well above 85% and 80% respectively regardless of the heat transfer fluid flow direction. The thermal power rate during discharging is stable between 74% and 93% with respect to the maximum input rate for both charging the storage from the top and from the bottom. All in all, packed bed thermal energy storage systems are found to be suitable for waste heat recovery in industrial processes. Only a marginal deterioration of the thermal performance of the storage has to be expected if the storage is required to be charged from the bottom.

1. Introduction

A packed bed thermal energy storage (PBTES) is a sensible type of thermal energy storage (TES) that uses a packed bed of solids as heat storage material, a gas (or liquid [1]) as heat transfer fluid (HTF) [2,3] and is capable of storing high-temperature heat. The fact that the HTF in a PBTES gets in direct contact with the storage material leads to an enhanced heat transfer and therefore high power rates compared to other storage technologies that use a gaseous medium as HTF [4,5]. Moreover, there is no need for heat exchanger tubes as it would be in other sensible and/or latent heat TES systems [6]. This reduces investment costs and increases the robustness of PBTES systems against aggressive/abrasive HTFs.

As the HTF can be any type of gas and the storage material can be any type of solids (rocks/gravel [7], slag [8], glass spheres [9], porcelain spheres [10], ceramic spheres [11], alumina spheres [12]) PBTES systems are usually cost-efficient and versatile in its application [13]. Furthermore, PBTES systems use one non-pressurized vessel as storage tank which further reduces investment costs compared to other storage technologies [14]. In addition to these economic advantages, PBTES

systems also have some interesting qualities from a technical point of view. Since PBTES systems take advantage of an effect called thermal stratification [15], they typically reach higher exergy efficiencies than conventional sensible heat TES systems [16,17] like Ruths steam storage [18] and hot water tanks. Thermal stratification means, that for a partially charged PBTES the storage volume is divided into a hot and a cold zone that are separated by a thin volume-slice which is called "thermocline" [19]. To charge the PBTES, hot HTF passes through the storage entering from the hot end. This expands the volume of the hot zone. To recover the stored heat, cold HTF passes through the packed bed entering from the cold end, which pushes back the thermocline and expands the cold zone [20]. In a well designed PBTES [21,22] the thermocline is as thin as possible which allows to recover heat at nearly the same temperature at which it was stored for most of the discharging period [23,24]. This effect leads to higher exergy efficiencies compared to TES technologies that do not take advantage of thermal stratification.

Based on these qualities a potential application of PBTES systems is waste heat recovery in the energy-intensive industry [25]. In their study on the selection of TES options for utilization of industrial waste

* Corresponding author.

E-mail addresses: paul.schwarzmayr@tuwien.ac.at (P. Schwarzmayr), rene.hofmann@tuwien.ac.at (R. Hofmann).

<https://doi.org/10.1016/j.apenergy.2024.122895>

Received 19 September 2023; Received in revised form 2 February 2024; Accepted 17 February 2024

0306-2619/© 2024 The Author(s). Published by Elsevier Ltd. This is an open access article under the CC BY license (<http://creativecommons.org/licenses/by/4.0/>).

Nomenclature	
Acronyms	
ASU	Air supply unit
EU	European Union
FWD	Forward
HTF	Heat transfer fluid
LD	Linz-Donawitz
PBTES	Packed bed thermal energy storage
REV	Reverse
RTD	Resistance temperature detector
SOC	State of charge
TES	Thermal energy storage
Roman symbols	
A	Volume-specific surface area of the packed bed in $\text{m}^2 \text{m}^{-3}$
B	Exergy in J
\dot{B}	Exergy in-/output rate in W
\hat{B}	Maximum gross exergy in-/output rate in W
C	Set of sample indices for charging
c	Specific heat capacity of storage material $\text{J kg}^{-1} \text{K}^{-1}$
c_p	Specific heat capacity at constant pressure for HTF in $\text{J kg}^{-1} \text{K}^{-1}$
M	Momentum of energy in J m
m	Mass in kg
MIX	MIX number
p	Pressure in Pa
Q	Heat in J
\dot{Q}	Heat/energy in-/output rate in W
\hat{Q}	Maximum gross heat/energy in-/output rate in W
R	Set of sample indices for recovery/discharging
S	Set of temperature sensors inside the packed bed $S = [1, 9]$
S	Entropy in J K^{-1}
SOC	State of charge
T	Temperature in K
U	Internal energy in J
W	Work in J
x	Vertical distance of temperature sensors to cold end of the storage in m
Greek symbols	
α	Heat transfer coefficient between packed bed and HTF in $\text{W m}^{-2} \text{K}^{-1}$
κ	Isentropic exponent of HTF ($\kappa = 1.4$)
η	Efficiency
ν	Specific volume of HTF in $\text{m}^3 \text{kg}^{-1}$
Subscripts	
B	Exergy
c	Cold
E	Energy
exp	Experimental
gen	Generation

h	Hot
htf	Heat transfer fluid
i	Sample index
j	Volume element index
loss	Losses to the surrounding
max	Maximum
min	Minimum
mix	Mixed
p	Pumping
Q	Heat
ref	Reference ($T_{\text{ref}} = 303.15 \text{ K}$, $p_{\text{ref}} = 101\,325 \text{ Pa}$)
sat	Saturation (losses)
str	Stratified
Superscripts	
+	Upper boundary of the SOC
-	Lower boundary of the SOC

heat, Manente et al. [26] state, that the integration of PBTES systems can significantly increase the efficiency and process steam output of industrial energy systems. By storing excess heat from industrial processes during periods of low heat demand and releasing the stored heat during periods of high heat demand, PBTES systems can contribute to the exploitation of the industry sector's enormous waste heat potential. The theoretical waste heat potential in the European Union (EU) industry was estimated to be 918 TWh in 2014 [27] which is nearly 8% of the EU's annual final energy consumption. As stated by Papapetrou et al. [28], approximately one third of this theoretical waste heat potential (304 TWh) is technically recoverable. By acting as a substitute for heat generated from burning natural gas, the utilization of this waste heat potential could significantly reduce annual CO_2 emissions.

The main barriers of implementing waste heat recovery in the energy-intensive industry are of economic and technological nature. On the one hand, waste heat recovery systems should be cost efficient and on the other hand they have to operate under very challenging conditions which makes them expensive. Table 1 provides a summary of recent publications in which the improvement of high-temperature industrial waste heat recovery using a TES was investigated. As industrial waste heat is almost always available in form of hot exhaust gas that is contaminated with high amounts of dust, waste heat recovery systems need to be designed to operate with gas-powder two phase flow as HTF. Powder that passes through the system may accumulate in the packed bed and could lead to a degradation of the thermal performance or even a clogging of the voids between the packed bed particles of the storage material [29]. In their studies on utilizing TES systems for the waste heat recovery in the iron and steel industry Keplinger et al. [30] and Ortega-Fernández et al. [31] tackled this issue by placing a gas-to-gas heat exchanger between the waste heat source and the storage (see Fig. 1). Similar studies were conducted by Slimani et al. [32] who investigated a horizontal flow PBTES that uses slag bricks as storage material. For detailed information about the design and analysis of horizontal flow PBTES systems the authors refer to Odenthal et al. [33] Soprani et al. [17]. Since gas-to-gas heat exchangers suffer from low exergy efficiencies and the lifetime of a heat exchanger that is operated with a gas-powder two phase exhaust gas will be short, this approach is not considered efficient from both a technological and an economic point of view. Therefore, the authors of this study propose the direct use of gas-powder two phase exhaust gas from a steel making process as HTF in a PBTES as it is shown in Fig. 1. They gray lines and components (gas-to-gas heat exchanger) in this figure represent the system as it was proposed by Keplinger

Table 1
Summary of studies that consider PBTES systems for waste heat recovery in the iron and steel industry.

Ref.	Objective	Approach	Aspects and results relevant for this work
Keplinger et al. [30]	Improve electric arc furnace waste heat recovery via thermocline TES integration	Dynamic simulation study	<ul style="list-style-type: none"> Hot water stratified storage is integrated via a hot-gas heat exchanger Thermocline storage integration enables decoupling of waste heat source and from steam production Maximum productivity and economic efficiency can be reached
Ortega-Fernández et al. [31]	Waste heat recovery from electric arc furnace exhaust gases using a TES	Case study	<ul style="list-style-type: none"> High temperature filter and flue-gas heat exchanger are used to protect PBTES from gas-powder two phase flow Operation planning to synchronize waste heat source and PBTES is of high importance System efficiency of around 65% is obtained
Slimani et al. [32]	Horizontal PBTES for waste heat recovery in the iron and steel industry	Numerical and economic study	<ul style="list-style-type: none"> Drop-out box and flue-gas heat exchanger are used to protect PBTES from gas-powder two phase flow Drop-out box and heat exchanger alone have a combined thermal efficiency of 45% PBTES waste heat recovery using slag as storage material is economically and ecologically attractive
Touzo et al. [34]	PBTES for high-temperature waste heat recovery	Experimental and numerical analysis	<ul style="list-style-type: none"> The issue of gas-powder two phase flow was not investigated Performance of commercial-scale PBTES was validated During cyclic operation the PBTES reaches a thermal efficiency of up to 90%

et al. [30] and Ortega-Fernández et al. [31]. The colored lines illustrate the integration of the PBTES for the direct use of industrial exhaust gas as HTF in a PBTES. This approach significantly reduces investment costs (no heat exchanger and less piping) and increases the exergy efficiency of the whole system. However, the challenges that arise when using gas-powder two phase exhaust gas as HTF in a PBTES are still in place.

In one of their previous studies [29] the authors already investigated effects like pressure drop and powder hold-up in a PBTES that is operated with a gas-powder two phase exhaust gas from a steel producing process. The results of this study revealed that the proposed approach is viable for the waste heat recovery from gas-powder two phase exhaust gas if certain measures are taken. In [29] it was found that 98% of the powder that is introduced into a PBTES with gas-powder two phase exhaust gas deposits inside the storage and is concentrated at the packed bed's surface at which the HTF enters the packed bed. Therefore it was suggested to switch the operating conditions of a PBTES so that it is charged from the bottom and discharged from the top. This way the powder hold-up inside the storage would be concentrated at the bottom surface of the packed bed where it can be easily removed via knocking/trembling mechanisms. Therefore one major adaption that has to be made compared to PBTES systems that operate in modern concentrated solar power (CSP) plants is the flow direction of the HTF during the charging and discharging periods. Since the natural choice of the HTF flow direction through a PBTES during charging is from top to bottom [35] only one study that investigates the thermal performance of a PBTES that is charged from bottom to top is available [36]. However, in this study only the standby operation of

a PBTES is considered. For a PBTES that is to be used for the waste heat recovery in a steel producing process, standby periods will be seldom and cycle durations will be short (40 min to 60 min). There are no studies that compare the performance of a PBTES in partial cycle operation for different flow directions of the HTF available to the authors. The remainder of this introductory section consist of a concise literature review of existing partial cycle studies and an elaboration of the research gap this paper aims to address. A short summary of this literature review is also provided in Table 2.

Comprehensive reviews considering experimental investigations on the partial cycle operation of PBTES systems were provided by Esence et al. [35] and Gautam et al. [2,3]. In their papers on packed bed thermocline storage performance Bayón et al. [37], Biencinto et al. [38] and Wang et al. [39] point out the importance of the operation strategy (partial extraction of the thermocline at the end of charging and discharging) on the performance of a PBTES in dynamic operation. Zavattoni et al. [40,41] conducted experiments considering the thermal stratification under charge/discharge cyclic conditions on their small-scale TES test rig and found that it takes up to 30 cycles until a steady state operation is established. Mertens et al. [42] investigated a PBTES for solar applications and highlighted that preheating is essential for the long term performance of a PBTES in partial cycle operation. They also state, that although this leads to an additional energy consumption during initial cycles, it also provides additional flexibility during the long term operation. Zanganeh et al. [43] numerically investigated an industrial scale gas-solid PBTES and stated, that the long-term performance of a PBTES is defined by its stabilized state. They found, that the duration of the stabilizing phase, both in terms of time and number of cycles can be controlled via operating parameters. Similar investigations were conducted by Bruch et al. [23] and Johnson et al. [44]. Bruch et al. experimentally studied an oil-rock PBTES in partial cycle operation and came to similar conclusions as Zanganeh et al.. Especially for short cycles, they found that thermocline degradation during partial cycle operation reduced the effective storage capacity by about 10%. The same conclusions were drawn by Cascetta et al. [45] who investigated a gas-solid PBTES under partial cycle operation. The numerical study of McTigue et al. [46] provides evidence on decreased efficiencies for long partial cycles especially if perturbations of cycle durations are involved. In their latest study on a pilot-scale oil-rock PBTES, Bruch et al. [24] investigated the impact of end-of-discharge criteria on the utilization rate of the storage capacity. They found, that by lowering the minimum discharge temperature, the utilization rate can be increased significantly. Since all these existing studies investigate the partial cycle operation for cut-off temperature-controlled cycles, the application of their results to a PBTES that is to be used for waste heat recovery in the

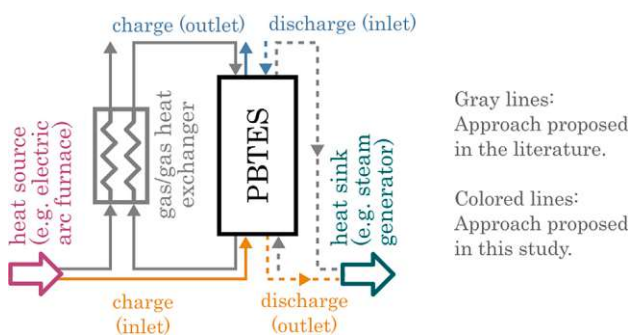


Fig. 1. Comparison of literature approach [30,31] and the system proposed in the present study.

Table 2
Summary of studies carried out to investigate the partial cycle operation of a PBTES.

Ref.	Objective	Approach	Results
Bayón et al. [37]	Exergy efficiency of a PBTES in partial cycle operation	Numerical study	<ul style="list-style-type: none"> Storage efficiency decreases during consecutive charge/discharge cycles This strong decrease can be relieved via partial thermocline extraction Without thermocline extraction, long term energy efficiency is below 50%
Bruch et al. [23]	Efficiency of an oil/rock PBTES in partial cycle operation	Numerical and experimental study	<ul style="list-style-type: none"> Valuable part of storage tank and/or thermal efficiency reduce during partial cycle operation Long-term efficiency in partial cycle operation is defined by a stabilized state which is reached after 10 cycles Thermocline control during long-term partial cycle operation is important
Bruch et al. [24]	Cycling behavior of a pilot-scale oil/rock PBTES	Experimental study	<ul style="list-style-type: none"> Stabilized state in partial cycle operation is independent on initial conditions Proper definition of end-of-cycle condition is important for efficient storage operation Energetic efficiencies of 88% to 92% were observed
Cascetta et al. [45]	Thermal behavior of a PBTES in repeated cycle operation	Experimental study	<ul style="list-style-type: none"> Thermocline degradation during partial cycle operation is significant Stabilized state is reached after 7 cycles Stabilized state can be controlled by design and operational parameters (mass flow, temperature threshold, aspect ratio)
Johnson et al. [44]	Exergy efficiency of a PBTES for ten charge–discharge cycles	Numerical study	<ul style="list-style-type: none"> Exergy losses during partial cycle operation are caused by thermocline degradation and heat losses to the surrounding Exergy efficiency in the stabilized state is 80% to 84% To improve the partial cycle performance of PBTES, the focus should be on minimizing thermocline degradation
Mertens et al. [42]	Dynamic simulation of a PBTES for CSP applications	Numerical study	<ul style="list-style-type: none"> Stabilized state is reached after 5 cycles Stabilized state energy efficiency is observed to be 95% Air/rock PBTES systems are an efficient and cost-effective alternative to molten-salt TES systems
Schwarzmayr et al. [36]	Efficiency of a PBTES in standby operation	Experimental study	<ul style="list-style-type: none"> Impact of HTF flow direction on thermocline degradation was investigated. For long standby periods, charging the PBTES from the bottom leads to significantly higher exergy losses If standby periods are short, charging a PBTES from the bottom does not lead to additional energy or exergy losses
Zanganeh et al. [43]	Testing of a pilot-scale PBTES for CSP applications	Numerical and experimental study	<ul style="list-style-type: none"> Thermocline degradation could be observed during partial cycle operation Stabilized state thermal efficiency was observed to be 95%
Zavattoni et al. [40]	Analysis of a PBTES under charge/discharge cyclic conditions	Numerical (CFD) study	<ul style="list-style-type: none"> Stabilized state is reached after 8–10 cycles Stabilized state thermal efficiency was observed to be 95% Pumping energy accounts for 7% of the input energy during charging

iron and steel industry is limited. When integrated into an industrial energy system, a TES has to follow the schedule of the upstream industrial process. Therefore, a time-controlled operation of the TES is more appropriate in this case. Under such operating conditions, end-of-charge and end-of-discharge criteria as defined by Bruch et al. [24] may not be satisfied for any cycle which has a negative impact on the exergy efficiency of the PBTES. Furthermore, as delineated in the previous paragraph, none of the mentioned studies (except [36], where the standby operation was studied) investigated a PBTES that is charged from the bottom and discharged from the top.

Therefore the goal and novelty of this work is the experimental investigation of the thermal performance of a PBTES in time-controlled partial cycle operation with a HTF charging flow direction from bottom to top. The motivation for this adapted operating strategy (shown in Fig. 1) – which stands in contrast to favorable operating conditions in terms of mitigating thermocline degradation – is the accumulation of powder hold-up in a PBTES that is charged with gas-powder two phase exhaust gas. Key performance indicators such as exergy efficiency, thermocline degradation and thermal power rates will be used to evaluate the proposed operating strategy. The results provided in this study will support industrial decision makers to assess the potential and economic benefits of a PBTES system for the waste heat recovery in their energy intensive processes.

The remainder of this paper is divided into four sections. The most important information and properties of the materials and the test rig that are used for the experimental investigations are provided in Section 2. At the end of Section 2 the experimental procedure as well as some important experimental operating parameters are summarized. Section 3 includes the main equations, uncertainty estimations and conceptual considerations that are necessary to understand to evaluation

of the measurement data. Experimental results as well as a summary and interpretation of the main findings are provided in Section 4. These main findings include reference values for energy/exergy efficiencies and maximum power rates for different operating conditions of the test rig. For convenience, some additional abbreviations will be used in the rest of this paper. Charging the PBTES from the top and discharging it from the bottom will be referred to as the FWD-mode, whereas charging the PBTES from the bottom and discharging is from the top will be referred to as the REV-mode.

2. Material and methods

2.1. Experimental setup

For the evaluation of the exergy efficiency and thermocline degradation of PBTES systems in partial cycle operation a lab-scale test rig of a vertical gas–solid PBTES was used. The main part of the test rig – the storage tank – is a vertical, slightly conical steel vessel that is filled with 891 kg of storage material. The conical design of the storage tank reduces thermo-mechanical stresses (thermal ratcheting see e.g. [47]) in the walls. LD-slag, a by-product from the iron and steel industry, is utilized as storage material. The choice of LD-slag as storage material is substantiated both by its low costs and excellent heat transfer properties. The geometric shape of the slag particles leads to an enhanced heat transfer between HTF and storage material and an even perfusion of the packed bed. Both have a positive impact on the thermal performance (power rate and storage capacity) of the TES. The whole test rig (storage tank and piping) is equipped with multiple layers of thermal insulation to reduce heat losses. In Fig. 2 photographs of the storage material and the test rig with and without thermal

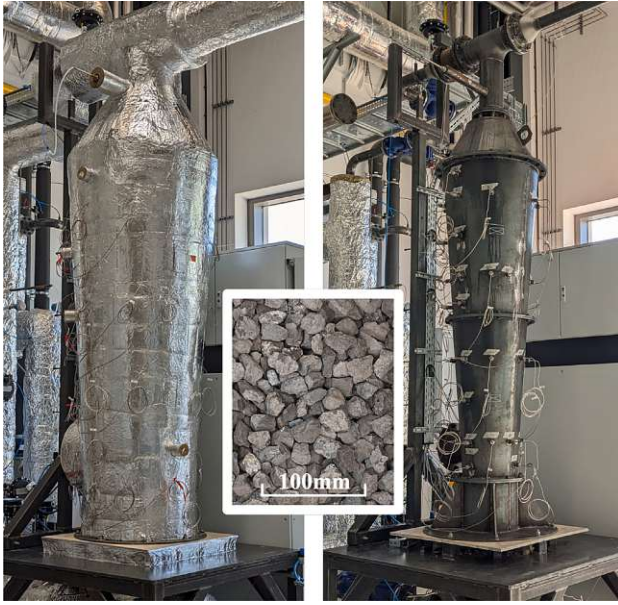


Fig. 2. PBTES test rig at the laboratory of TU Wien: with thermal insulation (left), storage material (center), without thermal insulation (right).
Source: Reprinted from [36].

insulation are shown. Detailed information about the test rig geometry, the utilized materials, the insulation and the operating conditions for the experiments are provided in Table 3.

In order to measure the thermal behavior of the experimental setup, the test rig is equipped with various temperature sensors. Two sensors are placed in the pipes that are connected to the top and bottom of the storage tank to measure the temperature of the HTF that enters/exits the packed bed (T_B and T_T). The temperature distribution inside the packed bed is measured with nine sensors that are evenly distributed along the center axis of the storage tank. To guarantee accurate measurements, four-wire resistance temperature detectors (RTD) class AA (or 1/3 DIN) PT100 sensors are utilized. The measurement uncertainty of the temperature sensors including all steps of signal conversion is less than $\pm 0.6^\circ\text{C}$ for a measured value of 300°C . To estimate exergy losses due to pumping work a piezoresistive differential pressure sensor is used to measure the pressure drop Δp between the packed bed in- and outlet pipes. This sensor was calibrated to an accuracy of $\pm 0.06\%$ of full scale before the experiments. Fig. 3 shows a simplified process flow diagram of the test rig including the sensor layout relevant for the investigations carried out in this work. For a detailed description of the sensor layout the authors refer to their previous study [36].

The PBTES test rig is provided with hot and cold HTF by an external air supply unit (ASU). The ASU is capable of supplying up to 400 kg h^{-1} of air with temperatures between ambient temperature and 400°C . The HTF mass flow that passes through the system is controlled by the ASU and is measured with a hot-wire anemometer. The measurement uncertainty of this sensor does not exceed 4% with respect to the measured value.

2.2. Experimental procedure

A PBTES that is operated at short charging/discharging periods and high power rates, can guarantee maximum exergy efficiency and flexibility when it is cycled around a partially charged ($\approx 50\%$) state [35]. The problem with such an operating strategy is that thermocline degradation may significantly reduce the storage's efficiency over time.

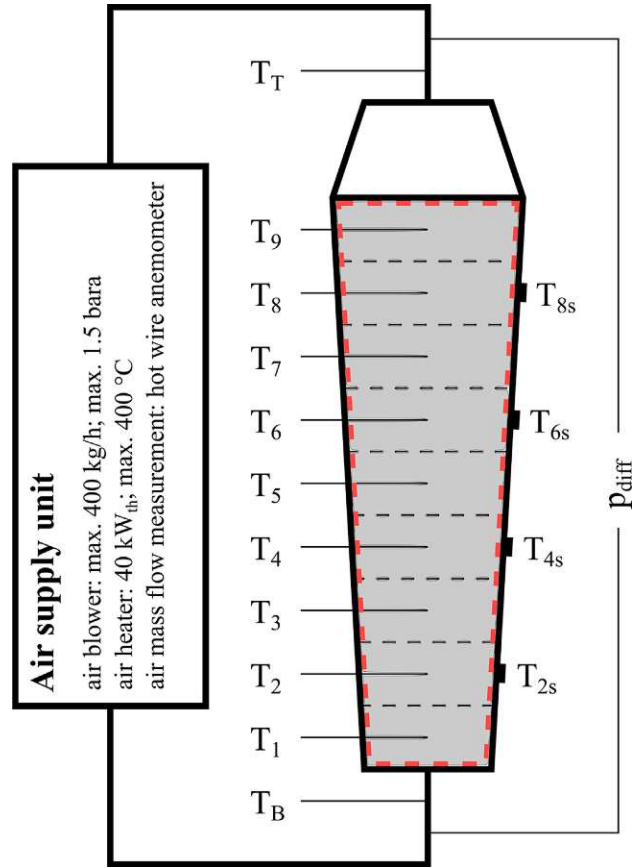


Fig. 3. Simplified process flow diagram of the PBTES test rig at the laboratory of TU Wien.
Source: Reprinted from [36].

Furthermore this effect may be even worse if the TES is designed to be operated in REV-mode.

In order to close the research gap described at the end of the introduction (Section 1), multiple experiments were conducted as part of this study. For a better understanding of the experimental procedure, Fig. 4 provides a schematic figure of the evolution (degradation) of the temperature profiles inside a PBTES during partial cycle operation in FWD-mode. As depicted in Fig. 4, there is a hot and a cold zone inside the packed bed throughout the whole process of partial cycle operation. Depending on the operating mode (charging or discharging) the thermocline moves downwards or upwards within the active zone of the packed bed. Based on the review of existing studies it is expected that the shape of the temperature profile inside the packed bed changes (degrades) throughout the partial cycle operation (compare Fig. 4a and b). The purpose of the experiments carried out in the course of this study is to investigate whether this effect (thermocline degradation) is more pronounced when the PBTES is operated in REV-mode rather than in FWD-mode. Therefore partial cycle experiments both in FWD- and REV-mode were conducted using the experimental setup presented in Section 2.1. Every experiment started with an empty storage (constant temperature of 30°C) that was then charged with hot air (300°C) until a state of charge (SOC) of approximately 50% was reached. In the next step, the storage was operated in partial cycle operation (between a lower and an upper SOC, SOC^- and SOC^+ respectively) where it was alternately charged and discharged with a HTF mass flow of 230 kg h^{-1} and very short cycle periods until a steady cycling operation was reached. The HTF temperatures during charging and

Table 3
Summary of parameters: Test rig geometry, data/properties of storage material, operating conditions.
Source: Adapted from [36].

Test rig	
Storage type	Vertical PBTES
Tank material	P295
Tank diameter	350 mm (bottom), 500 mm (middle), 650 mm (top)
Tank height	2050 mm
Storage volume	0.405 m ³
Thermal insulation	100 mm ceramic wool ($\lambda = 0.055 \text{ W m}^{-1} \text{ K}^{-1}$) 80 mm rock wool ($\lambda = 0.04 \text{ W m}^{-1} \text{ K}^{-1}$) 0.1 mm aluminum sheeting
Storage material	
Type of storage material	LD-slag (irregular shaped, partly porous)
Composition of storage material	CaO (24%–49%), SiO ₂ (6%–37%), Fe ₂ O ₃ (10%–36%), MgO (0%–13%), Al ₂ O ₃ (0%–7%), Cr ₂ O ₃ (0–0.55%)
Grain size	16 mm to 32 mm
Particle density	3800 kg m ⁻³
Fractional void volume	0.42
Bulk density	2200 kg m ⁻³
Specific heat capacity	900 J kg ⁻¹ K ⁻¹
Operating parameters	
Mass of storage material	891 kg
Air mass flow	230 kg h ⁻¹
Charging temperature	300 °C
Recovery temperature	30 °C
HTF mass flux	0.17 kg m ⁻² s ⁻¹ to 0.58 kg m ⁻² s ⁻¹
Cycle duration	40 min to 60 min

discharging were set to 300 °C and 40 °C respectively. This procedure was repeated for both FWD- and REV-mode operation of the storage and different charging/discharging periods (40 min to 60 min). The reason for time-controlled charging/discharging periods rather than SOC- or cut-of-temperature-controlled is the nature/characteristics of industrial processes. When integrated into an industrial energy system, the operation of a TES is determined by the strictly scheduled production plan of the upstream industrial process. This operating behavior is best simulated with time-controlled charging/discharging periods with a 40 min to 60 min cycle duration.

3. Theory and calculations

In this section all equations that are used for the post-processing of the measured data are provided and explained. The index i represents the sample number and the index j is used to represent the individual temperature sensors ($j \in S = [1,9]$) inside the packed bed. Before calculating energy/exergy efficiencies and evaluating thermocline degradation, the measured data is validated using the first and second law of thermodynamics applied to the storage material inside the storage tank (system boundaries are the same as in [36]). The energy balance (first law) of this thermodynamic system can be written as

$$\sum_{j \in S} dU_{i,j} = \delta Q_{\text{htf},i} - \delta Q_{\text{loss},i} \quad (1)$$

where the left side is the change in the system's internal energy and the right side is the sum of all heat crossing the system boundary. The change in the system's internal energy is defined by the caloric equation of state as

$$dU_{i,j} = m_j c(T) dT_{i,j} \quad (2)$$

where $T_{i,j}$ is the measured temperature value of each sensor located in the packed bed, m_j is the mass of storage material that is assigned to each temperature sensor and $c(T)$ is the specific heat capacity of the storage material which is assumed to be constant. The heat crossing

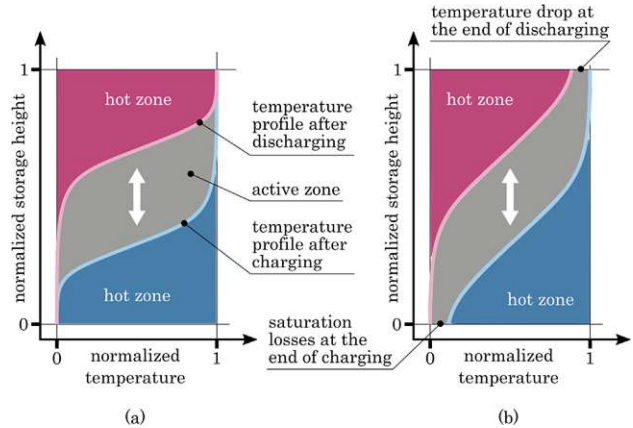


Fig. 4. Experimental procedure for partial cycle operation of a PBTES: (a) vertical temperature profile at the end of the first cycle's charging and discharging period, (b) vertical temperature profile at the end of the n th cycle's (where a steady cycling operation is established) charging and discharging period.

the system boundary due to heat transfer between HTF and storage material can be calculated as

$$\delta Q_{\text{htf},i} = \delta m_{\text{htf},i} \int_{T_{c,i}}^{T_{h,i}} c_p(T) dT. \quad (3)$$

where $\delta m_{\text{htf},i}$ is the amount of HTF that passes through the packed bed, $c_p(T)$ is the specific heat capacity of the HTF at isobaric conditions and $T_{c,i}$ and $T_{h,i}$ are the temperatures of the cold and hot HTF entering/exiting the packed bed respectively.

Analogously to the energy balance in Eq. (1) the entropy generation equation (second law) applied to the storage volume can be written as

$$\sum_{j \in S} dS_{i,j} = \delta S_{Q,i} + \delta S_{\text{gen},i} \quad (4)$$

where the left side is the change in system entropy and the right side is the sum of entropy crossing the system boundary due to heat transfer and the entropy generation due to irreversible effects. The change in system entropy is defined by the equation of state given in Eq. (5).

$$dS_{i,j} = m_j \frac{c(T)}{T} dT_{i,j} \quad (5)$$

The entropy introduced into the system due to heat crossing the system boundary is per definition

$$\delta S_{Q,i} = \sum_{j \in S} \frac{dU_{i,j}}{T_{\text{htf},i,j}} \quad (6)$$

where $T_{\text{htf},i,j}$ is the absolute temperature at which the heat that is equivalent to $dU_{i,j}$ crosses the system boundary. It is assumed, that the entropy transport due to heat losses to the surrounding is negligible compared to the entropy transport due to heat transfer between HTF and storage material. The impact of this assumption on the significance of the results presented in this study is discussed in Section 4. The absolute temperature $T_{\text{htf},i,j}$ is calculated using Eq. (7), where α is the heat transfer coefficient between HTF and storage material and A is the volume-specific surface of the packed bed. Both parameters were determined via model-based parameter optimization using a finite volume model of the test rig [48].

$$T_{\text{htf},i,j} = T_{i,j} + \frac{dU_{i,j}}{\alpha A} \quad (7)$$

Considering both Eqs. (1) and (4), the measured data is considered valid if the heat losses to the surrounding δQ_{loss} in Eq. (1) and the entropy generation $\delta S_{\text{gen},i}$ in Eq. (4) are positive.

The energy and exergy efficiency of the examined PBTES test rig in partial cycle operation are defined as

$$\eta_E = \frac{\sum_{i \in \mathcal{R}} \delta Q_{\text{htf},i}}{\sum_{i \in \mathcal{C}} \delta Q_{\text{htf},i} + \sum_{i \in \mathcal{C}} \delta Q_{\text{sat},i} + \sum_{i \in (\mathcal{C} \cup \mathcal{R})} \delta W_{p,i}} \quad (8)$$

and

$$\eta_B = \frac{\sum_{i \in \mathcal{R}} \delta B_{\text{htf},i}}{\sum_{i \in \mathcal{C}} \delta B_{\text{htf},i} + \sum_{i \in \mathcal{C}} \delta B_{\text{sat},i} + \sum_{i \in (\mathcal{C} \cup \mathcal{R})} \delta W_{p,i}} \quad (9)$$

The energy efficiency η_E is defined as the ratio of the heat that can be extracted from the test rig during a discharging period ($i \in \mathcal{R}$) to the amount of heat that is introduced into the system during the preceding charging period ($i \in \mathcal{C}$) plus the amount of work that is needed to pump the HTF through the packed bed during charging and discharging periods ($i \in (\mathcal{C} \cup \mathcal{R})$). The exergy efficiency is defined analogously to the energy efficiency as given in Eq. (9).

The exergy change that the HTF experiences when it passes through the packed bed can be calculated as

$$\delta B_{\text{htf},i} = \delta Q_{\text{htf},i} - T_{\text{ref}} \delta S_{\text{htf},i} \quad (10)$$

where T_{ref} is the reference temperature (30 °C = 303.15 K) and

$$\delta S_{\text{htf},i} = \delta m_{\text{htf},i} \int_{T_{\text{c},i}}^{T_{\text{h},i}} \frac{c_p(T)}{T} dT \quad (11)$$

It can be seen, that both the energy and exergy efficiency incorporate saturation losses ($\delta Q_{\text{sat},i}$ and $\delta B_{\text{sat},i}$) for the charging periods. These losses are caused by increased exhaust gas temperatures and can be calculated as

$$\delta Q_{\text{sat},i} = \delta m_{\text{htf},i} \int_{T_{\text{ref}}}^{T_{\text{c},i}} c_p(T) dT \quad \text{and} \quad \delta B_{\text{sat},i} = \delta Q_{\text{sat},i} - T_{\text{ref}} \delta S_{\text{sat},i} \quad (12)$$

where

$$\delta S_{\text{sat},i} = \delta m_{\text{htf},i} \int_{T_{\text{ref}}}^{T_{\text{c},i}} \frac{c_p(T)}{T} dT \quad (13)$$

$\delta S_{\text{sat},i}$ is the entropy difference between the HTF that exits the storage and the surrounding air.

The amount of pumping work $\delta W_{p,i}$ that is needed to overcome the pressure drop Δp_i caused by the packed bed can be calculated as

$$\delta W_{p,i} = \frac{1}{\eta_p} \delta m_{\text{htf},i} \int_{p_{\text{ref}}}^{p_{\text{ref}} + \Delta p_i} v dp \quad \text{with} \quad p v^\kappa = \text{const.} \quad (14)$$

where p_{ref} is the ambient pressure, Δp_i is the pressure drop of the packed bed measured during the experiments, v is the specific volume of the HTF passing through the packed bed, κ is the isentropic exponent of the HTF and η_p is the efficiency (assumed to be 0.35 [43]) of the aggregate that is utilized to pump the HTF through the packed bed.

For a more convenient data visualization in Section 4 the SOC is used to describe the amount of energy stored in the PBTES at a certain time. In this study the SOC is defined as

$$SOC_i = \frac{\sum_{j \in S} U_{i,j} - U_{\text{min}}}{U_{\text{max}} - U_{\text{min}}} \quad \text{where} \quad U_{i,j} = m_j \int_{T_{\text{ref}}}^{T_{i,j}} c(T) dT \quad (15)$$

U_{min} is the energy that is stored in a fully discharged storage ($T_j = 30^\circ\text{C} \forall j \in S = [1, 9]$) and U_{max} is the energy for a fully charged storage ($T_j = 300^\circ\text{C} \forall j \in S = [1, 9]$).

Finally, the MIX number [49] can be calculated, to quantify the thermocline degradation of the examined PBTES in partial cycle operation. The MIX number is a dimensionless number that was first defined by Andersen et al. [50] and is based on the momentum of energy. For the calculation of the momentum of energy, the amount

of energy that is stored in each vertical volume section $U_{i,j}$ is weighted with its vertical distance x_j from the cold end of the storage as

$$M_i = \sum_{j \in S} x_j U_{i,j} \quad (16)$$

With this definition, the MIX number is a suitable metric to describe the thermocline in a PBTES with an uneven distribution of the storage mass. Andersen et al. defined the MIX number as

$$MIX_i = \frac{M_{\text{str},i} - M_{\text{exp},i}}{M_{\text{str},i} - M_{\text{mix},i}} \quad (17)$$

where $M_{\text{exp},i}$ is the momentum of energy calculated from the measured data, $M_{\text{str},i}$ is the momentum of energy for an entirely stratified storage and $M_{\text{mix},i}$ is the momentum of energy of an entirely mixed storage. Both $M_{\text{str},i}$ and $M_{\text{mix},i}$ are calculated for a virtual storage with the same SOC as the real storage. With this definition, the MIX number is 0 if the real storage is perfectly stratified and 1 if it is perfectly mixed. Details on the calculation of the MIX number and the definition of an entirely stratified and mixed storage are provided by Oró et al. [15].

The impact of measurement uncertainties on the quality of the calculated results is estimated using the law of error propagation. The maximum errors of the measuring devices used for the experiments in this study are $\pm 4\%$ of the measured value for the air mass flow sensor and ± 0.6 K for the temperature sensors. With these two values the maximum errors in the calculated heat and exergy $\delta Q_{\text{htf},i}$ and $\delta B_{\text{htf},i}$ defined in Eqs. (3) and (10) are well below 4% of the calculated values. The uncertainties in the energy and exergy efficiency η_E and η_B are calculated using the repeatability of the utilized mass flow sensor ($\pm 0.5\%$). This results in a maximum error that is less than 1% of the calculated value for both quantities. Since these errors are nominal, they do not have any impact on the quality and significance of the results presented in this study.

4. Results and discussion

Before presenting and discussing the core results of this study the validity and significance of the measured data is clarified shortly. The first and second law are used for data validation as already presented in the beginning of Section 3. The experimental data satisfies the energy balance in Eq. (1) with average heat loss rates of 525 W and 287 W for charging and discharging respectively. Similarly, the second law in Eq. (4) is satisfied with an average entropy generation of 0.63 W K^{-1} for charging and 0.1 W K^{-1} for discharging. Since these values are all positive, the experimental data collected in the course of this study is considered valid.

Multiple experiments for the FWD- and REV-mode with different charging/discharging periods are carried out in the course of this study. The results reveal, that the length of the charging/discharging periods does not have a significant impact on the thermocline degradation. Therefore, only results from the experiments with charging/discharging periods of 60 min are discussed in the remainder of this section. Figs. 5 and 6 display the axial temperature distribution inside the test rig during the experiments where the TES was operated in FWD- and REV-mode respectively. The ordinate represents the dimensionless temperature where 0 corresponds to the ambient temperature (30 °C) and 1 corresponds to 300 °C. On the abscissa, the dimensionless height of the packed bed is plotted, where 0 corresponds to the bottom (0 m) and 1 to the total height of the packed bed (2.05 m). The blue lines and areas show the temperature profile inside the packed bed for the first charging/discharging cycle and the orange lines and areas show the temperature profile of the n th cycle where steady cycling is reached. For the given operating parameters steady cycling is reached after the 10th cycle (corresponding to less than 10 h) for the experiments carried out in this study. Besides the degradation of the thermocline, the most important observation that can be made in these figures are the temperature differences at both ends of the storage. During the first

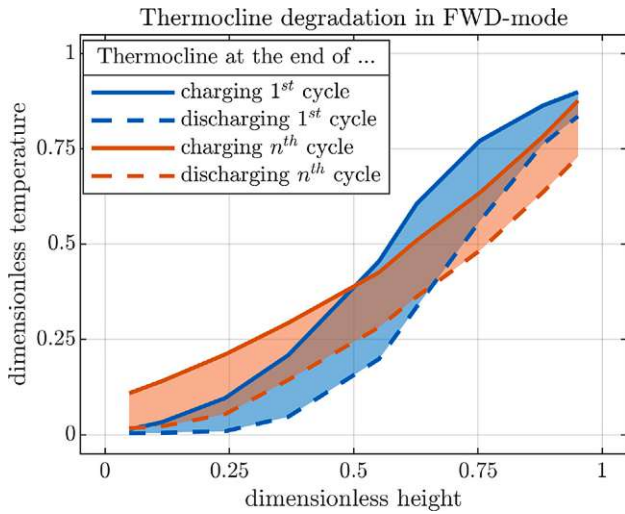


Fig. 5. Thermocline degradation of a PBTES in partial cycle operation (FWD-mode) with a cycle time of 1 h.

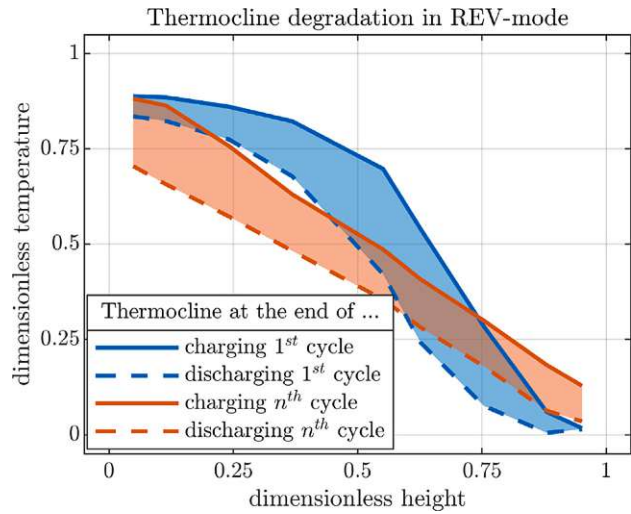


Fig. 6. Thermocline degradation of a PBTES in partial cycle operation (REV-mode) with a cycle time of 1 h.

cycle (blue lines and areas) the temperatures at the top and bottom end of the packed bed do not change significantly for both operating the TES in FWD- and REV-mode. For the n th cycle (red lines and areas), however, the temperature differences between the solid and dashed lines at the top and bottom ends of the packed bed are clearly bigger. This means that during charging, the exhaust temperatures of the HTF are above the ambient temperature leading to saturation losses. Likewise, the exhaust gas temperature during discharging is significantly lower than the charging temperature. Both effects lead to a deterioration of the energy and exergy efficiency of the storage, which will be confirmed later in this section.

As the axial distribution of the storage material mass in the examined test rig is not even, the comparison of the temperature profiles in Figs. 5 and 6 is not reasonable. To make statements on the difference in thermocline degradation between a PBTES that is operated in FWD-mode versus a PBTES that is operated in REV-mode, the MIX number as it is defined in Eq. (17) comes in handy. As the MIX number is calculated based on the momentum of energy the information of uneven mass distribution is also taken into account. Fig. 7 presents the results of evaluating the MIX number for the collected data. Again, the blue lines and area represent the FWD-mode and the orange lines and area represent the REV-mode. In this figure, the number of charging/discharging cycles is plotted on the abscissa. It can be observed, that for both the FWD- and REV-operation the MIX number in the first cycle is similar and starts to diverge with increasing number of cycles. In FWD-mode the MIX number seems to converge to an average value of approximately 0.18 whereas in REV-mode the MIX number is noticeably higher and still slightly rises after the 11th cycle. A corollary of these observations is, that when a PBTES is operated in partial cycle and REV-mode, a much faster and more pronounced degradation of the thermocline inside the packed bed has to be expected. In the following paragraphs, the impact of this accelerated thermocline degradation on the most important thermal key performance indicators is discussed.

In Fig. 8 the energy and exergy efficiency as they are defined in Eqs. (8) and (9) for both operating modes (FWD and REV) are illustrated. The evaluation of measurement data revealed, that the pumping work needed to overcome the pressure drop of the packed bed reduces the energy and exergy efficiency by less than 0.5% and 3% points respectively and is therefore negligible compared to the thermal effects. Notice, that the ordinate in this figure starts at 0.75. The blue and violet bars represent the energy and exergy efficiencies for the first

charging/discharging cycle. Efficiencies for the n th cycle, where steady cycling is reached, are displayed as orange and green bars. Naturally, all exergy efficiencies are lower than the energy efficiencies which is mainly caused by the temperature difference that is needed as a driving force to transfer heat from the HTF to the storage material and vice versa. Nevertheless, the exergy efficiencies achieved in the experiments of this study all are greater than 80%, which is higher than other sensible heat TES systems (Ruths steam storage, hot water tanks) of comparable size can accomplish. These results coincide with findings from Knobloch et al. and Soprani et al. [16,17]. Furthermore, the results in Fig. 8 reveal that both the energy and the exergy efficiency for the n th cycle are 5 to 6% points lower compared to the efficiencies in the first cycle. This is due to the increased impact of thermocline degradation on the storage's performance in the n th cycle. Since thermocline degradation leads to lower discharging temperatures and higher exhaust losses during charging both the energy and exergy efficiency are negatively influenced by this effect. An impact of the

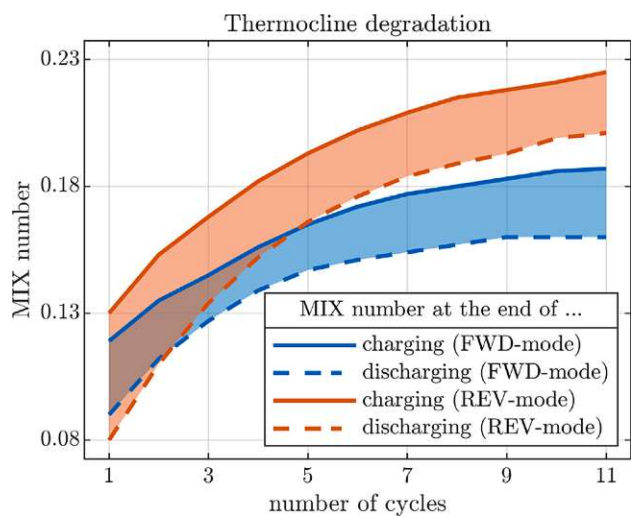


Fig. 7. Thermocline degradation of a PBTES in partial cycle operation with a cycle time of 1 h: MIX number.

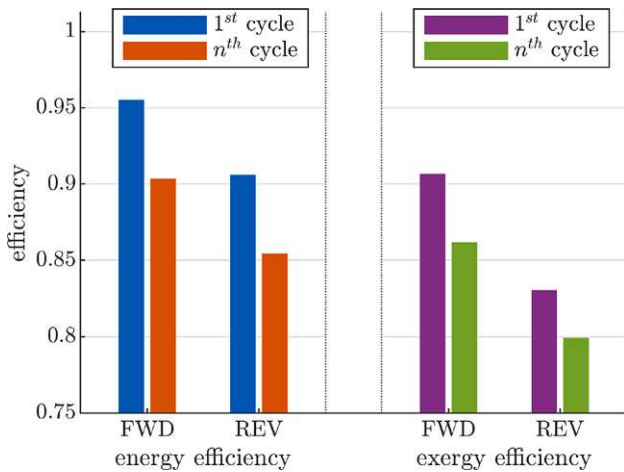


Fig. 8. Energy-/exergy roundtrip efficiency of a PBTES in partial cycle operation with a cycle time of 1 h.

operating mode (FWD or REV) on this degradation of the efficiencies cannot be observed. When comparing the FWD- and REV-operation, Fig. 8 indicates that the energy efficiency of a PBTES in REV-mode is lower by 5% points compared to the FWD-mode. This efficiency loss can be explained by increased heat losses to the surrounding via the metal grating on which the packed bed is sitting and a higher surface-to-volume ratio at the bottom half of the storage vessel. The losses of the exergy efficiency, when comparing the REV- and the FWD-operation, are between 6 to 7% points, which is mainly caused by the accelerated thermocline degradation that is also evident in Fig. 7.

Figs. 9 and 10 illustrate the energy and exergy in-/output rates that are accomplished for different experimental conditions. Positive

values on the ordinate are energy/exergy input rates when the storage is charged whereas negative values are output rates when the storage is discharged. All values are normalized to the maximum gross input rate that is observed during charging ($\dot{Q}_{htf} = 15.4 \text{ kW}$ and $\dot{B}_{htf} = 3.9 \text{ kW}$). The gross input rate is the sum of the energy/exergy rate transferred to the packed bed and the saturation losses ($\dot{Q}_{htf} + \dot{Q}_{sat}$ and $\dot{B}_{htf} + \dot{B}_{sat}$ respectively) and is plotted as a black solid line in Figs. 9 and 10. The dashed lines represent the in-/output rates that are reached in the first cycle of each experiment whereas the dotted lines are the in-/output rates achieved in the n th cycle after steady cycling is reached. The results from the experiments where the storage is operated in FWD- and REV-mode are plotted in blue and orange respectively. As documented in Section 2 the partial cycle experiments start with a storage that is charged to a state of charge of approximately 50%. During the partial cycle experiments the storage is cycled between a lower and an upper SOC (SOC^- and SOC^+ respectively). As SOC^- and SOC^+ are not exactly the same for every cycle, the x-axes in Figs. 9 and 10 are labeled with the variable names SOC^- and SOC^+ . For the experiments presented in Figs. 9 and 10 $SOC^- = 0.32$ to 0.38 and $SOC^+ = 0.48$ to 0.54 .

Considering the energy in-/output rate for the first cycles (dashed lines) in Fig. 9, exactly the same behavior is observed for the FWD- and the REV- mode. In the second half of the charging period both curves start to diverge from the solid black curve. This difference is caused by saturation losses due to an increase in the exhaust gas temperature. During the discharging period a fairly constant output rate with a maximum of 93% and 89% is reached in the FWD- and the REV-mode respectively. The difference between the two modes can be explained by higher heat losses via the metal grating at the bottom of the packed bed in the REV-mode. The energy in-/output rate for the n th cycles, which are plotted as dotted lines, indicate increased saturation losses throughout the whole charging period. Furthermore a degradation of the maximum output rate for both the FWD- (89%) and REV-mode (84%) can be observed. However, in both modes the energy output rate for the n th cycle (steady cycling) is well above 74% of the maximum gross input rate \dot{Q}_{htf} .

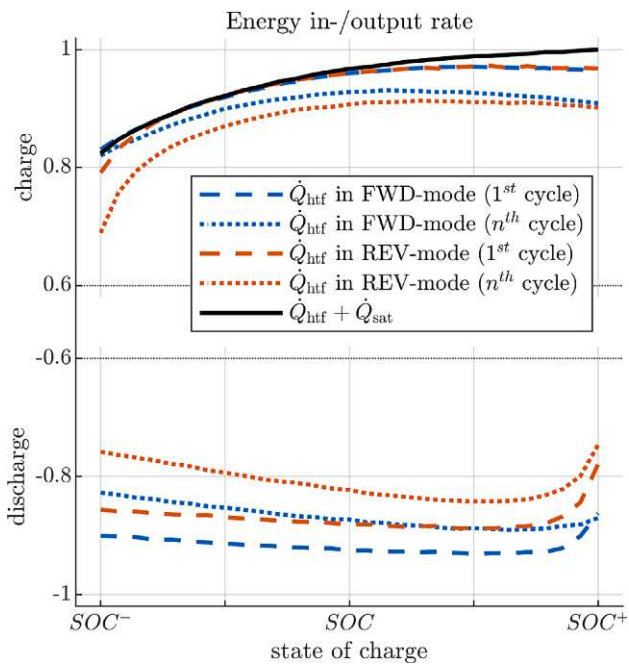


Fig. 9. Rate of energy in- and output of a PBTES in partial cycle operation with a cycle time of 1 h.

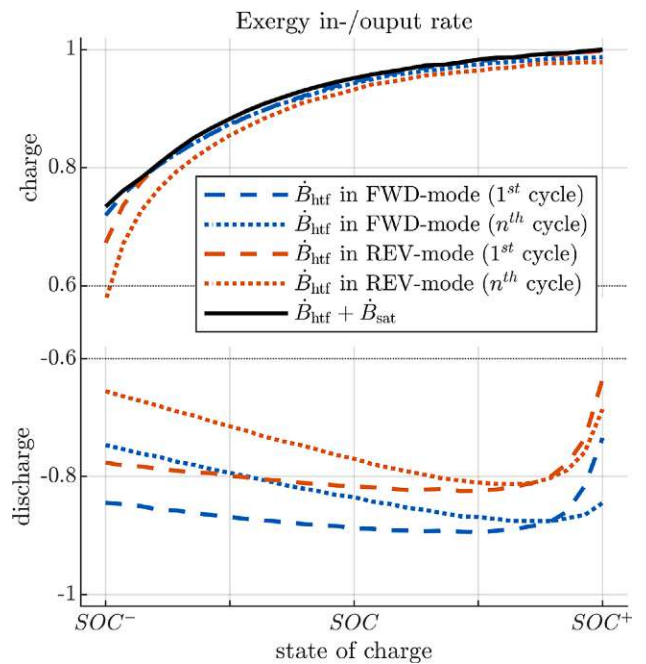


Fig. 10. Rate of exergy in- and output of a PBTES in partial cycle operation with a cycle time of 1 h.

Table 4

Summary of the main results: Energy/exergy efficiency are calculated according to Eqs. (8) and (9). Energy/exergy output rates are given as relative values with respect to the maximum gross input rates \dot{Q}_{htf} and \dot{B}_{htf} .

HTF flow direction	Cycle number	FWD-mode		REV-mode	
		1st	nth	1st	nth
Energy efficiency	η_E	95%	90%	90%	85%
Exergy efficiency	η_B	90%	86%	83%	80%
min. energy output rate	$\dot{Q}_{\text{htf}}/\hat{Q}_{\text{htf}}$	90%	82%	85%	75%
max. energy output rate		93%	89%	89%	84%
min. exergy output rate	$\dot{B}_{\text{htf}}/\hat{B}_{\text{htf}}$	84%	74%	77%	65%
max. exergy output rate		89%	87%	82%	81%

Regarding the exergy in-/output rate, similar deductions can be drawn from Fig. 10. Compared to the energy input rate, the exergy input rate during the charging periods does not diverge from the gross exergy input rate \hat{B}_{htf} in any experiment. That is because saturation losses occur at low temperatures near the ambient temperature and are therefor mostly composed of anergy. For the discharging process, the qualitative behavior of all the exergy curves is similar to the energy curves in Fig. 9. Again, in the first cycles a fairly constant output rate with a maximum of 89% and 82% can be observed for the FWD- and the REV-mode respectively. However, the degradation of the exergy output rate in the n th cycle is slightly more pronounced. For steady cycling the maximum exergy output rates for the FWD-mode and the REV-mode are 87% and 81% respectively. Still noteworthy, the exergy output rate is well above 65% of the maximum gross exergy input rate \hat{B}_{htf} for all experiments.

The results presented and discussed in this section provide important information about the thermal performance of PBTES systems that operate under challenging, not yet investigated, conditions. The most important key performance indicators that can be used to assess the suitability of PBTES systems for the waste heat recovery in industrial processes are summarized in Table 4. These reference values are valid for a PBTES with a design similar to the test rig used in this study as well as similar operating conditions.

5. Conclusion

The experiments presented in this work were conducted to assess the efficiency of packed bed thermal energy systems when they are operated with industrial exhaust gases. To facilitate the removal of powder particles, a packed bed thermal energy storage is required to be charged from the bottom and discharged from the top in this particular application. Since this is contrary to an optimal operation in terms of thermal efficiency, this study investigated the thermal performance of a packed bed thermal energy storage for different flow directions of the heat transfer fluid. To quantify the effect of the flow direction on the exergy efficiency and thermocline degradation, a lab-scale test rig of a packed bed thermal energy storage is used. Multiple partial cycle experiments in which the storage was periodically charged from the top and discharged from the bottom and vice versa were conducted and analyzed.

The results reveal that in a packed bed thermal energy storage in partial cycle operation, the thermocline gradually degrades until it reaches a steady state after approximately 10 cycles (equivalent to 10 h in this study). A slightly faster and more pronounced degradation of the thermocline could be observed when the storage was charged from the bottom and discharged from the top. Furthermore, the energy and exergy efficiency of a storage that has reached steady cycling after it was charged from the top and discharged from bottom are 90% and 86% respectively. These values are 5% points lower than the ones achieved in the first cycle. For a storage that has reached steady cycling after it was charged from the bottom and discharged from top the

energy and exergy efficiency are 85% and 80% respectively which are 3 to 5% points less than they were in the first cycle.

The energy and exergy in-/output rates were observed to be stable for all experiments. Despite minimum saturation losses during charging and slight reductions of the maximum output rates during discharging no substantial deterioration of the thermal performance of the storage could be detected. Energy output rates of 74% to 93% and exergy output rates of 65% to 89% with respect to the maximum input rates were measured.

CRedit authorship contribution statement

Paul Schwarzmayr: Writing – original draft, Visualization, Validation, Methodology, Investigation, Formal analysis, Data curation, Conceptualization. **Felix Birkelbach:** Writing – review & editing, Methodology, Formal analysis, Conceptualization. **Heimo Walter:** Writing – review & editing, Visualization, Supervision, Methodology, Formal analysis, Conceptualization. **René Hofmann:** Writing – review & editing, Validation, Supervision, Funding acquisition, Conceptualization,.

Declaration of competing interest

The authors declare that they have no known competing financial interests or personal relationships that could have appeared to influence the work reported in this paper.

Data availability

Data will be made available on request.

Acknowledgments

The authors acknowledge funding support of this work through the research project *5DIndustrialTwin* as part of the Austrian Climate and Energy Fund's initiative Energieforschung (e!MISSION) 6th call (KLIE/FFG project number 881140). Furthermore, the authors acknowledge TU Wien Bibliothek, Austria for financial support through its Open Access Funding programme.

References

- [1] Bai Y, Wang L, Lin L, Lin X, Peng L, Chen H. A performance analysis of the spray-type packed bed thermal energy storage for concentrating solar power generation. *J Energy Storage* 2022;51:104187. <http://dx.doi.org/10.1016/j.est.2022.104187>.
- [2] Gautam A, Saini RP. A review on sensible heat based packed bed solar thermal energy storage system for low temperature applications. *Sol Energy* 2020;207:937–56. <http://dx.doi.org/10.1016/j.solener.2020.07.027>.
- [3] Gautam A, Saini RP. A review on technical, applications and economic aspect of packed bed solar thermal energy storage system. *J Energy Storage* 2020;27:101046. <http://dx.doi.org/10.1016/j.est.2019.101046>.
- [4] Cui Z, Du Q, Gao J, Bie R, Li D. Development of a direct contact heat exchanger for energy and water recovery from humid flue gas. *Appl Therm Eng* 2020;173:115214. <http://dx.doi.org/10.1016/j.applthermaleng.2020.115214>.
- [5] Wang W, Li H, Guo S, He S, Ding J, Yan J, Yang J. Numerical simulation study on discharging process of the direct-contact phase change energy storage system. *Appl Energy* 2015;150:61–8. <http://dx.doi.org/10.1016/j.apenergy.2015.03.108>.
- [6] Scharinger-Urschitz G, Schwarzmayr P, Walter H, Haider M. Partial cycle operation of latent heat storage with finned tubes. *Appl Energy* 2020;280:115893. <http://dx.doi.org/10.1016/j.apenergy.2020.115893>.
- [7] Zanganeh G, Ambrosetti G, Pedretti A, Zavattoni S, Barbato M, Good P, Haselbacher A, Steinfeld A. A 3 m² parabolic trough CSP plant operating with air at up to 650 °C. In: 2014 international renewable and sustainable energy conference (IRSEC). 2014, p. 108–13. <http://dx.doi.org/10.1109/IRSEC.2014.7059884>, ISSN: 2380-7393.
- [8] Rong Y, Huang SY, Zhou H. Experimental study on storage performance of packed bed solar thermal energy storage system using steel slag. *J Energy Storage* 2024;78:110042. <http://dx.doi.org/10.1016/j.est.2023.110042>.
- [9] Mawire A, McPherson M, Heetkamp RRJvd, Mlatho SJP. Simulated performance of storage materials for pebble bed thermal energy storage (TES) systems. *Appl Energy* 2009;86(7):1246–52. <http://dx.doi.org/10.1016/j.apenergy.2008.09.009>.

- [10] Meier A, Winkler C, Wullemind D. Experiment for modelling high temperature rock bed storage. *Solar Energy Mater* 1991;24(1):255–64. [http://dx.doi.org/10.1016/0165-1633\(91\)90066-T](http://dx.doi.org/10.1016/0165-1633(91)90066-T).
- [11] Yang X, Yang X, Qin FG, Jiang R. Experimental investigation of a molten salt thermocline storage tank. *Int J Sustain Energy* 2014;35(6):606–14. <http://dx.doi.org/10.1080/14786451.2014.930465>, Publisher: Taylor & Francis.
- [12] Anderson R, Shiri S, Bindra H, Morris JF. Experimental results and modeling of energy storage and recovery in a packed bed of alumina particles. *Appl Energy* 2014;119:521–9. <http://dx.doi.org/10.1016/j.apenergy.2014.01.030>.
- [13] Kanojia N, Kaushik S, Singh M, Sah MK. Comprehensive review on packed bed thermal energy storage systems. In: Manik G, Kalia S, Sahoo SK, Sharma TK, Verma OP, editors. *Advances in mechanical engineering. Lecture notes in mechanical engineering*. Singapore: Springer; 2021, p. 165–73. http://dx.doi.org/10.1007/978-981-16-0942-8_15.
- [14] Al-Azawii MMS, Alhamdi SFH, Braun S, Hoffmann J-F, Calvet N, Anderson R. Thermocline in packed bed thermal energy storage during charge-discharge cycle using recycled ceramic materials - Commercial scale designs at high temperature. *J Energy Storage* 2023;64:107209. <http://dx.doi.org/10.1016/j.est.2023.107209>.
- [15] Oró E, Castell A, Chiu J, Martin V, Cabeza LF. Stratification analysis in packed bed thermal energy storage systems. *Appl Energy* 2013;109:476–87. <http://dx.doi.org/10.1016/j.apenergy.2012.12.082>.
- [16] Knobloch K, Muhammad Y, Costa MS, Moscoso FM, Bahl C, Alm O, Engelbrecht K. A partially underground rock bed thermal energy storage with a novel air flow configuration. *Appl Energy* 2022;315:118931. <http://dx.doi.org/10.1016/j.apenergy.2022.118931>.
- [17] Soprani S, Marongiu F, Christensen L, Alm O, Petersen KD, Ulrich T, Engelbrecht K. Design and testing of a horizontal rock bed for high temperature thermal energy storage. *Appl Energy* 2019;251:113345. <http://dx.doi.org/10.1016/j.apenergy.2019.113345>.
- [18] Dusek S, Hofmann R, Gruber S. Design analysis of a hybrid storage concept combining Ruths steam storage and latent thermal energy storage. *Appl Energy* 2019;251:113364. <http://dx.doi.org/10.1016/j.apenergy.2019.113364>.
- [19] Xie B, Baudin N, Soto J, Fan Y, Luo L. Chapter 10 - Thermocline packed bed thermal energy storage system: a review. In: Jeguirim M, editor. *Renewable energy production and distribution. Advances in renewable energy technologies*, vol. 1, Academic Press; 2022, p. 325–85. <http://dx.doi.org/10.1016/B978-0-323-91892-3.24001-6>.
- [20] Yang B, Bai F, Wang Y, Wang Z. Study on standby process of an air-based solid packed bed for flexible high-temperature heat storage: Experimental results and modelling. *Appl Energy* 2019;238:135–46. <http://dx.doi.org/10.1016/j.apenergy.2019.01.073>.
- [21] Marti J, Geissbühler L, Becattini V, Haselbacher A, Steinfeld A. Constrained multi-objective optimization of the thermocline packed-bed thermal-energy storage. *Appl Energy* 2018;216:694–708. <http://dx.doi.org/10.1016/j.apenergy.2017.12.072>.
- [22] Trevisan S, Jemmal Y, Guedez R, Laumert B. Packed bed thermal energy storage: A novel design methodology including quasi-dynamic boundary conditions and techno-economic optimization. *J Energy Storage* 2021;36:102441. <http://dx.doi.org/10.1016/j.est.2021.102441>.
- [23] Bruch A, Fourmigué JF, Couturier R. Experimental and numerical investigation of a pilot-scale thermal oil packed bed thermal storage system for CSP power plant. *Sol Energy* 2014;105:116–25. <http://dx.doi.org/10.1016/j.solener.2014.03.019>.
- [24] Bruch A, Molina S, Esence T, Fourmigué JF, Couturier R. Experimental investigation of cycling behaviour of pilot-scale thermal oil packed-bed thermal storage system. *Renew Energy* 2017;103:277–85. <http://dx.doi.org/10.1016/j.renene.2016.11.029>.
- [25] Miró L, Gasia J, Cabeza LF. Thermal energy storage (TES) for industrial waste heat (IWH) recovery: A review. *Appl Energy* 2016;179:284–301. <http://dx.doi.org/10.1016/j.apenergy.2016.06.147>.
- [26] Manente G, Ding Y, Sciacovelli A. A structured procedure for the selection of thermal energy storage options for utilization and conversion of industrial waste heat. *J Energy Storage* 2022;51:104411. <http://dx.doi.org/10.1016/j.est.2022.104411>.
- [27] Bianchi G, Panayiotou GP, Aresti L, Kalogirou SA, Florides GA, Tsamos K, Tassou SA, Christodoulides P. Estimating the waste heat recovery in the European Union Industry. *Energy Ecol Environ* 2019;4(5):211–21. <http://dx.doi.org/10.1007/s40974-019-00132-7>.
- [28] Papapetrou M, Kosmadakis G, Cipollina A, La Commare U, Micale G. Industrial waste heat: Estimation of the technically available resource in the EU per industrial sector, temperature level and country. *Appl Therm Eng* 2018;138:207–16. <http://dx.doi.org/10.1016/j.applthermaleng.2018.04.043>.
- [29] Schwarzmayr P, Birkelbach F, Walter H, Javernik F, Schwaiger M, Hofmann R. Packed bed thermal energy storage for waste heat recovery in the iron and steel industry: A cold model study on powder hold-up and pressure drop. *J Energy Storage* 2024;75:109735. <http://dx.doi.org/10.1016/j.est.2023.109735>.
- [30] Keplinger T, Haider M, Steinparzer T, Patrejko A, Trunner P, Haselgrübler M. Dynamic simulation of an electric arc furnace waste heat recovery system for steam production. *Appl Therm Eng* 2018;135:188–96. <http://dx.doi.org/10.1016/j.applthermaleng.2018.02.060>.
- [31] Ortega-Fernández I, Rodríguez-Aseguinolaza J. Thermal energy storage for waste heat recovery in the steelworks: The case study of the reslag project. *Appl Energy* 2019;237:708–19. <http://dx.doi.org/10.1016/j.apenergy.2019.01.007>.
- [32] Slimani H, Filali Baba Y, Ait Ousaleh H, Elharrak A, El Hamdani F, Bouzekri H, Al Mers A, Faik A. Horizontal thermal energy storage system for Moroccan steel and iron industry waste heat recovery: Numerical and economic study. *J Clean Prod* 2023;393:136176. <http://dx.doi.org/10.1016/j.jclepro.2023.136176>.
- [33] Odenthal C, Steinmann W-D, Zunft S. Analysis of a horizontal flow closed loop thermal energy storage system in pilot scale for high temperature applications – Part I: Experimental investigation of the plant. *Appl Energy* 2020;263:114573. <http://dx.doi.org/10.1016/j.apenergy.2020.114573>.
- [34] Touza A, Olives R, Dejean G, Pham Minh D, El Hafi M, Hoffmann J-F, Py X. Experimental and numerical analysis of a packed-bed thermal energy storage system designed to recover high temperature waste heat: an industrial scale up. *J Energy Storage* 2020;32:101894. <http://dx.doi.org/10.1016/j.est.2020.101894>.
- [35] Esence T, Bruch A, Molina S, Stutz B, Fourmigué J-F. A review on experience feedback and numerical modeling of packed-bed thermal energy storage systems. *Sol Energy* 2017;153:628–54. <http://dx.doi.org/10.1016/j.solener.2017.03.032>.
- [36] Schwarzmayr P, Birkelbach F, Walter H, Hofmann R. Standby efficiency and thermocline degradation of a packed bed thermal energy storage: An experimental study. *Appl Energy* 2023;337:120917. <http://dx.doi.org/10.1016/j.apenergy.2023.120917>.
- [37] Bayón R, Rivas E, Rojas E. Study of thermocline tank performance in dynamic processes and stand-by periods with an analytical function. *Energy Procedia* 2014;49:725–34. <http://dx.doi.org/10.1016/j.egypro.2014.03.078>.
- [38] Biencinto M, Bayón R, Rojas E, González L. Simulation and assessment of operation strategies for solar thermal power plants with a thermocline storage tank. *Sol Energy* 2014;103:456–72. <http://dx.doi.org/10.1016/j.solener.2014.02.037>.
- [39] Wang Y, Wang Z, Yuan G. Control strategy effect on storage performance for packed-bed thermal energy storage. *Sol Energy* 2023;253:73–84. <http://dx.doi.org/10.1016/j.solener.2023.02.012>.
- [40] Zavattoni SA, Barbato MC, Pedretti A, Zanganeh G, Steinfeld A. High temperature rock-bed TES system suitable for industrial-scale CSP plant – CFD analysis under charge/Discharge cyclic conditions. *Energy Procedia* 2014;46:124–33. <http://dx.doi.org/10.1016/j.egypro.2014.01.165>.
- [41] Zavattoni SA, Barbato MC, Pedretti A, Zanganeh G. Single-tank TES system – transient evaluation of thermal stratification according to the second-law of thermodynamics. *Energy Procedia* 2015;69:1068–77. <http://dx.doi.org/10.1016/j.egypro.2015.03.213>.
- [42] Mertens N, Alobaid F, Frigge L, Epple B. Dynamic simulation of integrated rock-bed thermocline storage for concentrated solar power. *Sol Energy* 2014;110:830–42. <http://dx.doi.org/10.1016/j.solener.2014.10.021>.
- [43] Zanganeh G, Pedretti A, Zavattoni S, Barbato M, Steinfeld A. Packed-bed thermal storage for concentrated solar power – Pilot-scale demonstration and industrial-scale design. *Sol Energy* 2012;86(10):3084–98. <http://dx.doi.org/10.1016/j.solener.2012.07.019>.
- [44] Johnson E, Bates L, Dower A, Bueno PC, Anderson R. Thermal energy storage with supercritical carbon dioxide in a packed bed: Modeling charge-discharge cycles. *J Supercrit Fluids* 2018;137:57–65. <http://dx.doi.org/10.1016/j.supflu.2018.03.009>.
- [45] Cascetta M, Cau G, Puddu P, Serra F. Experimental investigation of a packed bed thermal energy storage system. *J Phys Conf Ser* 2015;655(1):012018. <http://dx.doi.org/10.1088/1742-6596/655/1/012018>, Publisher: IOP Publishing.
- [46] McTigue JD, Markides CN, White AJ. Performance response of packed-bed thermal storage to cycle duration perturbations. *J Energy Storage* 2018;19:379–92. <http://dx.doi.org/10.1016/j.est.2018.08.016>.
- [47] Mitterlehner T, Kartnig G, Haider M. Analysis of the thermal ratcheting phenomenon in packed-bed thermal energy storage using Discrete Element Method. *FME Trans* 2020;48(2):427–31. <http://dx.doi.org/10.5937/fme2002427M>.
- [48] Schwarzmayr P, Birkelbach F, Kasper L, Hofmann R. Development of a digital twin platform for industrial energy systems. In: *Accelerated energy innovations and emerging technologies*, Vol. 25, Cambridge, USA: Energy Proceedings; 2022. <http://dx.doi.org/10.46855/energy-proceedings-9974>.
- [49] Haller MY, Cruickshank CA, Streicher W, Harrison SJ, Andersen E, Furbo S. Methods to determine stratification efficiency of thermal energy storage processes – Review and theoretical comparison. *Sol Energy* 2009;83(10):1847–60. <http://dx.doi.org/10.1016/j.solener.2009.06.019>.
- [50] Andersen E, Furbo S, Fan J. Multilayer fabric stratification pipes for solar tanks. *Sol Energy* 2007;81(10):1219–26. <http://dx.doi.org/10.1016/j.solener.2007.01.008>.

Contributions to international conferences

Publication 4

Development of a Digital Twin Platform for Industrial Energy Systems

by Paul Schwarzmayr, Felix Birkelbach, Lukas Kasper and René Hofmann; technical presentation at the (virtual) Applied Energy Symposium: MIT A+B in 2022

In this conference paper, the digital twin platform that was proposed in Publication 6 was implemented on the medium-scale PBTES test rig that was investigated in Publication 1 and 3. The bi-directional communication within the digital twin platform was tested with an ontology-supported automated soft sensor modeling service. The results of this paper show noticeable advantages of the digital twin platform for thermal energy storage devices that operate in a constantly changing and challenging environment.

Author contribution: Conceptualization, Methodology, Software, Data Curation, Writing - Original Draft, Visualization.

P. Schwarzmayr, F. Birkelbach, L. Kasper, and R. Hofmann (2022). "Development of a Digital Twin Platform for Industrial Energy Systems". In: Accelerated Energy Innovations and Emerging Technologies. Vol. 25. Cambridge, USA: Energy Proceedings.

DOI: 10.46855/energy-proceedings-9974

Abstract

The reduction of waste heat in energy-intensive industrial processes, in combination with digital technologies, will play a key role for the development and decarbonization of modern industrial energy systems. In the last few years, a significant share of the CO₂ related to energy was emitted by the industry sector. Since industrial processes often are batch processes, waste heat recovery in these processes requires thermal energy storage systems for closing the temporal gap between energy supply and demand. The ongoing digitalization in the field of industrial energy systems enables modern applications like digital twins to increase the efficiency of energy-intensive processes. This paper presents the implementation of a five-dimensional digital twin platform for a packed bed thermal energy storage test rig. The five-dimensional digital twin platform allows the development of services and applications in interdisciplinary teams and facilitates their interaction on a standardized platform. By that, the digital twin helps to make modern industrial energy systems more efficient.

Publication 5

Study on the Standby Characteristics of a Packed Bed Thermal Energy Storage: Experimental Results and Model-Based Parameter Optimization

by Paul Schwarzmayer, Felix Birkelbach, Heimo Walter and René Hofmann; technical presentation at the ASME Power Applied R&D Conference in Long Beach, California, 2023

In this study, the experimental results of Publication 1 were used to optimize unknown parameters of the medium-scale test rig. A one-dimensional finite volume model was developed and used for the model-based parameter optimization. The results include important thermo-physical properties of the storage material that were necessary for the data analysis in Publication 1 and 3 as well as a validated thermal model of the storage that represents the virtual entity in the digital twin platform developed in Publication 6.

Author contribution: Conceptualization, Methodology, Software, Validation, Formal analysis, Investigation, Writing - Original Draft, Visualization.

P. Schwarzmayer, F. Birkelbach, H. Walter, and R. Hofmann (Sept. 2023b). "Study on the Standby Characteristics of a Packed Bed Thermal Energy Storage: Experimental Results and Model Based Parameter Optimization". In: American Society of Mechanical Engineers Digital Collection.

DOI: [10.1115/POWER2023-108578](https://doi.org/10.1115/POWER2023-108578)

Abstract

In the present study the standby characteristics of a packed bed thermal energy storage are investigated experimentally and numerically. The results collected from the experiments are used for the development of a thermal model of the storage that will act as the virtual entity in a digital twin platform. A packed bed thermal energy storage is a sensible type of thermal energy storage that is capable of storing excess heat for several hours and even days. In this study experimental data from a lab-scale test rig is used to make statements on the thermal characteristics of the storage during standby periods. In addition, the experimental data and a finite volume model of the test rig are used for model-based parameter optimization. The developed model is able to predict the thermal behaviour of the storage in standby and can be utilized as the virtual entity in a digital twin platform. The evaluation of the measured data is done with first and second law analysis and nonlinear optimization. The results are contributing to the further development and deployment of packed bed thermal energy storage systems for waste heat recovery in industrial processes and to increasing flexibility of renewable power generating technologies.

Co-author publications

Publication 6

Toward a Practical Digital Twin Platform Tailored to the Requirements of Industrial Energy Systems

by Lukas Kasper, Felix Birkelbach, Paul Schwarzmayr, Gernot Steindl, Daniel Ramsauer and René Hofmann; published in Applied Sciences.

This paper proposed a five-dimensional digital twin platform for industrial energy systems. This digital twin platform was later implemented (4) and tested (7) on the PBTES test rig that was experimentally investigated in Publications 1 and 3.

Author contribution: Conceptualization, Methodology, Writing - Original Draft.

L. Kasper, F. Birkelbach, P. Schwarzmayr, G. Steindl, D. Ramsauer, and R. Hofmann (Jan. 2022). "Toward a Practical Digital Twin Platform Tailored to the Requirements of Industrial Energy Systems". In: Applied Sciences 12.14. Number: 14 Publisher: Multidisciplinary Digital Publishing Institute, p. 6981. ISSN: 2076-3417. DOI: 10.3390/app12146981

Abstract

Digitalization and concepts such as digital twins (DT) are expected to have enormous potential to improve efficiency in industry, in particular, in the energy sector. Although the number and maturity of DT concepts are increasing, there is still no standardized framework available for the implementation of DTs for industrial energy systems (IES). On the one hand, most proposals focus on the conceptual side of components and leave most implementation details unaddressed. Specific implementations, on the other hand, rarely follow recognized reference architectures and standards. Furthermore, most related work on DTs is done in manufacturing, which differs from DTs in energy systems in various aspects, regarding, for example, multiple time scales, strong nonlinearities, and uncertainties. In the present work, we identify the most important requirements for DTs of IES. We propose a DT platform based on the five-dimensional DT modeling concept with a low level of abstraction that is tailored to the identified requirements. We address current technical implementation barriers and provide practical solutions for them. Our work should pave the way to standardized DT platforms and the efficient encapsulation of DT service engineering by domain experts. Thus, DTs could be easy to implement in various IES-related use cases, host any desired models and services, and help get the most out of individual applications. This ultimately helps bridge the interdisciplinary gap between the latest research on DTs in the domain of computer science and industrial automation and the actual implementation and value creation in the traditional energy sector.

Publication 7

A digital twin-based adaptive optimization approach applied to waste heat recovery in green steel production: Development and experimental investigation

by Lukas Kasper, Paul Schwarzmayr, Felix Birkelbach, Florian Javernik, Michael Schwaiger and René Hofmann; published in Applied Energy.

The digital twin platform that was proposed in Publication 6 was implemented and experimentally evaluated using the PBTES test rig that was investigated in Publications 1 and 3. For these evaluations, micro-services from Publications 5 and 8 were utilized.

Author contribution: Conceptualization, Methodology, Software, Writing - Original Draft, Writing - Review and Editing, Visualization.

L. Kasper, P. Schwarzmayr, F. Birkelbach, F. Javernik, M. Schwaiger, and R. Hofmann (Jan. 2024). "A digital twin-based adaptive optimization approach applied to waste heat recovery in green steel production: Development and experimental investigation". In: Applied Energy 353, p. 122192. ISSN: 0306-2619.

DOI: 10.1016/j.apenergy.2023.122192

Abstract

Renewable-dominated power grids will require industries to run their processes in accordance with the availability of energy. At the same time, digitalization introduces new possibilities to leverage the untapped optimization potential to provide this flexibility. Mathematical optimization methods such as mixed integer linear programming (MILP) are widely used to predict optimal operation plans for industrial systems. MILP models are difficult to adapt, but the viability of the predicted plans relies on accurate underlying models of the actual behavior. New automation paradigms, such as the digital twin (DT), can overcome these current drawbacks. In this work, we present the implementation and experimental evaluation of several micro-services on a standardized five-dimensional DT platform that automates MILP model adaption and operation optimization. These micro-services guarantee that (1) deviations between the physical entity and its virtual entity models are detected, (2) the models are adapted accordingly, (3) subsequently linearized to suit the MILP approach and (4) used for live operational optimization. These novel services and DT workflows that orchestrate them were experimentally tested with a packed bed thermal energy storage test rig that acts as a physical entity. A waste heat recovery use case in steel production is used as the evaluation scenario. While the model error of a static simulation model would increase to 60 % over 7 days of operation, the model error remains well below 25 % as a result of successful model adaption. The prediction error of the optimization model remains in a typical magnitude of 10 to 20 % during the evaluation period, despite the degradation of the packed bed thermal energy storage power.

Publication 8**Operation planning with thermal storage units using MILP: comparison of heuristics for approximating non-linear operating behaviour**

by Felix Birkelbach, Lukas Kasper, Paul Schwarzmayr and René Hofmann; technical presentation at the Int. Conf. on ECOS in Las Palmas de Gran Canaria, Spain, 2023.

This conference paper compared the performance of different linearization algorithms for the modeling of thermal storage units and was selected for publication in a special issue of the Journal of Energy Storage. The journal paper is included as Publication 9 in this dissertation.

Author contribution: Methodology, Writing - Review and Editing, Visualization.

F. Birkelbach, L. Kasper, P. Schwarzmayr, and R. Hofmann (2023b). "Operation Planning with Thermal Storage Units Using MILP: Comparison of Heuristics for Approximating Non-Linear Operating Behavior". In: 36th Int. Conf. on Eff., Cost, Opt., Sim. and Env. Imp. of En. Sys. (ECOS 2023). Las Palmas De Gran Canaria, Spain: ECOS 2023, pp. 1345–1350.

DOI: 10.52202/069564-0122

Abstract

For operation planning in industrial energy systems mixed integer linear programming (MILP) is the go-to method because of its reliability and the huge advances in MILP algorithms in recent years. MILP is especially well suited for planning the use of storage units, even if including the non-linear operating behavior of thermal storage is still a big challenge — especially if partial load cycles are considered. To model the storage behavior, a multi-variate non-linear function has to be linearized and incorporated into the MILP model. The key to good performance in MILP is using as few linear pieces as possible to achieve the required accuracy. We consider two types of piecewise-linear models: triangulation on a grid and general triangulation. In this paper, we present different heuristics for computing efficient piecewise-linear approximations of nonlinear functions. As a use case, we consider the behavior of a thermal storage unit. We apply the heuristics to compute a piecewise-linear approximation of the non-linear operating behavior and discuss the results. We then compare the performance of the models in a MILP model for the operation planning of an energy system. For translating the piecewise-linear function to MILP we consider state-of-the-art approaches with a logarithmic number of binary variables. Our results show that gridded triangulation models in combination with logarithmic MILP formulations can be used for data-driven modeling of non-linear operating behavior of devices. We highlight the potential of this approach for realizing adaptable operation optimization of energy systems.

Publication 9**Modeling Partial Cycle Behavior of a Thermal Storage in MILP: Comparison of Heuristics for Approximating Non-Linear Operating Behavior**

by Felix Birkelbach, Lukas Kasper, Paul Schwarzmayr and René Hofmann; submitted to the Journal of Energy Storage.

In this paper, the development of a specialized micro-service that was used for the digital twin evaluation in Publication 7 was presented. The developed algorithm can be used to approximate the non-linear behavior of real-world devices with double-convex linear functions that are suitable for operational optimization using mixed integer linear programming.

Author contribution: Methodology, Writing - Review and Editing, Visualization.

F. Birkelbach, L. Kasper, P. Schwarzmayr, and R. Hofmann (2023a). Modeling Partial Cycle Behavior of a Thermal Storage in Milp: Comparison of Heuristics for Approximating Non-Linear Operating Behavior. *submitted to Journal of Energy Storage.*


DOI: [10.2139/ssrn.4656763](https://doi.org/10.2139/ssrn.4656763)

Abstract

For operation planning in industrial energy systems mixed integer linear programming (MILP) is the go-to method because of its reliability and significant advances in the area of MILP solvers in recent years. MILP is especially well suited for planning the use of storage units, even if including the non-linear operating behavior of thermal storages is still a big challenge – especially if partial load cycles are considered. To model the storage behavior, a multi-variate non-linear function has to be linearized and incorporated into the MILP model. The key for good performance in MILP is finding an approximation with as few linear pieces as possible that achieves the required accuracy. In this paper, we consider two different heuristics for computing piecewise linear approximations of non-linear functions. As a use case, we use a unit commitment (UC) problem of an energy system with a packed-bed thermal storage unit. We discuss properties of the approximation heuristics and apply them to compute piecewise-linear models of the non-linear operating behavior. We then compare the performance of the models in the UC problem. For translating the piecewise-linear function to MILP we consider state-of-the-art approaches with a logarithmic number of binary variables. Our results show that approximation with triangulation on a grid, in combination with logarithmic MILP formulation yields the best performance by a margin. With this approach, data-driven models of non-linear operating behavior can be derived also for other applications. We highlight the potential of this approach for realizing adaptable operation optimization of energy systems.

About the author

Paul Schwarzmayr was born in Haag am Hausruck, Austria in 1995. After finishing the high school for mechanical engineering (HTL) in Ried im Innkreis in 2014 he did his compulsory military service at the military band. Soon after, in 2015, he enrolled at TU Wien to study Chemical and Process Engineering, specializing on pressure vessel technology, plant construction, and the design and simulation of thermal power plants. During his studies, he worked as a tutor and teaching assistant at the Institute of Energy Systems and Thermodynamics at TU Wien. In 2021 he graduated with distinction.

The research he did in the course of his master's thesis motivated him to pursue a Ph.D. at the Institute of Energy Systems and Thermodynamics at TU Wien, where he focused on thermal energy storage and digital twin technologies and managed a research project called *5DIndustrialTwin*. The present dissertation is based on that research. An up-to-date record of the author's publications can be found at:  0000-0003-4735-3447.

